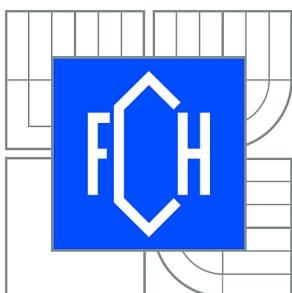# VYSOKÉ UČENÍ TECHNICKÉ V BRNĚ

BRNO UNIVERSITY OF TECHNOLOGY

FAKULTA CHEMICKÁ
ÚSTAV FYZIKÁLNÍ A SPOTŘEBNÍ CHEMIE

FACULTY OF CHEMISTRY
INSTITUTE OF PHYSICAL AND APPLIED CHEMISTRY

DUAL-FOCUS FCS IN COLLOIDAL RESEARCH

DVOUOHNISKOVÁ FCS VE VÝZKUMU KOLOIDŮ

DIPLOMOVÁ PRÁCE
MASTER'S THESIS

AUTOR PRÁCE   Bc. ROMANA CHOVANCOVÁ
AUTHOR

VEDOUCÍ PRÁCE   Ing. FILIP MRAVEC, Ph.D.
SUPERVISOR

BRNO 2015

Zadání diplomové práce

Číslo diplomové práce:	**FCH-DIP0856/2014**	Akademický rok:	**2014/2015**
Ústav:	Ústav fyzikální a spotřební chemie		
Student(ka):	**Bc. Romana Chovancová**		
Studijní program:	Spotřební chemie (N2806)		
Studijní obor:	Spotřební chemie (2806T002)		
Vedoucí práce	**Ing. Filip Mravec, Ph.D.**		
Konzultanti:			

Název diplomové práce:

Dvouohnisková FCS ve výzkumu koloidů

Zadání diplomové práce:

1. Zpracovat rešerši na využití techniky fluorescenční korelační spektroskopie ve výzkumu koloidů s přihlédnutím ke dvouohniskové technice a biopolymerům.

2. Na základě rešerše najít nejvhodnější model kalibrace a vyhodnocení pro experimenty s fluorescenčně značeným hyaluronanem.

3. Ověřit možnosti stanovení difúzních charakteristik fluorescenčně značeného hyaluronanu a zjistit vliv fyziologického prostředí a koncentrace hyaluronanu na tyto charakteristiky.

4. Zhodnotit a ověřit využití techniky dvoufokusové FCS pro studium fluorescenčně značeného hyaluronanu.

Termín odevzdání diplomové práce: 11.5.2015

Diplomová práce se odevzdává v děkanem stanoveném počtu exemplářů na sekretariát ústavu a v elektronické formě vedoucímu diplomové práce. Toto zadání je přílohou diplomové práce.

-    -   -

  Bc. Romana Chovancová   Ing. Filip Mravec, Ph.D.   prof. Ing. Miloslav Pekař, CSc.
       Student(ka)   Vedoucí práce   Ředitel ústavu

- -

prof. Ing. Martin Weiter, Ph.D.

V Brně, dne 30.1.2015   Děkan fakulty

ABSTRACT

This thesis deals with study of fluorescently labelled sodium rhodaminylamino hyaluronate (Hya-Rh, 40 kDa) by dual-focus fluorescence correlation spectroscopy (2f-FCS). At first, the overview of research was focused on use of the technique of FCS in colloidal chemistry and polymers, and then the utilisation overview of 2f-FCS method was summarised. At second, the most suitable model of preparation and storage of Hya-Rh solution for experiments was found on the basis of previous measurements. At third, the possibility of determining the diffusion characteristics of fluorescently labelled hyaluronan was verified as well as the influence of physiological environment and concentration of Hya-Rh on these characteristics. Subsequently, the influence of alkali metal ions on these characteristics was determined by measuring of diffusion coefficient values of Hya-Rh in presence of various concentrations of the alkali metal ions. Afterwards, the behaviour of Hya-Rh polymer molecules was studied in dependence on increasing concentration of very low molecular weight hyaluronan (VLMW HA, 404 kDa) in aqueous and physiological solutions. Finally, the evaluation and validation of use of 2f-FCS method for studying of fluorescently labelled hyaluronan solutions was described.

ABSTRAKT

Tato práce se zabývá studiem fluorescenčně značeného hyaluronanu, konkrétně rhodaminylamino hyaluronátu sodného (Hya-Rh, 40 kDa), pomocí dvouohniskové fluorescenční korelační spektroskopie (2f-FCS). Nejdříve byla prostudována literatura týkající se využití FCS techniky v koloidní chemii a při studiu polymerů, přičemž následně byly shrnuty veškeré poznatky o využití 2f-FCS metody. Na základě prvotních měření byl zjištěn vhodný postup přípravy a způsob uchovávání vzorku Hya-Rh používaném pro následující experimenty. Záhy byly prostudovány možné vlivy koncentrace Hya-Rh na jeho difúzní charakteristiky jak ve vodě, tak ve fyziologickém roztoku. Následně bylo studováno chování Hya-Rh a vliv koncentrace solí alkalických kovů ve vodných roztocích těchto solí a fluorescenčně značeného hyaluronanu. Poté bylo sledováno chování Hya-Rh v závislosti na koncentraci velmi nízkomolekulárního hyaluronanu (VLMW HA, 404 kDa) v čisté vodě i ve fyziologickém roztoku, přičemž získané výsledky byly mezi sebou porovnány. Nakonec bylo využití 2f-FCS metody celkově zhodnoceno a popsáno z hlediska studia chování fluorescenčně značeného hyaluronanu v roztocích.

KEYWORDS

Hyaluronic acid, dual-focus fluorescence correlation spectroscopy, absolute diffusion coefficient, fluorescently labelled hyaluronan, biopolymers, colloid solutions.

KLÍČOVÁ SLOVA

Kyselina hyaluronová, dvouohnisková fluorescenční korelační spektroskopie, absolutní difúzní koeficient, fluorescenčně značený hyaluronan, biopolymery, koloidní roztoky.

DECLARATION

I declare that the diploma thesis has been worked out by myself and that all the quotations from the used literary sources are accurate and complete. The content of the diploma thesis is the property of the Faculty of Chemistry of Brno University of Technology and all commercial uses are allowed only if approved by both the supervisor and the dean of the Faculty of Chemistry, BUT.

....
student's signature

CONTENT

1   INTRODUCTION

The hyaluronic acid is a publicly well-known compound and it is a subject of interest of many scientific groups in a relative with its potential usage as a drug delivery system and as a cancer tumour cure. In addition, study of hyaluronic acid brings better understanding of native tissues because this polysaccharide acts as a main part of extra-cellular matrix, so all transport between cells goes through this aqueous solution of this biopolymer. Furthermore, a usage of hyaluronic acid as a polyelectrolyte has a great potential in a thin film coating deposition process as well as for fibre production [1]. The behaviour of hyaluronic acid and its sodium salt in aqueous solutions at different conditions such as the influence of ionic strength, pH environment, hyaluronan concentration and molecular weight have already been studied by many researchers [2–5]. On the contrary, it is still not exactly known how the low molecular weight hyaluronan molecules behave in aqueous solutions, and how the macromolecular chains interact with each other at specific concentrations of hyaluronan even changed conditions. However, the study of diffusion characteristics of hyaluronan in solutions is one of the approaches how to answer these questions. Moreover, the molecular size of hyaluronan particles is observable with known diffusion coefficient values.

Nowadays, the determination of Brownian motion and associated diffusion coefficient is possible by many techniques, such as pulsed-field nuclear magnetic resonance (pfNMR), by ultracentrifugation or by dynamic light scattering spectroscopy (DLS). But for all these methods, it is necessary to have a quite high concentration of analysed material in the sample. Nevertheless, it is also possible to measure diffusion coefficient by fluorescence correlation spectroscopy (FCS). However, the concentration of analysed compound could be ranged around nanomolar and even in picomolar quantity. This leads to a robust technique, which facilitates investigations of extremely low concentrated biomolecules [6].

In past decade till now, researchers have devised some improvements of conventional FCS to avoid many optical and photo-physical artefacts as laser beam astigmatism, optical saturation or refractive index mismatch, which accompany the conventional FCS measurements and bring incorrect results [7]. One of the improvements is dual-focus fluorescence correlation spectroscopy (2f-FCS), which will be discussed here.

This thesis deals with study of diffusion characteristics and behaviour of macromolecules in solutions, in particular with fluorescently labelled hyaluronan in aqueous solutions, whereas the contemporary research overview of behaviour of hyaluronan in aqueous solutions is included. Subsequently, the actual background research of study of biomolecules and polymers by FCS is described. This theory is also focused on the implementation of 2f-FCS technique and explanation of the theoretical base, and it collects all applications which have ever been performed by this technique. Moreover, the assignment concerns the fluorescently labelled anionic polysaccharide and study of its diffusion characteristics under various conditions. In addition, behaviour of the low molecular weight polymer at different concentrations was studied for determining of the diluted to semi-diluted concentration transition.

2   THEORETICAL PART

2.1   Translational diffusion

Dissolved and dispersed particles in solution randomly collide with surrounding, thermally moving molecules of solvent, and thus the crashes induce thermal motion of these particles in the fluid medium too [8]. The global translational movement of dispersed particles in various directions is influenced by a force, which resultant determines the direction of the particle transport. Its mean velocity is expressed by equation (1) below:

$$\overline{\mu} = \sqrt{\frac{3k_B \cdot T}{m}}$$

(1)

where $\overline{\mu}$ is the mean velocity of translational movement, k_B means Boltzmann constant, T is thermodynamic temperature and m is weight. According to this relation, the mean velocity decreases with increasing weight and with increasing size of particles too. This fact causes that the motion is very fast for analytical dispersed particles, but it is decreasing for colloid particles. For bigger particles, especially with diameter higher than 4 μm, the movement disappears and these particles just vibrate in the same positions [9].
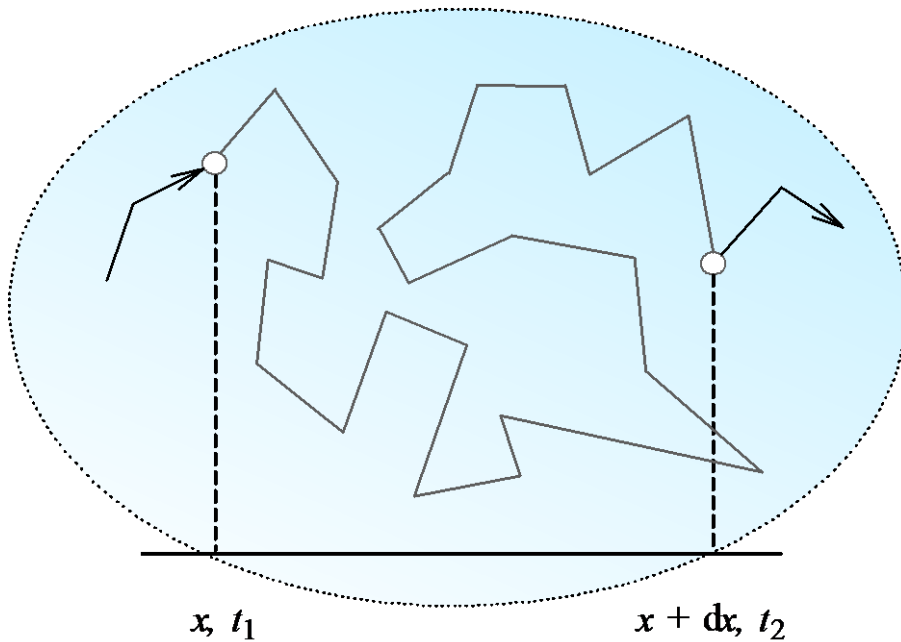
Figure 1: The picture of translational movement of particle in solution and its distance between position x and x + dx per change of time.

As a consequence, the translational thermal motions of dispersed particles in disperse medium lead to the movement down of the concentration gradient, and have tendency to isothermally balance chemical potentials as well as concentrations in the whole solution by Brownian movements. The effect is called translational diffusion. However, dispersed particles in solution collide with molecules of surrounding medium very fast and it is not possible exactly determine all various changes of directions and every individual velocity of

the movements in solutions. The shift of the particle in time can be explained as a difference between the distance x and $x + dx$ in time t, whereas the situation is described in Figure 1. According to the fact that particles move randomly in all directions per time, namely the *three-dimensional random walk* [10], the expression of the net distance of particles through the space by diffusion is determined by Gauss statistical distribution:

$$\langle x^2 \rangle (t) = \int_{-\infty}^{\infty} x^2 P(x,t) dx \tag{2}$$

where $\langle x^2 \rangle$ is a mean square distance of particle in time t and $P(x,t)$ is a frequency of the shift of particle in the distance x at time t. Subsequently, the term $P(x,t)$ is expressed as a probably distribution function:

$$P(x,t)dx = (2\pi K t)^{\frac{1}{2}} \cdot \exp\left(-\frac{x^2}{2Kt}\right) dx \tag{3}$$

where K is a constant. According to *Fick's first law of diffusion*, diffusion coefficient D is a proportional constant, which relates the intensity of diffusion flow q with difference of a concentration c per difference of the distance x, alias the space concentration gradient:

$$q = -D \cdot \left(\frac{\partial c}{\partial x}\right)_t \tag{4}$$

Then, the concentration can be formulated as a function of the probable distribution of the resulting displacements in a given time:

$$c(x,t) = n \cdot P(x,t) \tag{5}$$

Based on deduction, and if the *Fick's second law of diffusion*, which relates a first-order differential equation with respect to time to a second-order differential equation with respect to square distance:

$$\left(\frac{\partial c}{\partial t}\right)_x = D \cdot \left(\frac{\partial c^2}{\partial x^2}\right)_t \tag{6}$$

is considered, the root mean square distance of particle alias the mean displacement along the direction of the x-axis is exactly proportional to the square root of diffusion coefficient D and time interval t [11]. The relation is called *Einstein-Smoluchowski equation*:

$$\langle x^2 \rangle^{\frac{1}{2}} = \sqrt{2Dt} \tag{7}$$

In addition, the diffusion happens as a consequence of thermal motion to equalise a space distribution of dispersed particles. If the motive force of diffusion F relates to work, which is done for moving of particle from a place of higher concentration to the place of lower concentration to equate chemical potentials, the relation for one particle would be expressed by following equation (8):

$$F = -\frac{1}{N_A} \cdot \left(\frac{\partial \mu_i}{\partial x}\right)_t \tag{8}$$

where μ_i is a chemical potential of dispersed part and N_A is Avogadro's constant. When intensity of diffusion flow relates to concentration multiplied by velocity of the movement, expressed by the motive force divided by friction coefficient f_i, it can be written that the

intensity of diffusion flow q relates inversely to friction coefficient, and is proportional to the gradient of concentration of highly diluted solutions:

$$q = -\frac{k_B \cdot T}{f_i} \cdot \left(\frac{\partial c_i}{\partial x}\right)_t \text{ for } (c \to 0) \tag{9}$$

It is obvious, according to equation (4) and (8), that the diffusion coefficient is proportional to the temperature and inversely proportional to friction coefficient as is shown in *Einstein equation* [9]:

$$D_i = \frac{k_B \cdot T}{f_i} = \frac{R \cdot T}{N_A \cdot f_i} \tag{10}$$

Then, one can express the friction coefficient for a spherical particle from the well-known *Stokes equation* to determine the *Einstein-Stokes equation*:

$$D_i = \frac{k_B \cdot T}{6 \cdot \pi \cdot \eta_0 \cdot R_H} \tag{11}$$

where η_0 is a viscosity of solvent and R_H is a hydrodynamic radius of diffused particle. According to the equation (11), the velocity of the translational diffusion is inversely proportional to the size of particle, as was mentioned in the equation (1) [8].

2.2 Behaviour of macromolecules in solutions

Every polymer molecule is composed of atoms and chemical groups, which all refer to its chemical structure and namely *configuration* of the polymer chain. Then, the polymer molecule exhibits an arrangement in space of solution, in other words a three-dimensional shape of the molecule called *conformation*, whereby the dynamics of molecule is derived. However, polymer chain can occupy many different conformations in dependence on the environment and origin of polymer molecule structure because the form of polymer molecule does not depend only on interactions of polymer segments with molecules of solvent, but also on interactions of polymer segments with each other. Consequently, the behaviour of polymer molecules in solutions depends on many facts as the polymer structure composition and polymer length even molecular weight, the concentration of polymer, the kind of solvent and its polarity or the temperature [12].

2.2.1 Effect of solvent

Let's assume the dissolving of polymer in solvent and consider all the thermodynamic effects. The Gibbs energy of polymer dissolving in solvent ΔG_{diss} is composed of the enthalpy of dissolving ΔH_{diss} as a first part, and the entropy of dissolving ΔS_{diss} multiplied by temperature as a second part:

$$\Delta G_{diss} = \Delta H_{diss} - T \cdot \Delta S_{diss} \tag{12}$$

By the accomplishment of relations for these thermodynamics parameters which were derived by statistical thermodynamics, one can get the *Flory-Huggins equation*, whereas n is the molar amount and φ is a volume fraction of individual compositions as solvent and polymer, respectively:

$$\Delta G_{diss} = R \cdot T \cdot \left(n_1 \ln \varphi_1 + n_2 \ln \varphi_2 + \chi n_1 \varphi_2\right) \tag{13}$$

Moreover, the two first terms in brackets $n_1\ln\varphi_1$ and $n_2\ln\varphi_2$ are negative. The third one has generally a positive value, and relates with the enthalpy contribution. Thus, it is evident that the change of Gibbs energy of both, dissolving and mixing of the polymer and solvent, depends on the value of the non-dimensional Flory-Huggins interaction parameter χ. The parameter expresses interactions of two different compounds and a thermodynamic eligibility of solvent for dissolving of certain polymer. Therefore, the fact that the solvent is good or poor for given polymer system depends on the value of this parameter, in other words on an influence of a change of cohesion energy at the forming of the mixture polymer-solvent [11].

The behaviour of linear flexible polymer molecule in different solvents is shown in Figure 2, where the forms of polymer in good, poor and theta solvents are compared. As can be seen, the character of solvent possesses polymer chain forming different conformations. In good solvent, polymer chains are swelled caused by the interactions of polymer-solvent are thermodynamically favourable than interactions between segments of polymer chain. As a consequence, the polymer chain expands and the excluded volume increases. On the contrary, polymer acts as a random coil in the theta (θ) solvent, where the interactions polymer-solvent equal to the interactions polymer-polymer, and the value of excluded volume is zero. Finally, the shrinking of polymer conformation form occurs in poor solvent, and the whole polymer molecule can contract in globule caused by the preference of polymer-polymer interactions. Moreover, the solvent quality factor α is expressed by [12]:

$$\alpha = \sqrt{\frac{\langle R^2 \rangle}{\langle R^2 \rangle_\theta}} \tag{14}$$

where $\langle R^2 \rangle$ is a quadratic mean distance of ends of polymer chain in certain solvent and the term θ indicate the quadratic mean distance of ends in theta solvent. If value of α is greater than number 1, the excluded volume is positive, polymer swells and the solvent is good for that kind of polymer. If the value of α is smaller than 1, the solvent is poor, excluded volume has negative value and polymer shrinks. Moreover, a phase separation happens in extreme cases.

Good solvent   Theta solvent   Poor solvent
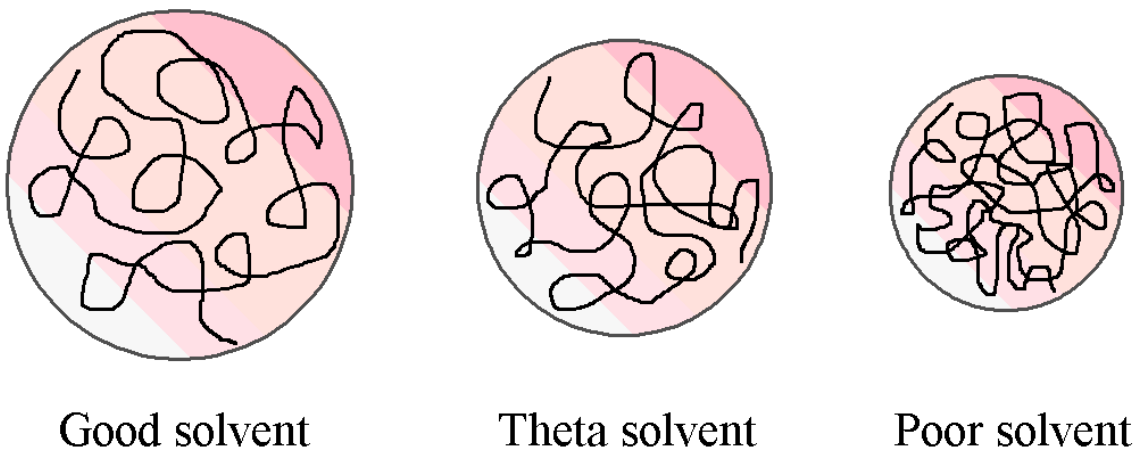
Figure 2: The comparison of effect of solvent on the volume of polymer molecule.

2.2.2 Polymer concentration regimes

In addition, solutions of polymers exhibit specific properties in dependence on the polymer concentration, which has especially influence on the polymer dynamics and viscosity as a consequence that the mobility and dimensions of polymer molecule have changed.
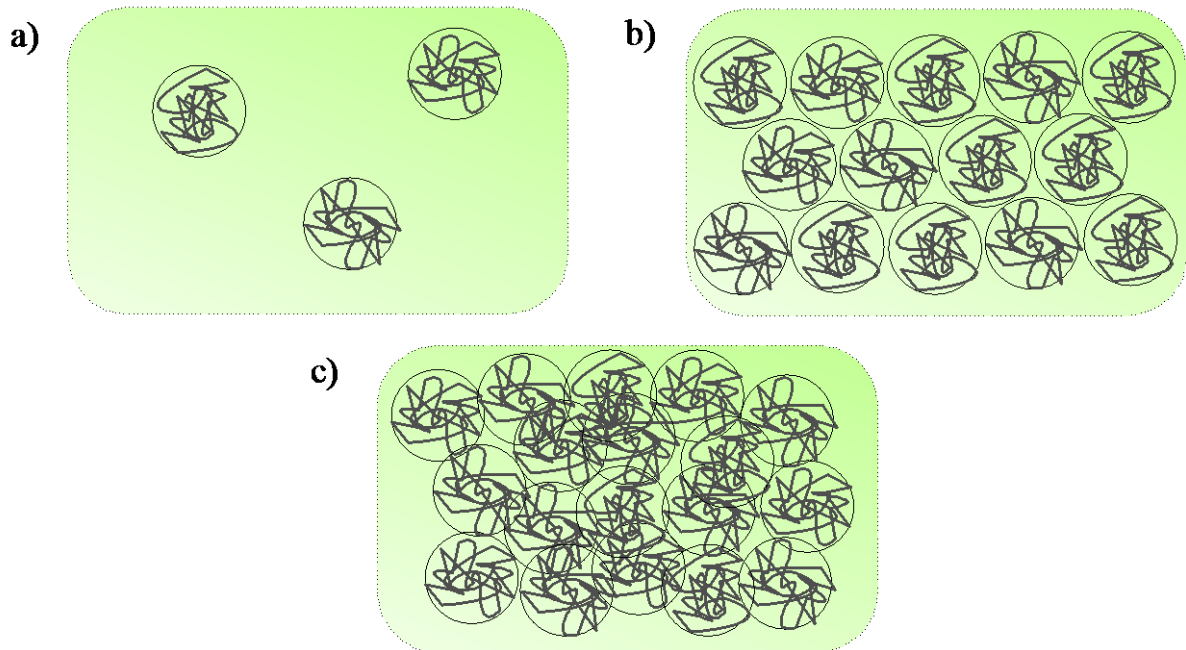
Figure 3: The picture of transitions between diluted (a), semi-diluted (b) and concentrated (c) solutions of polymer.

Diluted solutions of macromolecules are defined as concentration heterogeneous mixtures because macromolecular coils are separated from each other by bulk of solvent, as is shown in Figure 3. Polymer molecules do not interact with each other, move independently [13] and their shape is given by the suitability of the solvent. If the concentration of polymer is increasing, the polymer coils start to overlap. After reaching of the *chain overlap concentration c**, the solution changes to the semi-diluted concentration regime. The polymer chains begin to interact with each other, and the polymer-polymer interactions are repulsive or positive in dependence on the use of good or poor solvent, respectively. For mixtures in theta solvent, the value of $c*$ is inversely proportional to a limiting viscosity number $[\eta]$, which relates with the contribution of polymer to the viscosity of solution [11]:

$$c* \sim \frac{1}{[\eta]_\theta} \tag{15}$$

Then, the polymer coils start to interpenetrate to each other with more increased concentration, and the solution cross over from the semi-diluted to the concentrated regime after passing the *critical entanglement concentration c***. Figure 3 shows three pictures of polymer solution transitions from the diluted to the semi-diluted and the concentrated mode, where polymer coils are considered as spheres for better visualisation. However, the real coils do not have defined surfaces. Since that, the transitions between concentration modes are not

significant when the concentration of polymer changes slightly, but are extended in larger concentration ranges. Consequently, the solution becomes a polymer melt without any solvent with further increasing of concentration of polymer [13]. A net of polymer entanglements is formed, and the shape of polymer molecules is similar as in theta solvent because the interactions between segments are only present there, and the molecule do not shrink or swell [12]. In addition, the representation of polymer solution transitions is shown in Table 1 with appropriate range of polymer concentration in solvent, where c_P is a mass concentration of polymer in solution, ρ_P is a bulk density of polymer solution and φ_2 is the volume fraction of the polymer [11].

Table 1: The description of concentration regimes with values of polymer concentration

Concentration of polymer c_P equals to:	Concentration regime
$\left(0, c*\right)$	Diluted solution
$\left(c*, c**\right)$	Semi-diluted solution
$\left(c**, \rho_P\varphi_2\right\rangle$	Concentrated solution
ρ_P	Polymer melt

2.2.3 Polyelectrolytes

As was referred, the polymer structure composition can also affect the general behaviour of polymer in solution such as hydrogen bonds, presence of functional and polar or non-polar groups. Mainly in case of soluble polymers, the presence of any group creating a charge can greatly change polymer conformation. These kinds of groups are able to partly or completely dissociate [14], and thereby form polycations or polyanions with surrounding counter ions in solution.

Bonds between counter ions and charged groups of polymer can differ, and two types of these bonds are commonly distinguished. At first, the localised bond forms ion pairs between charged groups of polymer and oppositely charged ions as a consequence of electrostatic attractive forces. Moreover, this type of bond usually appears at higher concentration of ions, and a tendency of its forming is increasing with larger valences of ions, with decreasing radius of ions and with decreasing permittivity of the solvent. At second, the non-localised bond is also formed, whereas it is based on non-specific interactions between ions and charge of polymer dissociated groups.

However, molecule of flexible polyelectrolyte behaves differently in solution with or without presence of ions because small molecules of ions affect electrostatic interactions and increase the ionic strength. The differences are most significant at high dilutions. Polyelectrolyte is dissociated and its counter ions move to the space in case of the diluted solution without presence of ions. As a consequence, the identical charged chains are repelling, so the whole coil expands and forms a stretched form. On the contrary, the polyelectrolyte stretched effect disappears with increasing concentration of ions. In case of semi-diluted solutions without ions, the density of charge and concentration of counter ions are higher than in diluted solutions. So the polymer molecule starts to shrink and compress with increasing concentration forming extended polymer coil [14].

2.2.4 Diffusion of macromolecules

The diffusion phenomenon is not only related to move against the concentration gradient, but occurs also in equilibrated solutions such as polymer systems. It is known as a *self-diffusion* process, which describes site-exchanges of molecules through the solution in the same phase [13]. However, different kinds of movements occur in polymer solutions. As first, the micro-Brownian movements take place, which concern a moving of polymer segments and continuous changes of conformation. They are generally faster than second, macro-Brownian movements, which are responsible for translational movement of the whole polymer molecule or particle in polymer solution. Since that, the molecular dynamic of polymers in solutions is more difficult because not only the movement of whole molecule, but also micro-conformation movements and motions of chain segments participate in the diffusion process. Thus, diffusion of macromolecules cannot be easily described by elementary theories mentioned in section 2.1 [11]. Hence, new improved theories and models of diffusion processes in polymer solutions were suggested based on experimental results.

It was already approved that properties of polymer solutions, mainly diffusion characteristics, vary with increasing concentration of polymer, and apparent shift in the mode of diffusion appears when the solution cross over from one concentration regime to the other one [15]. Thus, the self-diffusion coefficient of probe is a function of concentration of polymer. The proportionality of diffusion coefficient on concentration of polymer alias the power law dependence has already been conceived as is shown in equation (16), where a is a scaling factor and b is an exponential factor. Unfortunately, the law is not valid for objects with different molecular weights [15]:

$$D = ac^b \tag{16}$$

Thus, the dependence on molecular weight has to be considered. Diffusion coefficient dependence on the molar mass M of polymer is expressed by equation (17) below [11]:

$$D = \sqrt[3]{\frac{2}{9\pi^2}} \cdot k_{\mathrm{B}} \cdot \sqrt[3]{\mathrm{N_A}} \cdot \left(\frac{T \cdot \sqrt[3]{\rho}}{\eta_0} \right) \cdot \sqrt[3]{M} \tag{17}$$

where ρ expresses a density of polymer solution. Equation (17) is valid only for spheres with defined surface, but polymer coils possess hydrated surface and their shapes are not ideal. So the following general expression more suits for the description of polymer diffusion, even though the relation is unfortunately not generally useful for wide range of molecular weights:

$$D = \mathrm{K} \cdot M^R \tag{18}$$

where K is a constant and an exponential term R differentiates for various molecular forms and interactions in solutions [16]. According to Rouse model, which considers polymer chains as beads and springs, the diffusion coefficient is proportional to molecular weight and concentration of polymer in diluted and semi-diluted solutions as is expressed below [17]:

$$D \sim M^{-1} \cdot c^{-\frac{1-\upsilon}{3\upsilon-1}} \tag{19}$$

where the term υ is Flory exponent, which depends on the excluded volume and the suitability of solvent. The following proportionality is valid for concentrated solutions, where entanglements are formed and reptation model is enforced [17]:

$$D \sim M^{-2} \cdot c^{\frac{2-\upsilon}{1-3\upsilon}} \tag{20}$$

The dependence of diffusion coefficient on concentration and molar mass of certain probe vary for different concentration regimes of polymer solution, as the proportional factors are obvious from equation (19) and (20). However, *Phillies et al.* [18] introduced an equation, which can sufficiently express the dependence of diffusion coefficient on concentration in wide range of molecular weights and in all concentration regimes [13, 15]:

$$D = D_0 \cdot \exp\left(-a \cdot c^b\right) \tag{21}$$

where D_0 is the diffusion coefficient in pure solvent and *a* and *b* are factors, which contain the contribution of molecular size, molecular weight, hydrodynamic interactions, etc. [13, 16, 18, 19]. Thus, the *Phillies equation* is valid either for low molecular weight diffusive compounds or also for diffusion of macromolecules [16].

2.3 Hyaluronic acid

Hyaluronic acid is a linear, unbranched polysaccharide, which belongs in group of glycosaminoglycans. The structure is composed of repeating monomer units formed of β-(1→4)-D-glucuronic acid β-(1→3)-N-acetyl-D-glucosamine disaccharide, whereas this main disaccharide unit of hyaluronic acid is shown in Figure 4. Because of the presence of carboxylate groups, hyaluronic acid dissociates in aqueous solutions forming hyaluronan as a negatively charged polyanion. Hyaluronic acid is fully dissociated at pH higher than 6 [2], and the effect causes dissolving of hyaluronic acid in water, while in non-dissociated form it is insoluble [20].
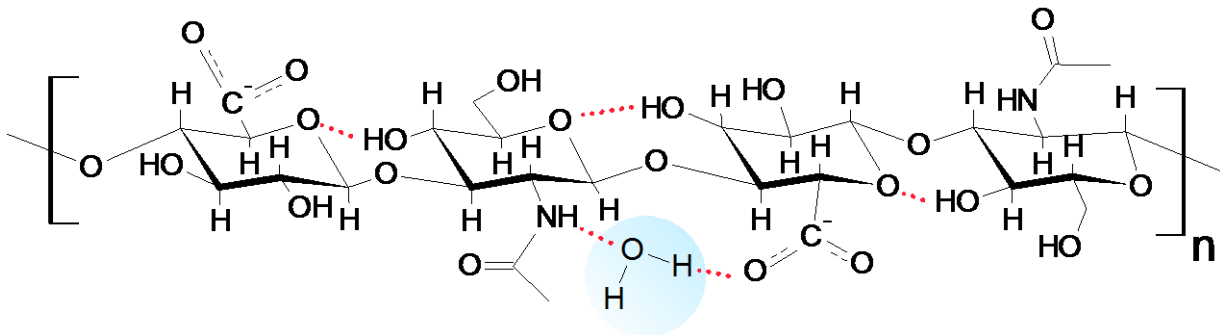
Figure 4: Structure of hyaluronic acid in dissociated form in aqueous solution, where hydrogen bonds are marked by red dotted lines [20].

Moreover, glycosidic bonds are stabilized by intramolecular hydrogen bonds, and all disaccharide units are twisted throw 180 degrees to each other. This organization brings a called two-fold helix structure in solutions, where water molecules act as a main stabilization agent by formation of intermolecular hydrogen bonds [20]. In steric point of view, hydrogens of sugar rings possess axial positions, while hydroxyl and other voluminous groups are in more favourable equatorial positions, so the structure is energetically very stable [21]. In addition, the axial hydrogens form hydrophobic patch, which causes amphiphilic behaviour of hyaluronan molecule and its ribbon-like structure in solution [20].

Nevertheless, sodium salt of hyaluronic acid occurs in all vertebrate bodies as one of main structural component in tissues because it contributes to formation of extracellular matrix, and creates environment for cell adhesion, migration and division [22]. Moreover, this unique compound has many essential physiological functions as lubrication, hydration and regulations of many processes in tissues as for example transport of fluids or diffusion of macromolecules in living organism.

Let's note some places and concentrations of hyaluronan occurring in human body. For example, 200 mg·L^{-1} of hyaluronan occurs in skin tissue, about 140-340 mg·L^{-1} in vitreous humour, 4.1 mg·L^{-1} in an umbilical cord and 1.4–3.6 mg·L^{-1} in synovial fluid [23]. However, properties and functions of hyaluronan depend on its molecular weight, which can vary from tens to thousands of kDa units. According to the molecular weight and functionality, two significant types of hyaluronan are distinguished. The low molecular weight hyaluronan (LMW HA) is known as a biomolecule, which main property is a supporting of inflammation processes, and acts as an anti-cancer tumour agent. The second one is high molecular weight hyaluronan (HMW HA), which restricts inflammations and stimulates formation of tumour metastasis [24]. The potential usage of hyaluronan is evident and nowadays, many research projects are in progress of studying hyaluronan utilisation as a humectant or a lubricant, as a drug delivery system or as a scaffold for cell treatment and producing in regenerative medicine.

2.3.1 Contemporary research of hyaluronic acid behaviour in aqueous solution

As was already reported, the observation of hyaluronan behaviour in aqueous solutions was aim of many research works. This section highlights the general knowledge about this topic. It was mentioned above that water molecules stabilize the two-fold helix structure of hyaluronan in solution by hydrogen bonds. So the molecule of hyaluronan possesses a large space volume in diluted regime, when the coil is expanded and polymer-solvent interactions are favourable.

According to *Almond* and *Sheehan* [3], hyaluronic acid molecules form coil-like structures above molecular weight of 10 kDa at pH 2, when the acidic groups are not dissociated. *Gribbon* by cooperation with *Heng* and *Hardingham* [4], studied the presence of intermolecular hydrogen bonding and electrostatic interactions of hyaluronan aqueous solutions as well as self-diffusion and tracer diffusion coefficients of hyaluronan (500 and 830 kDa) aqueous solutions by confocal fluorescence after photo-bleaching (FRAP) measurements. It was determined that the system is composed of domains of coils and is generally inhomogeneous, which brings different diffusion velocities between low and high molecular weight tracers, whereas low molecular weight tracers can freely diffuse through the space, while bulky and high molecular weight tracers diffuse much slower [21]. Moreover, polymer chains usually create aggregates because of hydrophobic interactions between non-polar parts of chains. Subsequently, domains start to overlap with increasing concentration of polymer, and form dynamic nets with meshwork and entanglements [2, 25, 26]. This leads to formation of superstructures, which can be associated by hydrophobic intermolecular interactions between polymer chains [27].

Then, *Almond* and *Harbinger* [5] declared by x-ray diffraction and NMR measurements that hyaluronic acid chain in solution can be comparable to a stiffened random coil.

Moreover, they used confocal-FRAP analysis to study self-diffusion of labelled hyaluronan (830 kDa) in dependence of pH and presence of salts and established a value for c^*, the concentration when chain-chain interactions appear. Furthermore, computational methods were also used for determination of hyaluronan dynamics [26, 28].

Great overview about experimental methods using for determination of hydrodynamic behaviour of hyaluronan in solutions and its physical dependencies can be found in work of *Cowman* and *Matsuoka* [29]. One of the approaches is also studying of hydrodynamic characteristics by rheological measurements, whereas wide studies of viscosity behaviour were performed. For reference, one can note the work of *Bilerová* [30], who focused on observation of deeper knowledge about samples of hyaluronan, which differed by concentration and molecular weight too. Finally, *Hejná* [24] studied the size of hyaluronan particles and ways of their preparation using DLS. It was determined that particles possess smaller sizes in physiological solutions at present of salt than in aqueous solutions.

2.3.2 Labelled hyaluronic acid

The idea of fluorescence labelling of hyaluronan macromolecular chains has already been accomplished. At first, *Gribbon et al.* [4] used Fluorescein amine labelled hyaluronan. At second, *Almond* and *Harbinger* [5] used Fluorescein isothiocyanate labelled hyaluronan for FRAP analysis to determine hydrodynamic properties of hyaluronan in aqueous solution, as was mentioned in section 2.3.1. *Fudala et al.* [31] successfully prepared hyaluronan labelled by Fluorescein amine even Rhodamine B amine, and these two fluorescently labelled hyaluronan samples were used for fluorescence resonance energy transfer (FRET) analysis for determination of kinetics of degradation process by enzyme hyaluronidase. Then, *Rich et al.* implemented one of this approaches, while they prepared hyaluronan molecules labelled by Fluorescein amine and used it in study of hyaluronidase activity by FCS and fluorescence life-time correlation spectroscopy (FLCS) [32, 33]. In addition, *Halasová* [34] used fluorescently labelled hyaluronan for study of its diffusion characteristics in aqueous solution at different concentration of surfactants by FCS.
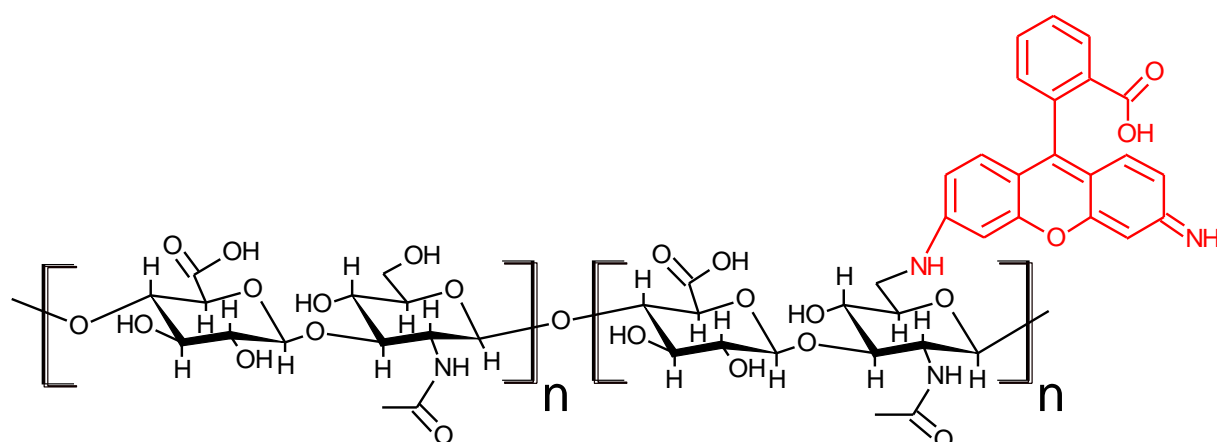

Figure 5: Structure of hyaluronic acid labelled by Rhodamine 110 (Hya-Rh).

Nowadays, fluorescently labelled hyaluronic acid is commercially available in two forms – with Rhodamine 110 or Fluorescein as synthesized, covalently bounded fluorescent parts, whereas Rhodamine 110 is bounded by imino group to the fifth carbon of sugar circle in N-acetyl-D-glucosamine unit, as is shown in Figure 5. According to the location of bonding and presumption mentioned by *Meunier* and *Wilkinson* [35], it was considered that the fluorescent label does not affect significantly the conformation and hydrodynamic behaviour of hyaluronan polymer chain.

2.3.2.1 Rhodamine 110

Rhodamine 110 belongs to organic fluorescent probes family. It has a wide conjugative bonded system with π electrons, and then it contains amino, imino and carboxylic group. This green-fluorescent dye is usually commercially offered as a chloride derivative, which is slightly soluble in water and is used as a fluorophore standard. The absorption has maximum at 496 nm and the emission maximum at 520 nm of wavelength. The excitation even the emission spectrum in water are both shown in Figure 6 [36].
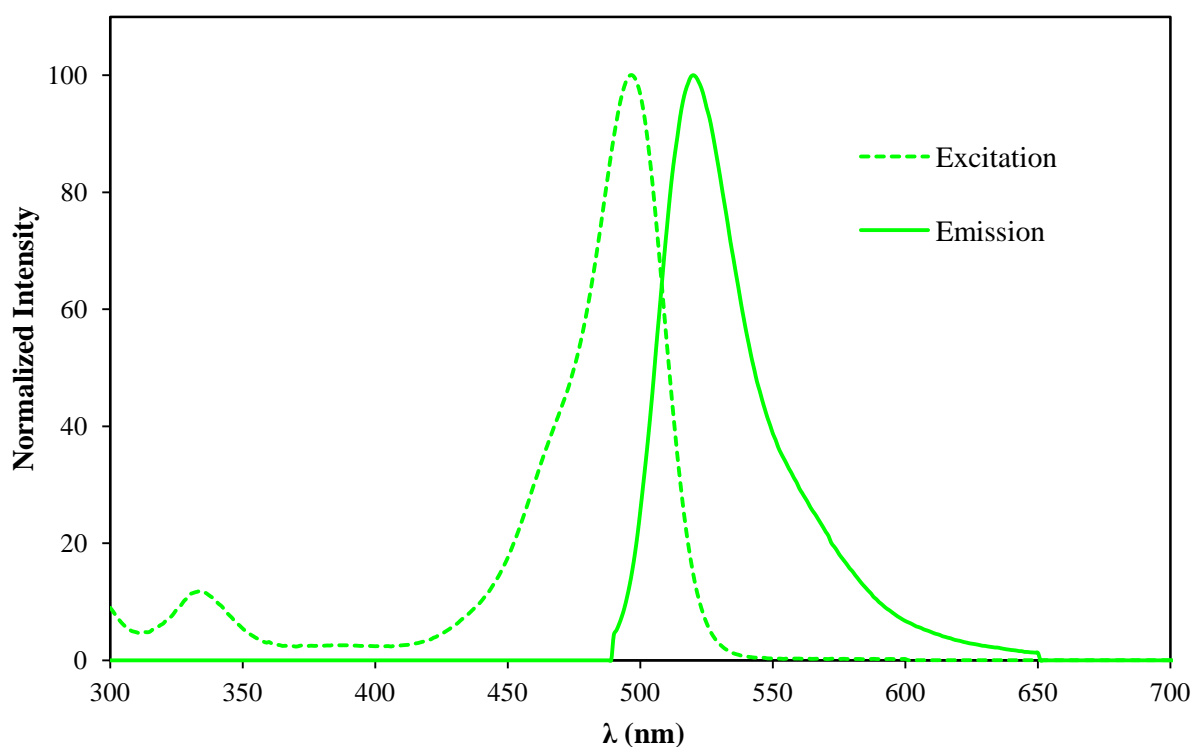
Figure 6: Excitation and emission spectra of Rhodamine 110 in water.

2.4 Single molecule detection and fluorescence correlation spectroscopy

Before a decade of years, *Elson*, *Magde* and *Webb* [6] investigated a special technique, which had a good potential to enable and facilitate studying of single molecules in liquor media. The technique is called fluorescence correlation spectroscopy (FCS) and originates from fluorescence fluctuation spectroscopy. Hence, FCS is based on evaluating of temporal

fluctuations of fluorescence intensity from molecules present in a small, specific detection volume. The monitored molecules come through the detection volume; however, the fluctuations are a response to blinking of the emitting fluorescence light. In other words, the fluctuations are caused by emitting fluorescence photons corresponding to the crossing of electrons from single excited state into the ground state, and dark non-emitting effects, such as an inner conversion, intersystem crossing into triplet state or simply molecule's leaving of the detection volume caused by translational diffusion. The entire process of electronics mechanism is well known from Jabłoński diagram (see Appendix 1). Subsequently, an idea about the single molecule detection has become feasible since the discovery of high resolution detection photon counting systems and laser excitation in confocal optics [37].

2.4.1 Principles of fluorescence correlation spectroscopy

According to the mentioned facts, fluorescence correlation spectroscopy enables to study translational diffusion and other effects depending on different time scales [38], as is demonstrated in Figure 7 [7]. However, the concentration of the sample has to be in nanomolar to picomolar range because it is possible to detect the incomings and outcomings of fluorescent molecules through the detection volume only at this small concentration, and fluorescence fluctuations correspond to the diffusive motion is observed as is explained below.

The fluctuation of concentration is together with the osmotic pressure one of the thermodynamic after-effects of random Brownian motion. In a defined, very small volume with a few dispersed particles, it is possible to note local changes of concentration in time as a consequence of diffusion movement, and the changes are called fluctuations. Equation (22) expresses the mean square concentration fluctuation, whereas δc represents the deviation of the mean concentration, which is equal to the mean, time-dependent change between immediate concentration c and its mean value in time $\langle c \rangle$:

$$\left\langle (\delta c)^2 \right\rangle = \left\langle \left(c - \langle c \rangle \right)^2 \right\rangle \tag{22}$$

According to Boltzmann statistical distribution of one particle in fluid medium, the probability of fluctuation is given by the probability density function:

$$P(\delta c) = \mathrm{K} \cdot \exp\left(-\frac{\delta G}{k_B \cdot T} \right)^2 \tag{23}$$

where δG means the deviation of Gibbs energy as a response of the difference of chemical potentials during the fluctuation process. After derivations, the relation between the mean square of concentration fluctuation is given by equation (24), and indicates that it is inversely proportional to square root of number of dispersed particles N [9]:

$$\frac{\sqrt{\left\langle (\delta c)^2 \right\rangle}}{c} = \sqrt{\frac{1}{N}} \tag{24}$$

Then, it is obvious that with increasing number of molecules and increasing detection volume, the fluctuation process is less observable. To simplify this statement, one can assume it for instance in the situation of looking for your wife or husband in very crowded area compared with looking for her or him at home in a living room. It would be much easier to

find her or him at home in one room, where you can specify exactly the occurring place, than in a shopping centre with many other people where the specification of the place is impossible [7]. Thus, the fluorescent signal of only a few molecules can be detected in the small detection volume generated by laser beam. Hence, one can measure diffusion, concentration, interactions or reactions between molecules and particles, which are either fluorescently labelled or fluorescent in their origin [37].
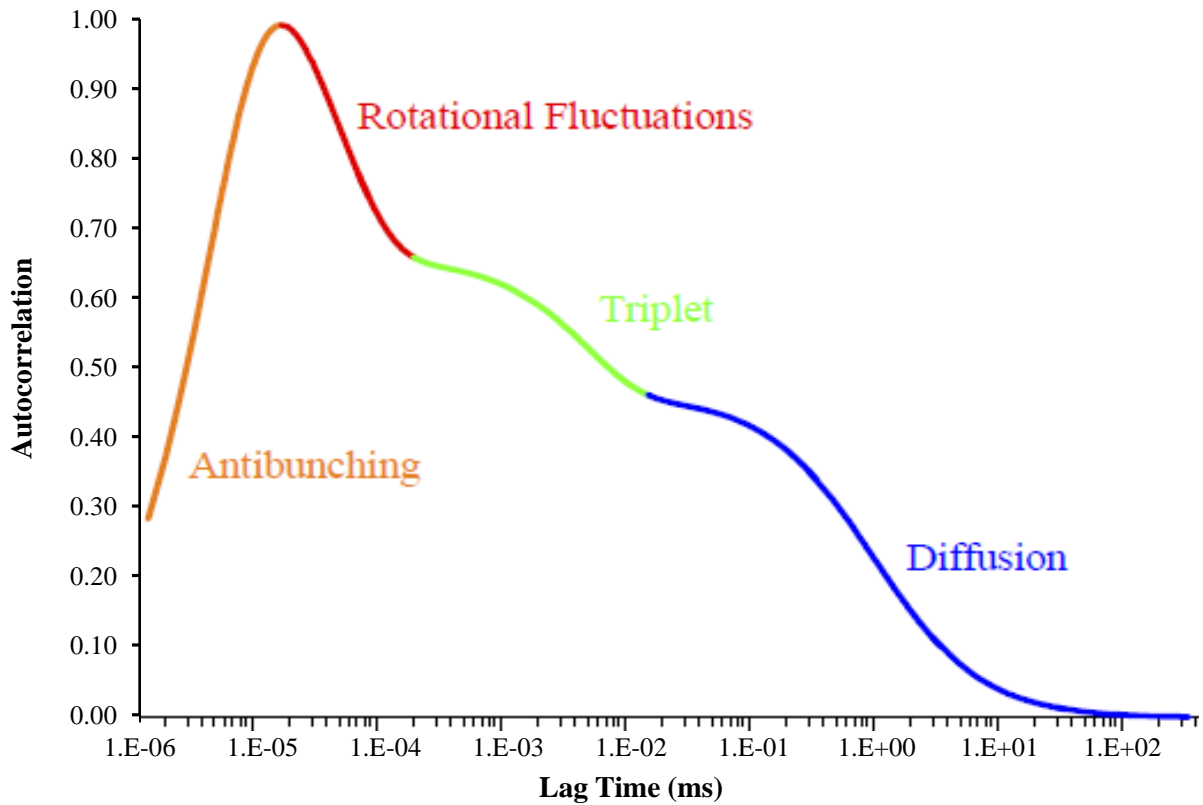

Figure 7: The demonstration of effects detected by FCS [7].

Moreover, the determination of the translational diffusion is based on detection of numbers of photons generated by fluorescent molecule, and this signal is evaluated by a second-order correlation function:

$$G_{ACF}(\tau) = \langle I(t) \cdot I(t+\tau) \rangle \tag{25}$$

where $G_{ACF}(\tau)$ expresses the autocorrelation function (ACF) and I means the intensity of fluorescence in a given time, whereas the term corresponds to the average of all values in time as is marked by triangular brackets. Hence, the autocorrelation function indicates the probability of detecting of photons in time $t+\tau$, if there was a detection of photon at time t. As the molecule moves through the detection volume, this function denotes the velocity of the movement and the concentration of particles in detection volume as a time dependent components of $G_{ACF}(\tau)$. Thus, at the beginning a large probability is there that the photons are emitted by similar particle, but the probability is decreasing with increasing time because the particle moves by Brownian motion and leaves the detection volume [38].

19
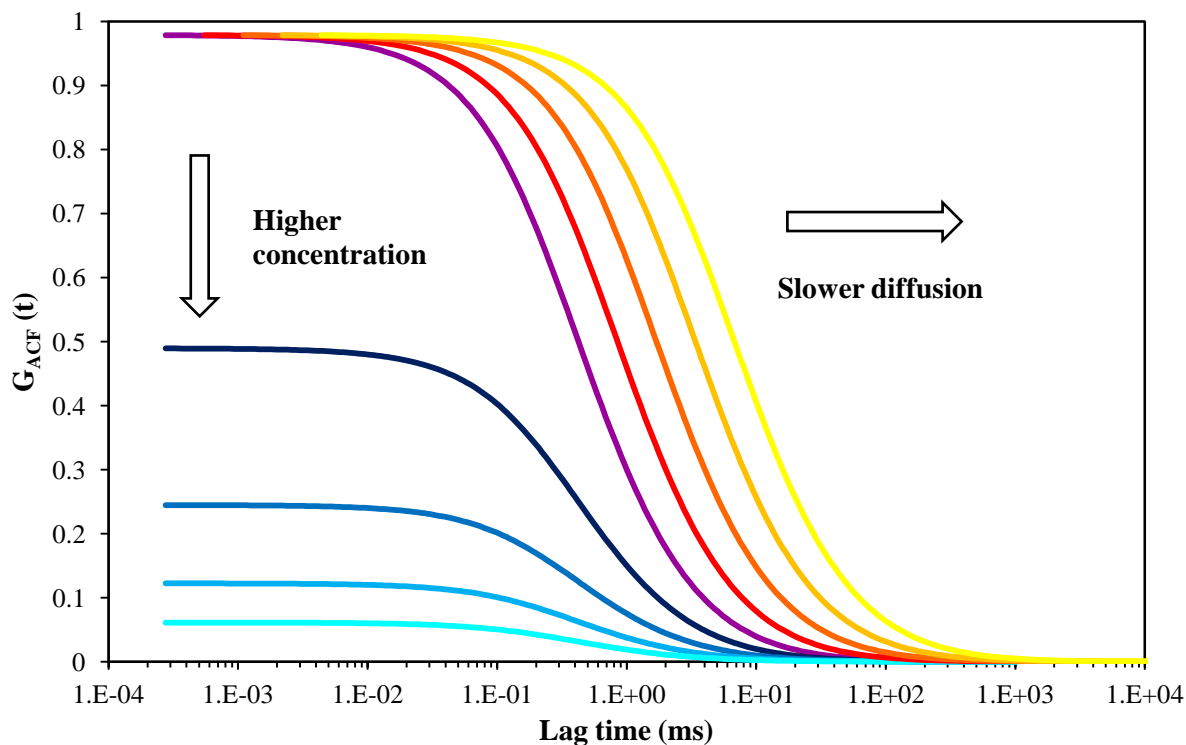
Figure 8: The description of trends of correlation curves with decreasing diffusion velocity and increasing concentration of observed compound.

Consequently, the value of $G_{ACF}(\tau)$ in initial time is decreasing with increasing concentration because of the inversed dependence of fluctuations on the number of molecules as is described in equation (24) leading to sensitivity limitation of FCS. On the other side, the slower the diffusion of fluorescent molecule the larger shift to the higher lag times can be expected. Hence, the diffusion coefficient has smaller value with increasing size of particle according to the *Einstein-Stokes equation* (11), and the entire translational diffusion process is slower. The description of behaviour of autocorrelation curve is shown in Figure 8.

2.4.2 Contemporary research overview about using of FCS

With FCS it is feasible to observe information about translational diffusion of detecting molecules in solutions and within a membrane, or to check transport of studied system. All of these phenomena and their corresponding shapes of autocorrelation functions are shown in Figure 9 [7]. Since that, increased usage of this technique in biophysics, biochemistry, biotechnology and drug delivery system studies is observable [39].

As an example, FCS finds applications in study of concentration and aggregation processes, diffusion and mobility of tracer analysis, molecular interactions, active transport phenomena, conformational changes of proteins and biopolymers, enzyme kinetics, structural formation and organisation, binding interactions between proteins and nucleic acids or binding to membrane receptors. All of these mentioned applications can be used to study of living cell, embryos and also artificial membranes. The work of *Macháň* and *Wohland* [40]

brings review of all these utilisations, whereas they have focused on summarization of utilisation of FCS in bioscience research for last five years.
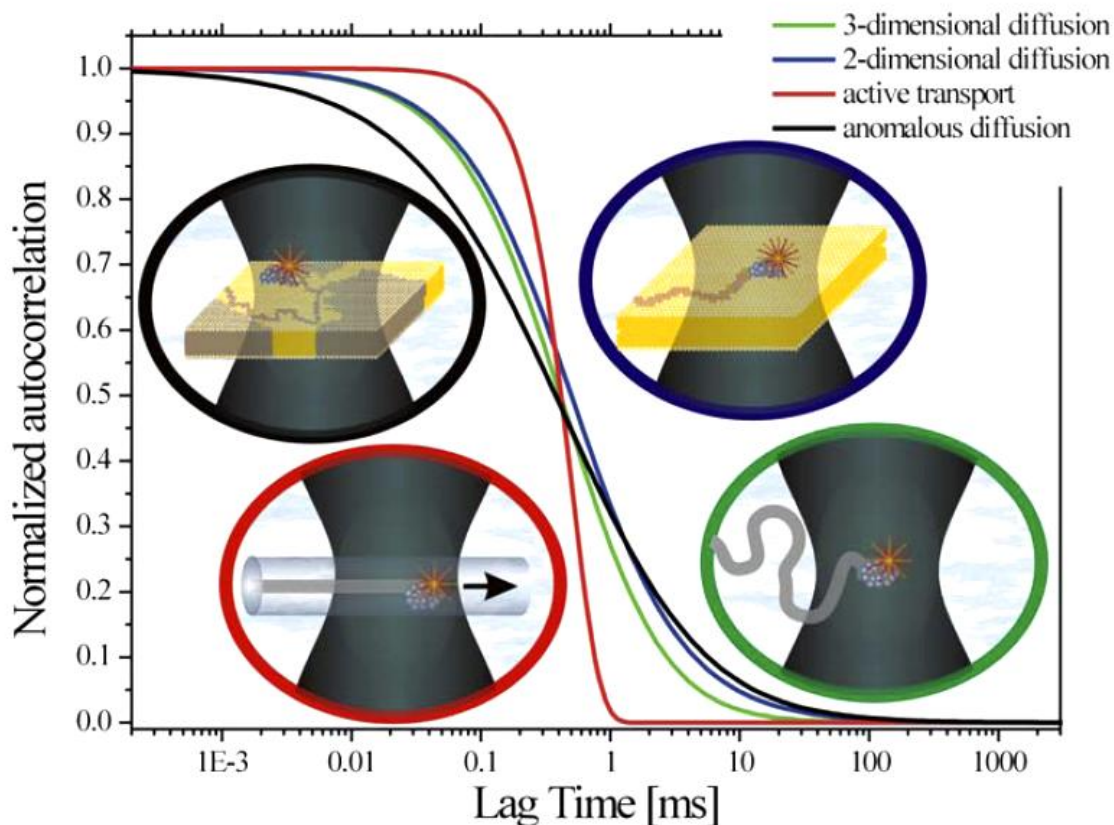
Figure 9: The schema of use of fluorescence correlation spectroscopy and appropriate autocorrelation functions of measurements [7].

Moreover, *Koynov* and *Butt* [41] highlighted the study of colloid systems and fluid interfaces by FCS in their work. They suggested the FCS as a method for measuring of hydrodynamic characteristics of colloid particles and macromolecules to determine their association and behaviour in solutions. In addition, they mentioned and discussed use of FCS in study of micellization processes and size of micelles of surfactants as well as of block copolymers by using of fluorescent probes. Then, it is necessary to note again works of *Halasová* [34] and *Rich et al.* [32], both have already been mentioned in section 2.3.2, which are about the research of hyaluronan using FCS method.

Also the utilization of FCS technique is widely increasing in polymer science, so some of FCS studies which are focused on investigations of polymer diluted to semi-diluted and concentrated transitions will be noted here.

H. Zettl et al. [42] described synthesis of polystyrene labelled by Rhodamine B which diffusion in toluene was studied by FCS as a function of molecular weight. Consequently, they found a scaling equation, which defined the dependence of diffusion coefficient on the molecular weight for the polystyrene-toluene system. The aim of work of *Liu et al.* [43] was

determination of diluted to semi-diluted concentration regime transition of polystyrene-toluene system, whereas dye-labelled polystyrene chains were used. Subsequently, they have fitted obtained data with the Phillies stretched exponential function mentioned in equation (21). On the contrary, the polystyrene-toluene system was also studied by *Grabowski* and *Mukhopadhyay* [44]. However, they specialized in study of polymer concentration ranges above the overlap concentration at different temperatures.

Cherdhirankorn et al. [45] measured by FCS diffusion coefficients of various low and high molecular weight tracers in dependence on broad concentration range of polystyrene in polystyrene-acetophenone mixture. Their measurement confirmed that hydrodynamic behaviour of polymeric probes depends on molecular weight of polymer matrix, and in special cases leads the trend described by Phillies.

U. Zettl et al. [46, 47] distinguished two diffusion coefficients, which can be obtained by FCS. At first, the self-diffusion coefficient corresponds to the thermal motion of probe molecule in polymer solution, and at second the cooperative diffusion coefficient can be obtained in semi-diluted concentration regimes due to long-range interactions between numbers of molecules in polymer nets. Then, they compared results of labelled polystyrene tracers in polystyrene-toluene solutions obtained by FCS and DLS, and determined that the cooperative diffusion coefficient is independent on molecular weight of polymer tracer.

Michelman-Ribeiro et al. [48] focused on study of diffusion characteristics of several tracers which differed by molecular weight and size through aqueous solution of poly(vinyl alcohol). The concentration of polymer varied from diluted to semi-diluted concentration regime, and it was found that the diffusion coefficient exponentially decreases with increasing polymer concentration for particles larger than formed polymer meshes, whereas authors explain this fact as a consequence of increasing viscosity. For particles with approximately similar size as polymer meshes, the diffusion coefficient dependence behaved according to Phillies model and the value of factor *b* was determined.

Furthermore, *Pristinski et al.* [49] studied hydrodynamic behaviour and translational diffusion of fluorescently labelled poly(methacrylic acid) as a weak polyelectrolyte in aqueous solutions in diluted regimes. They also contributed to determination of its hydrodynamic size at different values of pH and ionic strength. In addition, the dependence of diffusion coefficient of labelled polymer on concentration of unlabelled polymer molecules was obtained and signalized interchain domain formation.

Finally, work of *Papadakis et al.* [50] brought a great overview of this research from last few years, and summarised all aspects of FCS measurements in study of polymers. Moreover, authors discussed all perspectives, advantages and examples of using FCS in polymer research, especially influence of polymer concentration, pH, temperature even ionic strength, and obtained results were compared with other methods.

2.4.3 Deficiencies of the one focus fluorescence correlation spectroscopy

It was already investigated that many different conditions of the measurement and optical artefacts heavily influence FCS results [51]. The first one is a refractive index mismatch between sample solvent and immersion medium of the objective. The second is cover slide thickness, which could also highly distort obtained data, and the third is laser beam

astigmatism. In the end, the last disadvantage is the dependence on optical saturation. It was documented that with increasing excitation power the values of diffusion coefficient changes significantly [52].

2.5 Dual-focus fluorescence correlation spectroscopy

Because there are many deficiencies which are a big disadvantage of classical, one focus FCS, new robust method called 2f-FCS was investigated. On the contrast to the conventional FCS, it is independent on all the optical artefacts and one can measure diffusion without any reference sample [52, 53]. The difference to the one-focus FCS is based on the usage of transformed optical set-up and improved mathematical and statistical calculations of detected signals.
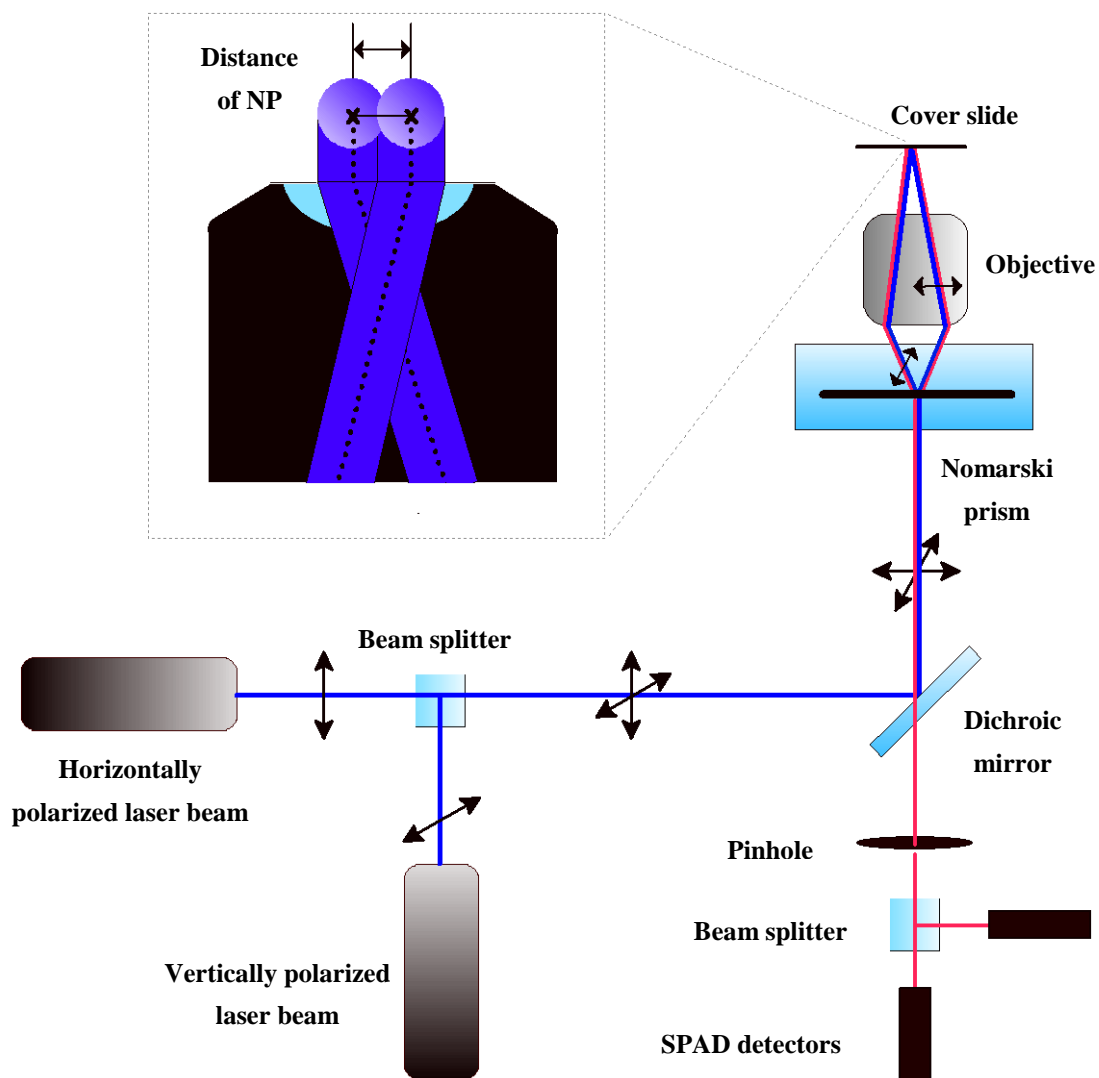
2.5.1 Measurement set-up

Figure 10: The optical set-up of 2f-FCS measurement.

The instrument for FCS is called fluorescence confocal microscope. The measurement set-up for 2f-FCS is composed of two identical, linearly polarized alternately pulsed laser diodes, which are synchronized by pulsed interleaved excitation mode (PIE). Both pulsed beams are combined by polarization beam splitter into one sequent pulsed beam with orthogonal polarization, which passes by dichroic mirror and leads to the objective, where goes through the Nomarski prism so called DIC prism according to its use in differential interference contrast microscopy. The prism divides beam into two directions and sets in two laterally shifted foci alias excitation volumes according to the different polarization orientation. Since here the name of the 2f-FCS technique generates.

Then, the emitting fluorescence in sample is collected by objective back to the dichroic mirror, where the signal is separated from excitation light. Further, the fluorescence light goes through $150\,\mu m$ sized pinhole and then to single photon avalanche diodes (SPAD) as detectors with single photon counting electronics unit which is able to record detected photons with picoseconds temporal resolution. It is notable, that the signal which goes to the detectors is similar; however, the difference between signals of each focus is that they are separated in time by PIE, so two time different fluorescence curves are obtained [54].

The picture of optical set-up of inverted epifluorescent microscope is shown in Figure 10. In addition, the manual describing how to adjust and prepare the instrument for measurement by 2f-FCS is attached in Appendix 2.

2.5.2 Principle of 2f-FCS

The whole idea is also based on evaluating of fluorescence intensity as in conventional FCS. The fluorescence fluctuations in time are detected and analysed by statistical ACF, which is calculated from different times of photons comings to the detector. Furthermore, the crosscorrelation function (CCF) between both foci is also calculated. This function correlates just photons from both foci and describes the probability of detecting photon at the time $t + \tau$ in the second focus, if there was a photon signal at time t in the first focus, and vice versa [52]:

$$G_{CCF}(\tau) = \left\langle I_1(t) \cdot I_2(t+\tau) \right\rangle \tag{26}$$

where I_1 is the fluorescence intensity in the first focus and I_2 in the second focus. As can be seen in Figure 11, where ACF and CCF curves obtained by measurement of Atto488-COOH in water are demonstrated, it is obvious that the trend of CCF curve has almost two times smaller amplitude that ACF curve caused by different computational base of each function.

Then, the precise determination of detection volume is necessary for calculation of diffusion coefficient, whereas it is described by molecule detection function (MDF) $U(\mathbf{r})$. This function relates with probability of excitation and detection of an emitted photon from a molecule at given position $\mathbf{r}$ in one of detection volumes. Therefore, CCF is generated by following general expression [54]:

$$G_{CCF}(t,\delta) = \varepsilon_1 \varepsilon_2 c \int d\mathbf{r}_1 \int d\mathbf{r}_2 U(\mathbf{r}_2) \frac{1}{(4\pi Dt)^{\frac{3}{2}}} \exp\left(-\frac{(\mathbf{r}_2 - \mathbf{r}_1 - \hat{\mathbf{x}}\delta)^2}{4Dt}\right) U(\mathbf{r}_1) \tag{27}$$

where δ is the distance of Nomarski prism alias the value of shift between both foci, $\hat{\mathbf{x}}$ represents unit vector along x axis, and terms ε_1 and ε_2 are factors related with excitation

power and detection efficiency in each detection volume. For determination of each ACF, the similar equation is valid, but the value of δ is set to zero and terms ε_1 and ε_2 are replaced to $\varepsilon_1{}^2$ and $\varepsilon_2{}^2$.

Consequently, the calculations of autocorrelation curves of each focus and crosscorrelation curves between them are processed by highly advanced statistical computations based on two conditions. At first, the value of shift between both foci has to be known and at second, the two-parameter model fitting has to be performed. Finally, if the magnification of the objective, the excitation and emission wavelength, the parameter of Nomarski prism, the pinhole size and refractive index of immersion medium are known, the absolute value of diffusion coefficient can by calculated by mathematical computation of MATLAB script [55].
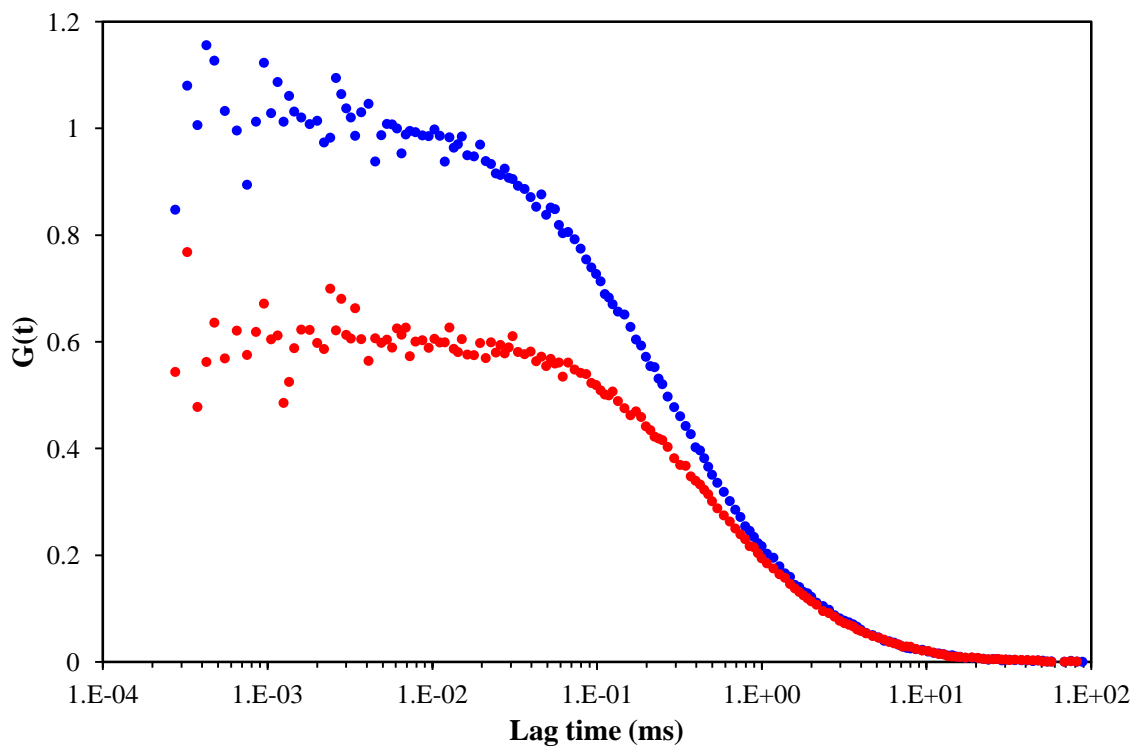
Figure 11: The comparison of trends of autocorrelation (blue dots) and crosscorrelation (red dots) curves of fluorescent probe Atto488-COOH in water.

2.5.3 Determination of the distance of Nomarski prism

For evaluation and determination of the absolute diffusion coefficient of measured system, it is necessary to precisely know the distance between both foci which is given by parameter of Nomarski prism. Furthermore, the distance of Nomarski prism is independent on refractive index mismatch, cover slide thickness and laser beam astigmatism. However, it is changing with excitation wavelength of used laser. Then, it is dependent on used objective with given magnification and of course on used DIC prism because every manufacture has different parameters [54].

There exist three pathways how to determine the parameter. Firstly, by using of fluorescently labelled beads with size range around 100 nm, secondly by using of probe with known diffusion coefficient, and thirdly by using z-scan of giant unilamelar vesicles (GUV) in lipid bilayers.

2.5.3.1 Using nanobeads

The first way how to determine the distance of foci is by using of fluorescently labelled nanobeads, approximately in the range of 100 nm with a known diffusion coefficient and hydrodynamic radius, for example measured by DLS experiments. The distance is then founded by comparing the results of calculated hydrodynamic radius obtained by 2f-FCS with measured values obtained by DLS [57]. The advantage of this pathway is the fact that these particles are fluorescently labelled in the whole spectrum of used lasers, typical excitation/emission wavelengths are 365/430 nm, 505/515 nm, 560/580 nm and 660/680 nm simultaneously, so it enables determination of the distance of Nomarski prism by using of one identical sample for all used excitation wavelengths.

2.5.3.2 Using fluorescence probe with defined diffusion coefficient

The second way is to choose a fluorescence probe, which is stable, accessible in laboratory and in particular with defined diffusion coefficient. The probe also has to have excitation spectrum in the range of used laser diodes. After performing the 2f-FCS measurement at known temperature, it is feasible to calculate the diffusion coefficient by MATLAB routine and determine the distance, which is corresponding to the defined value. This method is the most simple; however, one has to select the right probe for the excitation laser at given wavelength and perform the measurement every time, when the excitation conditions are changed.

2.5.3.3 Giant unilamelar vesicles (GUV) z-scan

The last way is using of fluorescently labelled GUV in lipid bilayers, whereas one can determine the diffusion time by measuring of fluorescence fluctuations in different positions of the *z* axis with respect to the focus plane. Then with known value of diffusion time, one can calculate parameters of detection volume and compare the value of calculated diffusion coefficient with value determined by 2f-FCS at given distance of Nomarski prism [55].

2.5.4 Use of dual-focus fluorescence correlation spectroscopy in research

2f-FCS is a relatively novel method which enables to measure translational diffusion coefficient of studied systems at nanomolar concentrations, and therefore enables to monitor hydrodynamic radius of detecting molecules related to the molecular size, binding parameters of ions or biomolecules, conformational changes, protein folding/unfolding, etc. All the measurements are performed only with some changes in measurement set-up of conventional FCS; however, these measurements have very high accuracy in contrast to the one focus FCS. In all fields where the conventional FCS is applicable, the potential utilization of 2f-FCS technique can be found.

In 2007, *Dertinger* and *Enderlein et al.* devised the 2f FCS technique. They mathematically described and implemented this method. Subsequently, they compared the data fitting model with recorded MDF, and results successfully coincided with the mathematical model. They also determined the absolute diffusion coefficient of red fluorescent dye Atto655-COOH and compared it with values measured by pfNMR, whereas both values corresponded [54]. Hence, 2f-FCS has a good potential for measuring of absolute diffusion coefficients and could become one of widely used technique in bioscience research. Obviously, the observed system has to be labelled by commercially available fluorescent dyes [52].

Then, the independent on photophysics and optical artefacts was proved by measuring of diffusion coefficients of two fluorescent dyes Atto655-COOH and cyanine Cy5-COOH upon different conditions e.g. excitation power. Further, *Dertinger* [55] performed several applications of this method. Measurements of translational diffusion of proteins and related complexes which enables quantifying the conformational changes of macromolecules were presented. For example, hydrodynamic radius of two calcium-binding proteins recoverin and calmodulin was observed in the dependence on free calcium concentration. Consequently, 2f-FCS measurements with extended fit for data evaluation were applied in study of planar diffusion within membranes, whereas the results of diffusion of lipids in phospholipid bilayers were in a good agreement with z-scan FCS measurements.

Müller et al. [56, 57] then published an extended model for data fitting for measurements of colloid particles and macromolecules. In addition, they discussed and impacted an analysis model for differently labelled fluorescent particles. It was found that for larger particles it is necessary to use a more improved and extended model of fitting calculations where is included the influence of labelling and the size of particle.

Then, *Müller* and *Richtering* [57, 58, 59] investigated diffusion measurements of temperature-sensitive microgel (poly-*n*-isopropylacrylamide) with fluorescently labelled monomers by Rhodamine B in aqueous media. Measurements of this system were performed in temperature sealed cell with accuracy of ±0.1 K. According the well-known *Einstein-Stokes equation* (11), the diffusion coefficient is dependent on temperature and viscosity of the media, which is in case of water strongly dependent on temperature too. Since that, it is necessary to control the temperature during the measurement very precisely and the utilization of the special cell enables to measure thermo responsive polymers or colloids.

Arbour et al. [60] applied 2f-FCS measurement to the study of the velocity profile in a microfluidic channel, and results were compared with the theory. *Loman et al.* [61] performed measurements of rotational diffusion of large biomolecules, such as human serum albumin, aldolase and ovalbumin by using of 2f-FCS measurement set-up.

Weiß et al. [62] studied theoretically and experimentally the application of 2f-FCS for the measurement of diffusion coefficients of lipids in highly stable free-standing black lipid membranes in the dependence on lipid ion valence and concentration in solvent buffer. In addition, they researched protein diffusion within black lipid membranes to determine a logarithmic dependence of diffusion coefficient on hydrodynamic radii for proteins. [63]

Maffre et al. [64] used dual-focus FCS in studying of adsorption of human blood serum proteins onto nanoparticles (with diameter of approximately 12 nm) composed from

fluorescently labelled polymer and coated by FePt with negatively charged groups on the surface. The growing of hydrodynamic radius with increasing proteins concentration was determined, and it was suggested that proteins form monolayer. This understanding of dynamic corona properties leads to safer use of nanoparticles in medical applications.

Wong et al. [65] studied assembling of fluorescently labelled polyelectrolyte by so-called layer-by-layer technique onto soft, porous and differently fluorescent labelled thermoresponsive nanogels. The studied system was made of Fluorescein isothiocyanate labelled poly(L-lysine) as polyelectrolyte and poly(N-isopropylacrylamide-co-acrylic acid-co-Rhodamine) as nanogel. Thus, they observed two fluorescence signals of both used dyes during the volume phase transition. Both of them had common values of diffusion coefficient indicating one single entity of polyelectrolyte and the nanogel template at different temperatures. This fact represents a possibility of using of any charged molecules on microgels, and provides their application in drug delivery and target systems.

Ries et al. [66] brought an idea about studying of binding between fluorescently labelled biomolecules by dual-colour as well as by dual-focus fluorescence correlation spectroscopy simultaneously. This combination enables better understanding and quantitative studies of binding on biological membranes without any difficult calibration of the overlap of detection volumes corresponding to conventional dual-colour FCS.

On the other side, *Korlann et al*. [67] described a new method called polarization-modulation dual-focus fluorescence correlation spectroscopy (pmFCS). This technique is based on 2f-FCS which measurement set-up contains two linearly pulsed polarized beams. However, for pmFCS the polarization of the excitation beam is modulated by a resonance-electro-optical modulator. So the optical set-up of confocal microscope needs easier implement than the established 2f-FCS. According the authors, this new technique also enables to measure absolute diffusion coefficients of fluorescent molecules with high robust against optical saturation effect. *Štefl et al*. [68] experimentally applied pmFCS and confirmed usage of this new approach in study of two model membrane systems and for different excitation wavelengths.

3 EXPERIMENTAL PART

The aim of the experimental part was at the beginning to find out and check, if fluorescently labelled hyaluronan is possibly available to measure by FCS technique, especially by 2f-FCS method. The sodium rhodaminylamino hyaluronate (Hya-Rh) was purchased from CPN Ltd. Dolní Dobrouč (Czech Republic) and used for the study. Determined structure by NMR spectroscopy attached by the manufacturer is shown in Figure 5. In addition, the degree of labelling was determined to 2 % by ^{1}H NMR spectroscopy. According to size exclusion chromatography measurements with multi-angle laser light scattering detection (SEC-MALLS), the molar mass of the sample was determined to 40 kDa, so it means that HyaRh molecules in aqueous solution possess the shape between rods and coils (see Appendix 3).

The calibration and also the procedure of effective preparation of samples for 2f-FCS measurements were devised and enhanced to successfully determine the diffusion coefficient of labelled polymer. Then, diffusion characteristics of labelled hyaluronan were measured and discussed as a function of influence of ionic strength even presence of different alkali metal ions. Furthermore, values of diffusion coefficient of labelled hyaluronan in solution of very low molecular weight hyaluronan (VLMW HA) with M_w of 404 kDa were studied in the dependence on concentration of the VLMW HA at different conditions such as in pure aqueous solution and physiological solution of 0.15 mol·L^{-1} NaCl. However, after every 2f-FCS measurement it was necessary to determine the parameter of Nomarski prism, which is very important component in 2f-FCS measurement set-up. For these measurements, Atto488-COOH and Oregon Green 488 were used. Finally, the analysis of measured data was performed, and the behaviour of hyaluronan in solution at different concentrations and conditions was studied.

3.1 Used chemicals

The list of used chemicals with corresponding chemical abstract service registry number (CAS) and number of batch (NB) is shown in Table 2.

Table 2: The list of used chemicals

Chemicals:	Manufacturer:	Specification:
Water Milli Q	Millipore academic	
Hya-Rh	CPN Ltd.	NB: 11122012
VLMW Hyaluronan sodium	Bioland Sochibios	NB: 1130607
Rhodamine 110 Chloride	Sigma-Aldrich Ltd.	CAS: 13558-31-1, NB: BCBJ9806V
LiCl	Lach-Ner Ltd.	CAS: 7447-41-8, NB: 307950505
NaCl	Lach-Ner Ltd.	CAS: 7647-14-5, NB: PP/2009/06278
NaCl	Merck KGaA	CAS: 7647-14-5, NB: K43305504217
KCl	Lach-Ner Ltd.	CAS: 7447-40-7, NB: 304120306
CsCl	Lach-Ner Ltd.	CAS: 7647-17-8, NB: 318931205
Oregon Green 488	Invitrogen Karlsruhe	NB: D6145
Atto488-COOH	Sigma-Aldrich Ltd.	NB: 1480709V

3.2 Used instruments

The measurements were performed at the University of Göttingen in Germany, in the Faculty of Physics, and at the University of Technology in Czech Republic, in the Faculty of Chemistry. The lists of used instruments at each workplace are shown below in Table 3 and Table 4.

Table 3: The list of used instruments at the University of Göttingen, Germany

Instrument:	Specification:
UV-VIS spectrophotometer	JASCO V-6500 Spectrophotometer
Size exclusion chromatograph	JASCO MD-20840PLUS SEC CHROMGRAM
Fluorescence spectrophotometer	JASCO FP 6500 spectrofluorometer
Time-resolved confocal microscope	Microtime 200 PicoQuant GmbH with water immersion objective Olympus, UPLSAPO 60XW

Table 4: The list of used instruments at the Brno University of Technology, Czech Republic

Instrument:	Specification:
UV-VIS spectrophotometer	HITACHI U3900
Fluorescence spectrophotometer	Fluorolog HORIBA Jobin Yvon
Time-resolved confocal microscope	Microtime 200 PicoQuant GmbH with water immersion objective Olympus, UPLSAPO 60XW

3.3 Preparation of samples for measurements

3.3.1 Preparation of stock solutions

3.3.1.1 Preparation of stock solutions of fluorescence probes

For preparation of stock solution of Atto488-COOH, Rhodamine 110 and Oregon Green 488, 0.001 g of each probe was dissolved in water and stored in a fridge at 4 °C. Before every 2f-FCS measurement, the stock solution was diluted to the final nanomolar concentration by water, and the temperature was adjusted to the laboratory temperature of 22 °C.

3.3.1.2 Preparation of stock solution of labelled hyaluronan

At the beginning, 0.001 g of fluorescently labelled hyaluronan Hya-Rh was dissolved in water and stirred for at least 24 hours. Then, the volume was adjusted to 50 ml, so the total concentration was 20 mg·L^{-1}. However, the sample was highly contaminated by free probe, which had to be separated. Then, certain amount of stock solution of fluorescently labelled hyaluronan was injected to SEC column, and the fraction of labelled polysaccharide without free probe was collected. Finally, this amount of few millilitres was stored in fridge at 4 °C for maximally 3 days because of the beginning of degradation processes.

3.3.1.3 *Preparation of stock solutions of salts*

For measurements of influence of ionic strength and presence of ions on the behaviour of fluorescently labelled hyaluronan, the exact amounts of LiCl, NaCl, KCl and CsCl were weighted, and then dissolved in water. After completed dissolving of salt in water, the volume of each stock solution was adjusted to exact concentration of certain stock solution.

3.3.1.4 *Preparation of stock solution of VLMW hyaluronan*

For the measurements in presence of VLMW HA, amount of 0.075 g of VLMW HA was dissolved in pure water and in 0.15 mol·L^{-1} solution of sodium chloride. The solution was stirred at least for next 24 hours, and then the volume was adjusted to 25 ml to get a stock solution with the total concentration of 3 g·L^{-1} of VLMW HA in aqueous and physiological solution.

3.3.2 Preparation of samples for 2f-FCS measurements

For every sample measured by 2f-FCS, certain amount of stock solution of labelled hyaluronan was piped to Eppendorf tubes. At the beginning, five different amounts of labelled hyaluronan, especially 1, 3, 5, 10 and 15 μL of storage solution of Hya-Rh, were diluted by water or physiological solution, and the final volume of each sample was 1 ml. This was done in reason to get a concentration range of Hya-Rh solutions, whereas all samples were prepared in three series.

Then, in dependence on concentration of labelled hyaluronan and FCS signal determined by previous checking measurements, certain amount of fresh stock solution of labelled hyaluronan was piped to Eppendorf tubes. The amount of labelled hyaluronan usually ranged between 5 to 10 μl of storage solution. For measurements of the influence of alkali metal ions, samples in concentration range from 0.000 1 mol·L^{-1} to 1 mol·L^{-1} of LiCl, NaCl, KCl and CsCl were prepared. Afterwards, samples with presence of unlabelled hyaluronan were prepared from 0.001 g·L^{-1} to 3 g·L^{-1} of VLMW HA in aqueous solution and in physiological solution too. All samples were prepared in three series of concentration range by dilution of stock solutions and the whole volume of every sample was 1 ml. It is important to note that the similar concentration of labelled hyaluronan was in each sample for certain kind of measurement. The samples were always prepared one day before 2f-FCS measurement and after preparation, stirred for 30 s. Then, they were left in a dark place at laboratory temperature until the next day.

3.4 Instrument and measurement set-up

3.4.1 Size exclusion chromatography separation

1 mL of prepared labelled hyaluronan aqueous solution was injected to SEC column (SUPERDEX^{TM} PEPTIDE 10/300 GL) with pore size for compounds in range from 0.1 kDa to 7 kDa. The measurement time was set to 120 min and the flow was 0.5 ml per min. As a mobile phase was used pure water. The UV-VIS absorption signal was detected in three series of detector channels at 230 nm, 280 nm and 500 nm of wavelength. Eluted labelled hyaluronan without probe contamination was collected into vials of volume 1 ml and

afterwards, the whole amount of collected labelled hyaluronan was mixed together to obtain the storage solution of Hya-Rh.

3.4.2 Fluorescence spectroscopy measurements

Measurements of emission and excitation spectra of Rhodamine 110 and Hya-Rh before and after performing of SEC separation process were measured by fluorescence spectrophotometer. The range of excitation spectra was set from 400 nm to 550 nm with 1 nm step of wavelength and emission wavelength at 570 nm. The emission spectra were measured between 450 nm to 650 nm with 1 nm step of wavelength and 430 nm of excitation wavelength. Finally, all values of fluorescence intensities were normalised.

3.4.3 2f-FCS measurements

The 2f-FCS measurements were performed with the inverted epifluorescent time-resolved confocal microscope. Horizontally and vertically polarized lasers of 470 nm wavelength (LDH Series) were used as an excitation source. The excitation power for measurement of labelled hyaluronan was usually set to 15 μW for both lasers together with 50 ps pulse duration and overall repetition rate 40 MHz. The z470/640rpc dichroic mirror and an emission filters HQ520/35 were used. The size of pinhole was 150 μm and two SPAD detectors were used for detection of fluorescence signal. Time of each measurement was from 5 to 10 min, according to the counting rate and the brightness of measured fluorescent molecules.

After all the measurements, it was necessary to standardize the distance of Nomarski prism. As a method to accomplish this standardization, the method of using the fluorescent probe with known diffusion coefficient was selected. For the excitation wavelength 470 nm, the probe ATTO488-COOH and Oregon Green 488 were used [70]. Subsequently, the 2f-FCS measurement was performed. The temperature was noted and used for recalculation of precise diffusion coefficient of certain probe at the measurement temperature by the *Einstein-Stokes equation* (11).

3.4.3.1 Analysis and data fitting

For analysis of measured data, software SymphoTime64 or Matlab version R2013 were used. In case of usage of SymphoTime64 for data analysis, the calculation programme Matlab version R2009 was used then for data fitting.

As was mentioned in section 2.5.2, the CCF and ACF functions are related with MDF $U(\mathbf{r})$, which can be expressed by following equation [55]:

$$U(\mathbf{r}) = \frac{\kappa(z)}{w^2(z)} \exp\left[-\frac{2}{w^2(z)}\left(x^2 + y^2\right)\right] \tag{28}$$

where x, y, and z are Cartesian coordinates and z axis goes along the optical axis. $w(z)$, $\kappa(z)$ and $R(z)$ are expressed by equations below:
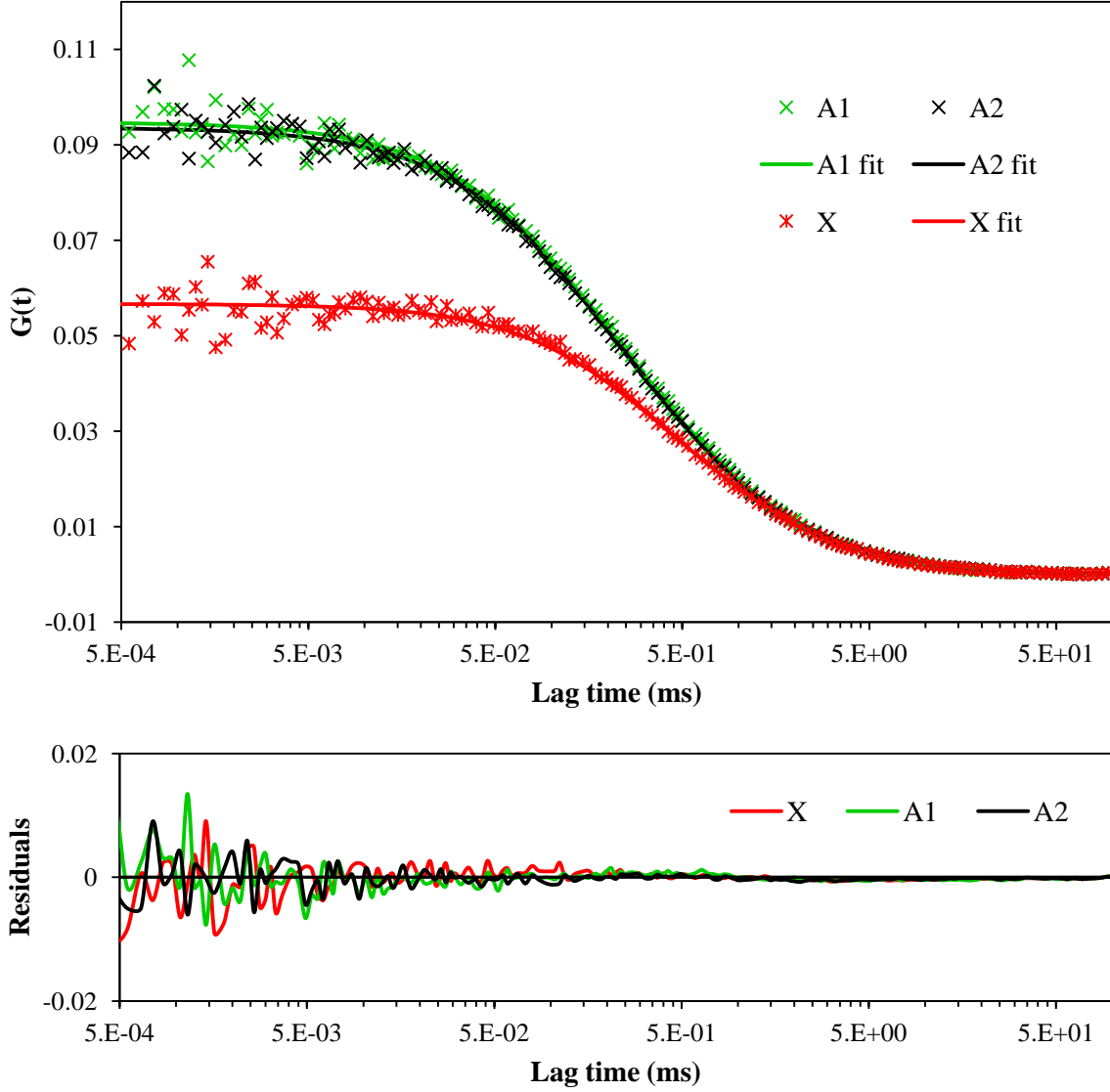
$$w(z) = w_0\left[1 + \left(\frac{\lambda_{ex} z}{\pi w_0^2 j}\right)^2\right]^{\frac{1}{2}} \tag{29}$$

$$\kappa(z) = 1 - \exp\left[-\frac{2h^2}{R^2(z)}\right] \tag{30}$$

$$R(z) = R_0\left[1 + \left(\frac{\lambda_{em}z}{\pi R_0^2 j}\right)^2\right]^{\frac{1}{2}} \tag{31}$$

whereas $\kappa(z)$ denotes eccentricity of detection volume, and $w(z)$ and $R(z)$ denote radius of detection volume.

Figure 12: The comparison of analyzed values and fitted curves with appropriate residual values for Atto488-COOH in aqueous solution. The A1 and A2 mean ACF for the first and the second volume, respectively, and X means CCF between both volumes.

Therefore, if the excitation wavelength λ_{ex}, the emission wavelength λ_{em}, refractive index of medium j, the radius of pinhole divided by magnification of objective h are all known, the

recorded correlation curves can be fitted with R_0 and w_0 as unknown parameters according to the following general equation:

$$G(t, \delta) = \frac{c}{4} \sqrt{\frac{\pi}{Dt}} \int dz_1 \int dz_2 \frac{\kappa(z_1)\kappa(z_2)\exp\left[-\frac{(z_1 - z_2)^2}{4Dt} - \frac{2\delta^2}{8Dt + w^2(z_1) + w^2(z_2)}\right]}{8Dt + w^2(z_1) + w^2(z_2)} \qquad (32)$$

and the absolute value of diffusion coefficient D can be determined. The comparison and description of ACFs of each foci and CCF are shown in Figure 12 with related fitting curves. Moreover, residuals curves of each fitting are also included.

In this thesis, all observed values of D of Hya-Rh were plotted against increasing concentration of various compounds according to the specific conditions and properties, which were measured. Obtained D values of Hya-Rh for three series of concentration ranges were always averaged, whereas the deviation curves were calculated by selective standard deviation and were shown in plot figure. Then, from known values of diffusion coefficient the hydrodynamic values of Hya-Rh were calculated by *Einstein-Stokes equation* (11), whereas the temperature was always 22 °C.

In addition, during 2f-FCS measurements values of counting rate as counts per second (CPS) units, number of $G(t_0)$ in zero lag time and molecular brightness as counts per second per molecule (CPSM) were also recorded, which all can also bring some important information about studied system as concentration and number of molecules in detection volume or signal to noise ratio.

Unfortunately, the concentration of used Hya-Rh was not accurately known for any kind of 2f-FCS measurement because of the SEC separation process. Hence, the approximate concentration was estimated for measurements of dependence of concentration of Hya-Rh on its diffusion characteristics by FCS and by information from the manufacturer. The free probe Atto488-COOH was used as a reference and the FCS measurement was performed at similar conditions. It was determined that the value of $G(t_0)$ of single detection channel relates with concentration of 1 nmol·L^{-1}. The sample concentrations were recalculated according to it and noted. However, these concentration values were not accurate, and since that these concentrations are described as approximate concentrations c_{App} of Hya-Rh.

4   RESULTS AND DISCUSSION

4.1   Preparation of fluorescently labelled hyaluronan solutions

At the beginning, it was necessary to find out if the labelled hyaluronan sample is measurable by FCS. Therefore, a conventional FCS measurement was performed to observe the diffusion time and also the adequate range of concentration of Hya-Rh, which can be subsequently used for next 2f-FCS measurements.
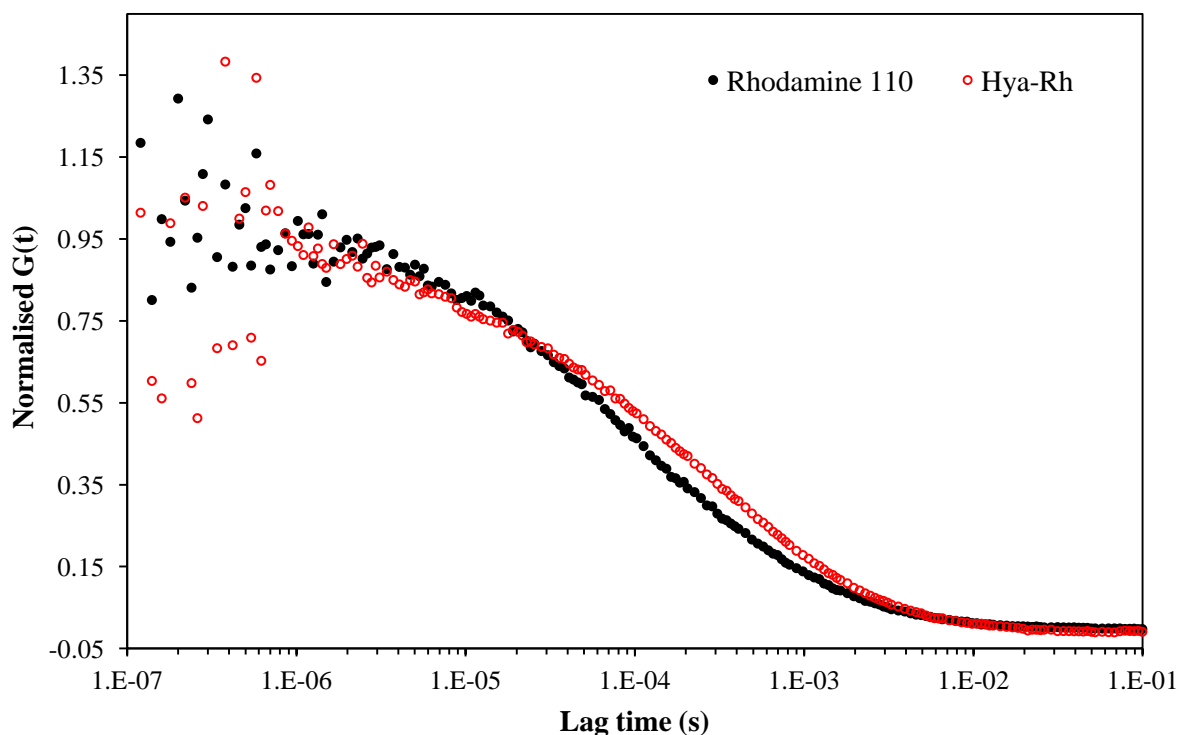
Figure 13: The comparison of normalised ACF curves of Rhodamine 110 and Hya-Rh in aqueous solution, obtained by conventional FCS experiment.

It was determined that a good signal to noise ratio and also acceptable value of $G(t_0)$ in time zero is observable at concentration of 100 μg·L^{-1} of Hya-Rh. Then, the observed ACF curve of Hya-Rh was necessary to compare with the signal of Rhodamine 110 as a free probe, so conventional FCS measurement of Rhodamine 110 at concentration of 10×10^{-9} mol·L^{-1} was performed too. Hence, to contrast the ACF curves of Hya-Rh and Rhodamine 110, values of both ACF curves were normalised and depicted in Figure 13. However, the ACF curves of Hya-Rh and Rhodamine 110, both dissolved in pure water, were almost similar, even if a slight shift of ACF curve of Hya-Rh to larger diffusion time is observable. This difference can be caused by many reasons, but the main discrepancy is in the range of diffusion time, when a larger molecule as the labelled hyaluronan has almost similar diffusion time as a much smaller free probe molecule. Because the decay of ACF of Hya-Rh along the lag time axis was almost similar to ACF of free probe, it denotes that the signal of sample of labelled hyaluronan did not relate to diffusion of a large molecule as could be expected for molecule of labelled polymer, which possess larger space than molecules of free probe, and then moves

slower. Based on these recognitions, it was concluded that the samples of labelled hyaluronan Hya-Rh can be highly contaminated by free probe, which was used for the synthesis process and was not probably separated, or the free probe could be released to the sample as a consequence of degradation process. So the obtained ACF curve of Hya-Rh contained contribution of fluorescence signal of free Rhodamine 110 molecules as well as molecules of Hya-Rh. Therefore, it was decided that the free probe molecules would be separated by SEC to get a pure sample of labelled hyaluronan without any impurities in solution. The description and example of data observed by SEC separation process is shown in Appendix 4.

Subsequently, after performing of SEC separation, the obtained ACF curve of Hya-Rh had changed, as is shown in Figure 14, where normalised ACF curves of Hya-Rh before and after SEC separation are plotted. The shift along the lag time axis was significant, and it proved that the sample of labelled hyaluronan was contaminated by free probe molecules, and even though it has followed storage instruction, the degradation of sample can be observed.

Moreover, excitation and emission spectra of Rhodamine 110 and Hya-Rh before and after SEC separation were measured to confirm that all these samples differ. As can be seen in Figure 15, the excitation and emission maximum of each sample is shifted, whereas the excitation and emission spectra of Rhodamine 110 reach the maximum at 496 and 520 nm, respectively, spectra of Hya-Rh before SEC at 500 and 525 nm, and spectra of Hya-Rh after SEC at 512 and 539 nm. These differences denote changed and non-identical character of each sample. However, the normalised spectra do not show the original distribution of intensity at each wavelength. The spectra of HyaRh before SEC should in origin embody the superposition of spectra of HyaRh after SEC and Rhodamine 110 together, which means that both signals of clear HyaRh after SEC and Rhodamine 110 present in sample of HyaRh can contribute to the spectra of HyaRh before SEC.

In addition, the possible change of signal of Hya-Rh during the storage time was also required to check because the molecular size of measured samples could be changed during the storage in solution as a consequence of the degradation of hyaluronan, and some change of Hya-Rh response could be found. The two ACF curves of first focus for Hya-Rh measured third and twentieth day after preparation were compared by using of normalisation, as is shown in Figure 16. Moreover, the comparison of ACF curves of first focus for HyaRh measured both at the third day after preparation is shown in Figure 17. Then, it is evident that the ACF curve for sample measured twentieth day after preparation changed and one of the reasons can be the degradation process, since the molecular brightness decreased and this fact caused higher contribution of noise. On the contrary, both ACF curves measured the third day were almost similar.

Hence before every usage of Hya-Rh for any FCS measurements, it was necessary to prepare the storage solution of Hya-Rh by separation of free probe impurities to entirely get a signal of fluorescently labelled polymer molecules. Because of the possible degradation, every storage solution of Hya-Rh was maximally stored for three days and since that, a fresh solution was always prepared by dissolving of solid Hya-Rh in water, then separated from free probe by SEC and stored at the same conditions.
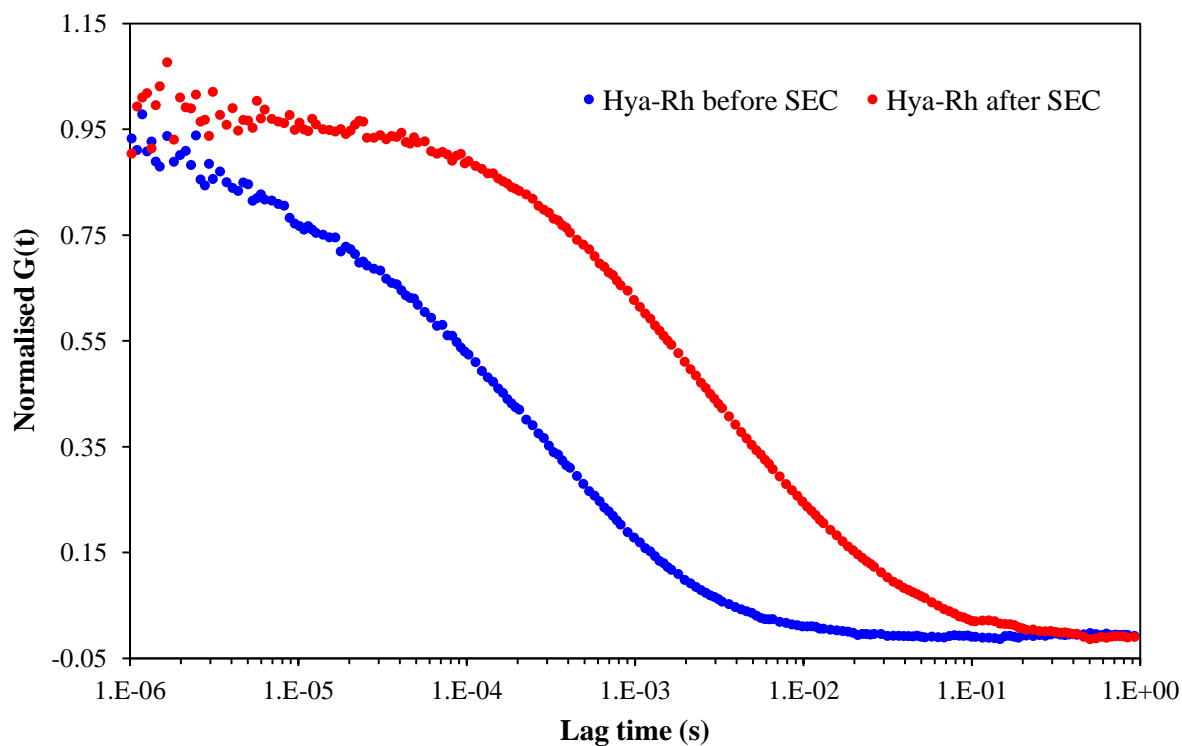
Figure 14: The comparison of normalised ACF curves of Hya-Rh before and after SEC separation process in aqueous solution obtained by FCS measurement.
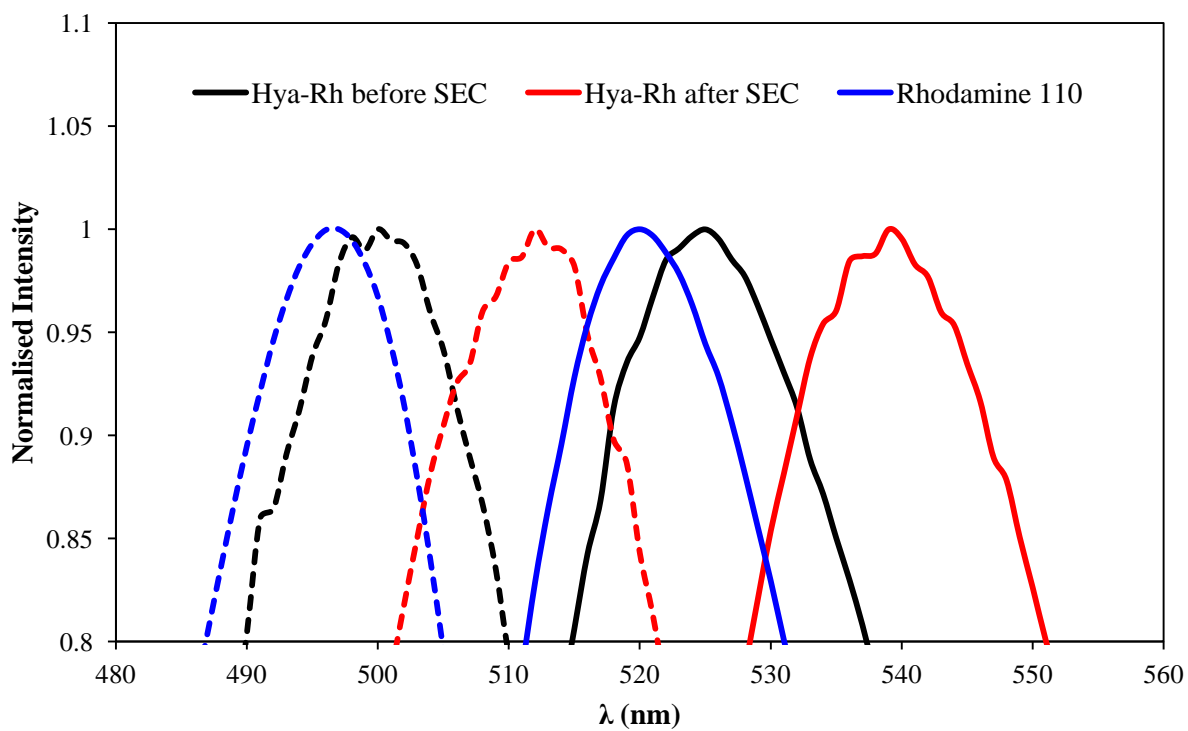
Figure 15: The comparison between emission (lines) and excitation (dashed lines) spectra of Hya-Rh before SEC separation, Hya-Rh after SEC separation and Rhodamine 110.
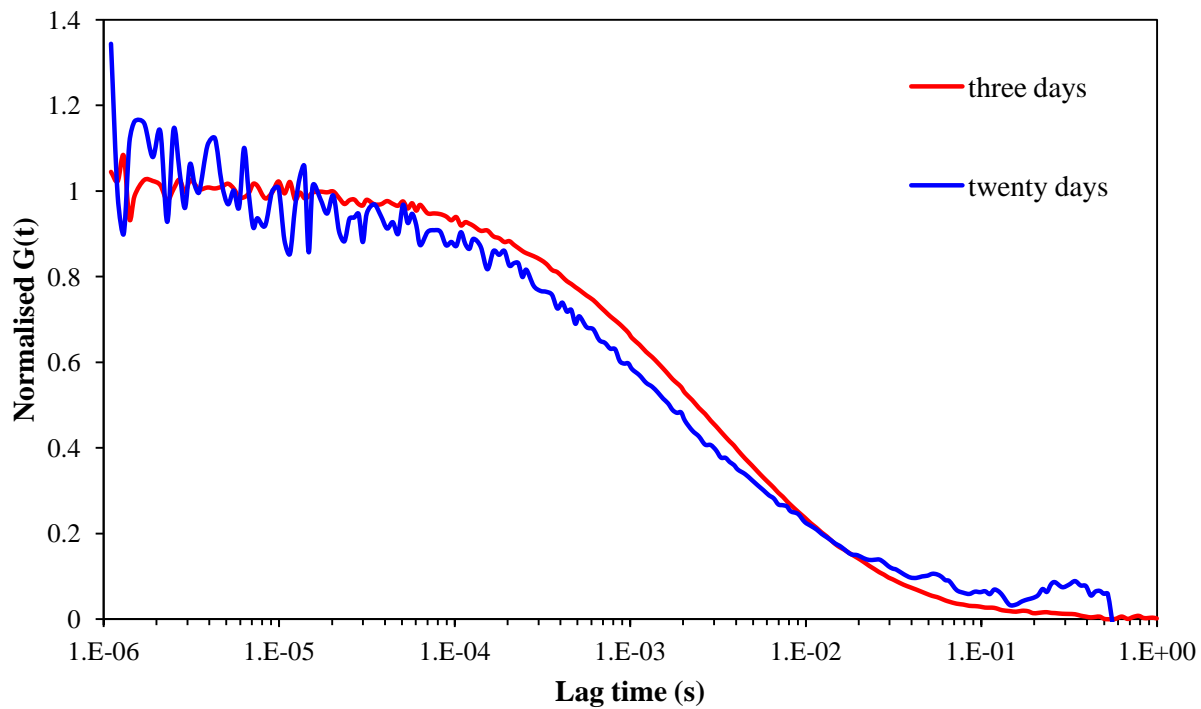
Figure 16: The comparison of ACF curves of first focus for samples of storage solution of Hya-Rh measured in different time after preparation.
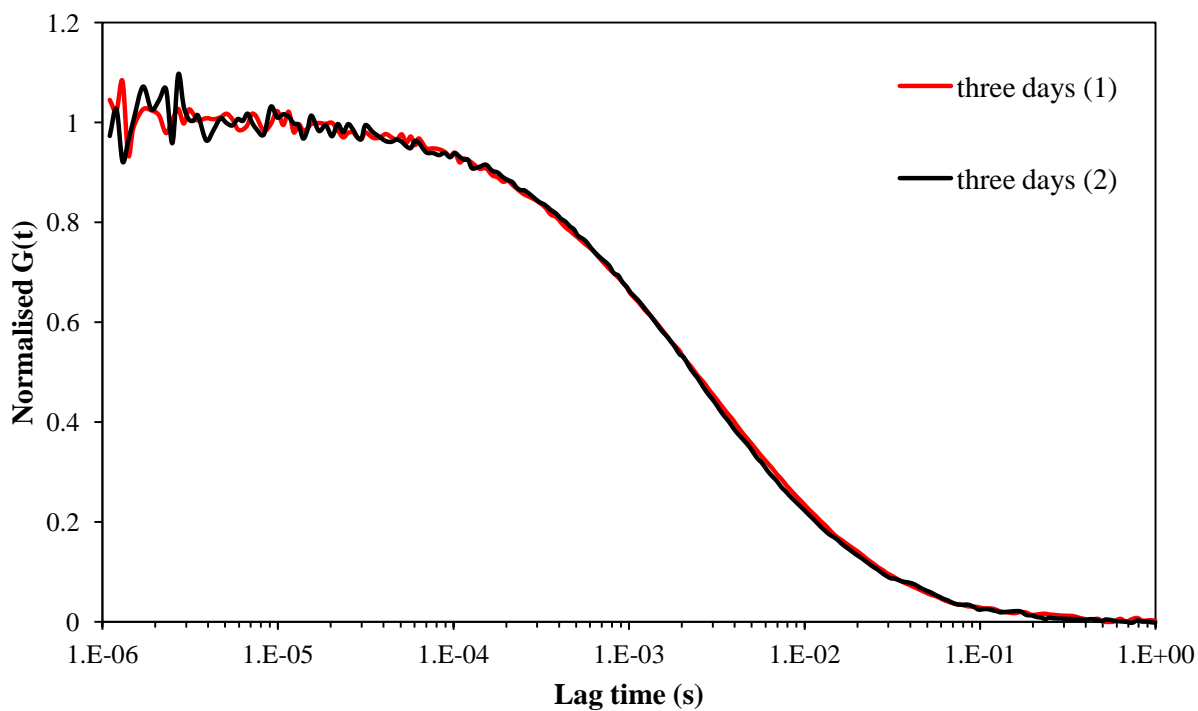
Figure 17: The comparison of ACF curves of first focus for samples of storage solution of Hya-Rh measured in the same time after preparation and stored at the same conditions.

4.2 Influence of Hya-Rh concentration on its diffusion characteristics

Since the exact value of concentration of Hya-Rh used for 2f-FCS measurements was not accurately known after SEC separation process and the concentration of Hya-Rh varied for every 2f-FCS measurements because of adjusting of good signal to noise ratio, the diffusion coefficient values and related hydrodynamic radii of labelled hyaluronan was measured in dependence on its concentration to determine any changes or influences of the concentration. All of these measurements were performed in water as well as in physiological solution.

4.2.1 Aqueous solution

At the beginning, the samples with different amount of Hya-Rh were prepared and subsequently measured by 2f-FCS. Obtained data of diffusion coefficients and approximate concentrations of Hya-Rh in solution are plotted in Figure 18. As can be seen, the values varied for different concentrations and slight increasing of diffusion coefficient of Hya-Rh molecules with increasing concentration of Hya-Rh can be noted.

Subsequently, the average values of diffusion coefficient and hydrodynamic radius for each sample of Hya-Rh at different concentration in water are shown in Table 5 with appropriate deviation values, which do not change significantly in dependence on concentration of Hya-Rh. However, the values are affected by deviations given by three series of measurements. The polydispersity of measured labelled polymer molecules can be considered as one of the reasons of deviations because the polymer molecules do not possess exactly similar molecular weight, and these deficiencies can be revealed by the measurement of diffusion coefficients.

The additional information about counting rates, molecule brightness and number of $G(t_0)$ calculated as an average of values measured in each detector are also included in Table 5. According to these data, the counting rate was increasing with increasing concentration of Hya-Rh, whereas the number of $G(t_0)$ was decreasing because of increasing number of molecules in detection volumes. The molecular brightness did not change significantly, but for sample with lowest concentration of Hya-Rh brightness slightly differed from other values at higher concentration of Hya-Rh.

Table 5: The values of diffusion coefficient, hydrodynamic radius, appropriate concentration and information of 2f-FCS measurement for samples of Hya-Rh in water

c_{App} (mol·L^{-1})	D (cm^2·s^{-1})	R_H (nm)	Counting rate (CPS)	$G(t_0)$	Brightness (CPSM)
2.3×10^{-10}	$(3.02 \pm 0.08) \times 10^{-7}$	74 ± 2	3 444	0.88	2 996
5.6×10^{-10}	$(3.10 \pm 0.07) \times 10^{-7}$	73 ± 2	9 263	0.36	3 338
9.1×10^{-10}	$(3.05 \pm 0.11) \times 10^{-7}$	74 ± 3	14 691	0.22	3 316
1.7×10^{-9}	$(3.19 \pm 0.08) \times 10^{-7}$	71 ± 2	28 050	0.12	3 387
2.5×10^{-9}	$(3.20 \pm 0.07) \times 10^{-7}$	71 ± 2	43 307	0.08	3 327
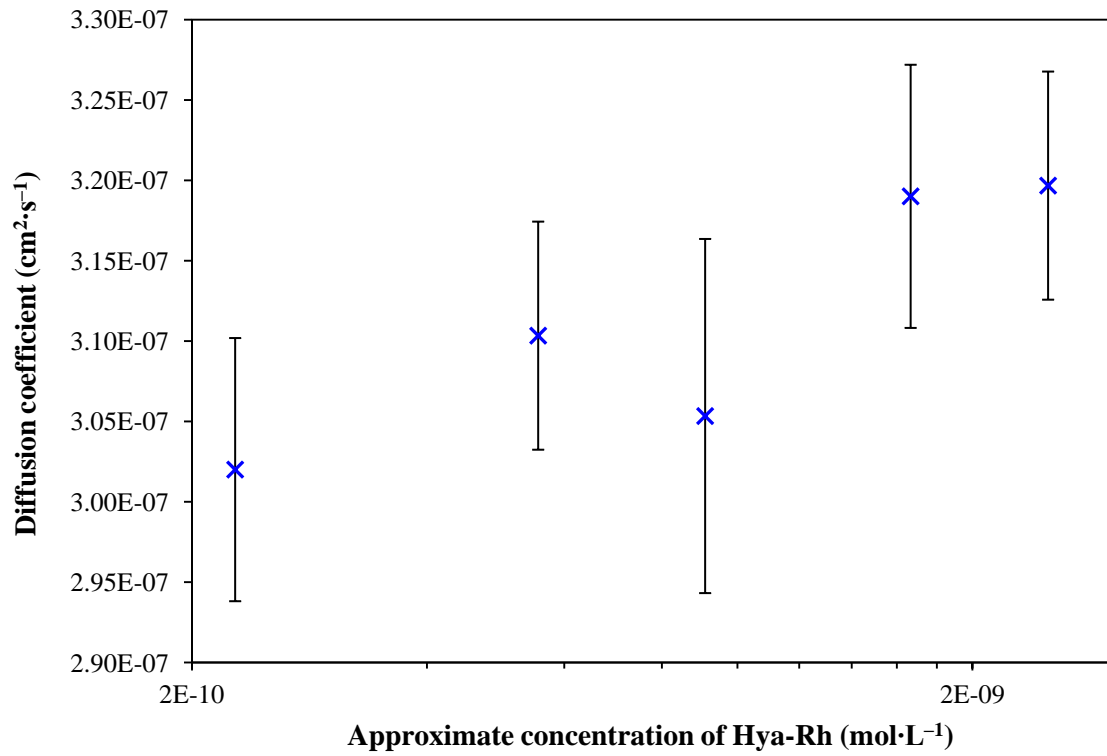
Figure 18: The dependence of diffusion coefficients and hydrodynamic radii of Hya-Rh on approximated concentration of Hya-Rh in water.
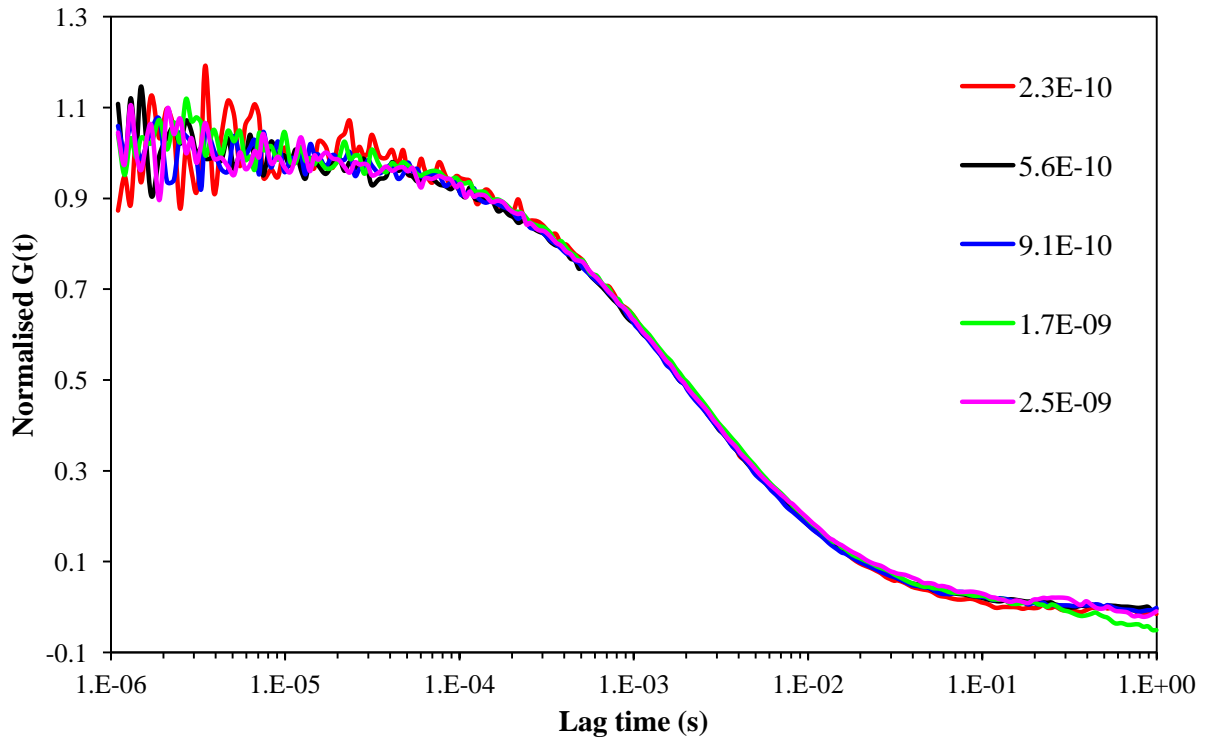
Figure 19: The comparison of normalised ACF curves of first focus measured with different concentration of Hya-Rh in aqueous solution.

40

Afterwards, the normalisation of all ACF curves of first focus for samples of different concentration of Hya-Rh was determined and plotted in Figure 19. Hence, there is no evident shift along the lag time axis, which means that the diffusion coefficient and then hydrodynamic radius values are not dependent on the concentration of Hya-Rh, and with increasing concentration of Hya-Rh any significant change in diffusion was not observed.
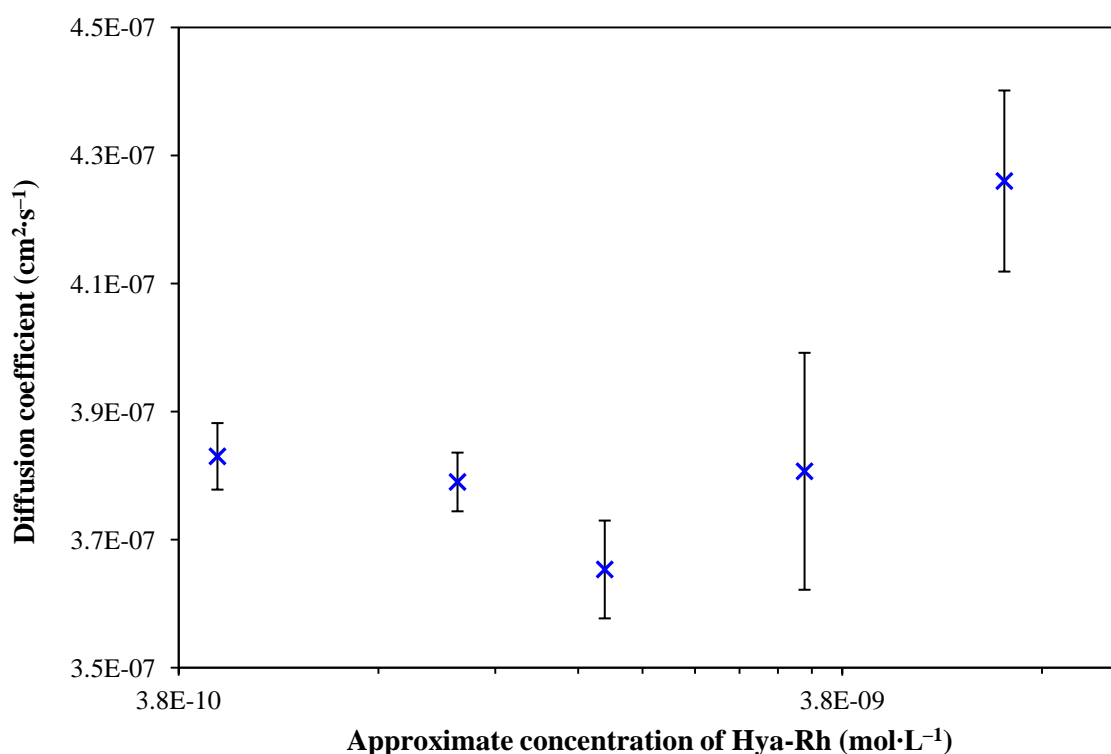
4.2.2 Physiological solution

The behaviour of diffusion characteristics of Hya-Rh in dependence on its concentration was also determined in physiological solution because the 0.15 mol·L^{-1} concentration of NaCl ions can influence the behaviour of charged chains of Hya-Rh. As is shown in Figure 20, the values of diffusion coefficient are not significantly changing with increasing approximate concentration of Hya-Rh; however, the change of diffusion rate is apparent for value at $6.7 \times 10^{-9} \text{ mol·L}^{-1}$ of approximate concentration of Hya-Rh, whereas this value contains larger deviation. The values are also shown in Table 6 with appropriate standard deviations, which increase with increasing concentration of studied polymer. If the values are compared with values of diffusion coefficient of Hya-Rh in aqueous solution, it is obvious that the diffusion characteristics are different in physiological solution, whereas polymer chains of Hya-Rh shrink in presence of ions. Then the whole molecules possess smaller size and move faster in the physiological solution.

For better understanding what is happening with Hya-Rh molecules in dependence on its concentration, the information about molecule brightness, counting rate and $G(t_0)$ were recorded and are also shown in Table 6. It can be seen that according to the theory, the values of $G(t_0)$ are decreasing and the values of counting rate are increasing with increasing concentration of polymer molecules in detection volumes. However, the brightness is changing and main difference between values below and above the $1.0 \times 10^{-9} \text{ mol·L}^{-1}$ of approximate concentration can be noted. It can be caused by fact that the brightness is not the absolute molecular brightness, or the conformational changes of polymer molecule could influence the interaction between fluorescent label, polymer chain and solvent, so the emission may change.

Therefore, the comparison of normalised ACF curves of first focus measured with different concentration of Hya-Rh in physiological solution was also concerned, and can be seen in Figure 21. All decays of normalised ACF curves along the lag time axis are almost similar except the normalised ACF curve for solution of $6.7 \times 10^{-9} \text{ mol·L}^{-1}$ of approximate concentration. This fact can be caused by presence of aggregates and larger particles, which cause the discrepancy of ACF curve in larger lag time values. However, one can disputes against this explanation. At first, the diffusion coefficient value is higher than at lower concentrations which denote smaller and faster particles, and at second, the concentration values were far away from concentration, where the polymer chains start to overlap and where is higher probability of association. Even if the concentration is very small, the probability of making of aggregates is not zero. Moreover, polymer molecules can possess more stable statements as associated systems at higher concentration of ions, and according to the behaviour of polyelectrolyte molecules in ion solution, this can be one of suggestion how this effect could be explained. However, the deficiency in the ACF curve can be also caused by

presence of some other different species denoting that the sample was not homogenous but heterogeneous.

Finally, the normalisation of both values of sample series was determined for the ACF curves of first focus for sample of Hya-Rh in physiological solution at highest concentration of Hya-Rh, as is shown in Figure 22. There can be seen that the decay along the lag time axis and the shape of both curves are almost similar. It can denote the fact that some change happens at this concentration of Hya-Rh in physiological solution. There is also some possibility that it can be caused by the performance of detector because the counting rate was higher than 100 000 CPS and then the detector can give some artefacts. Therefore, it was concluded that this highest concentration of Hya-Rh will not be used for following measurements.


Figure 20: The dependence of diffusion coefficients and hydrodynamic radii of Hya-Rh on approximate concentration of Hya-Rh in physiological solution.

Table 6: The values of diffusion coefficient, hydrodynamic radius, appropriate concentration and information of 2f-FCS measurement for samples of Hya-Rh in physiological solution

c_{App} (mol·L^{-1})	D (cm^2·s^{-1})	R_H (nm)	Counting rate (CPS)	G(t$_0$)	Brightness (CPSM)
4.4×10^{-10}	$(3.83 \pm 0.05) \times 10^{-7}$	59 ± 1	6 860	0.46	2 983
1.0×10^{-9}	$(3.79 \pm 0.05) \times 10^{-7}$	60 ± 1	16 538	0.20	3 257
1.7×10^{-9}	$(3.65 \pm 0.08) \times 10^{-7}$	62 ± 1	35 987	0.12	4 212
3.3×10^{-9}	$(3.81 \pm 0.19) \times 10^{-7}$	59 ± 3	66 573	0.06	3 605
6.7×10^{-9}	$(4.26 \pm 0.14) \times 10^{-7}$	51 ± 3	136 994	0.03	4 257
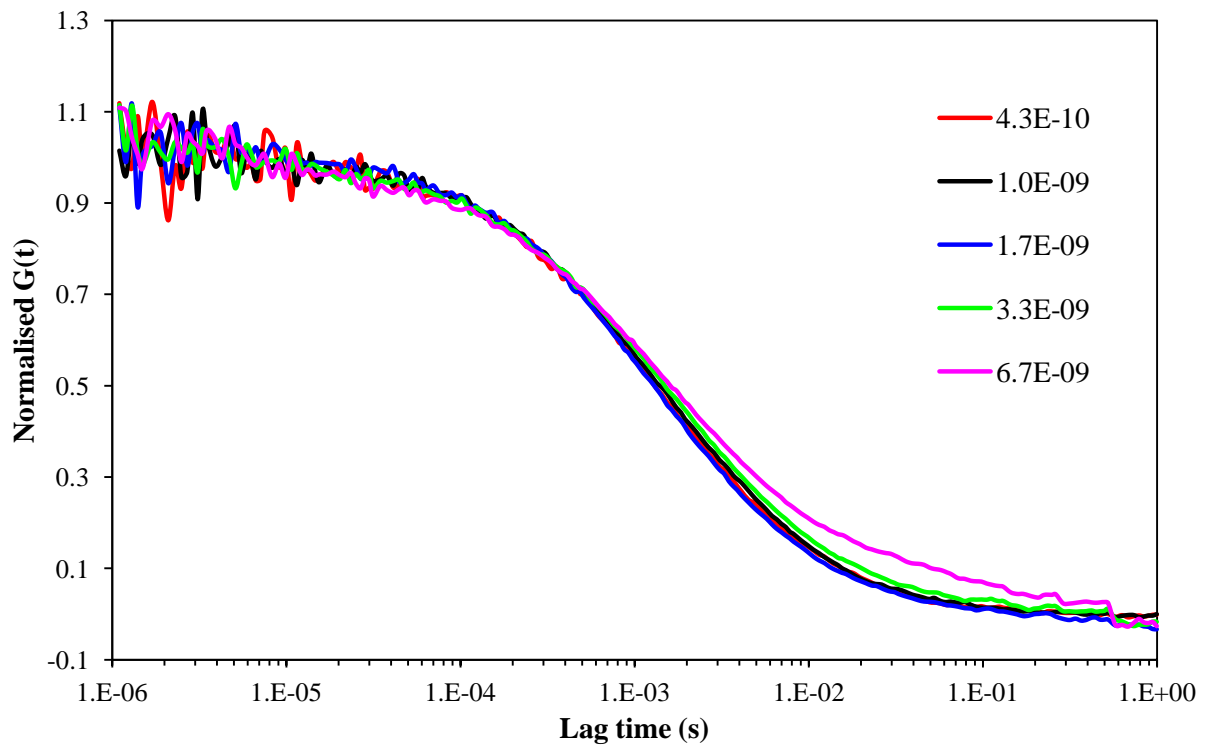
Figure 21: The comparison of normalised ACF curves of first focus measured with different concentration of Hya-Rh in physiological solution.
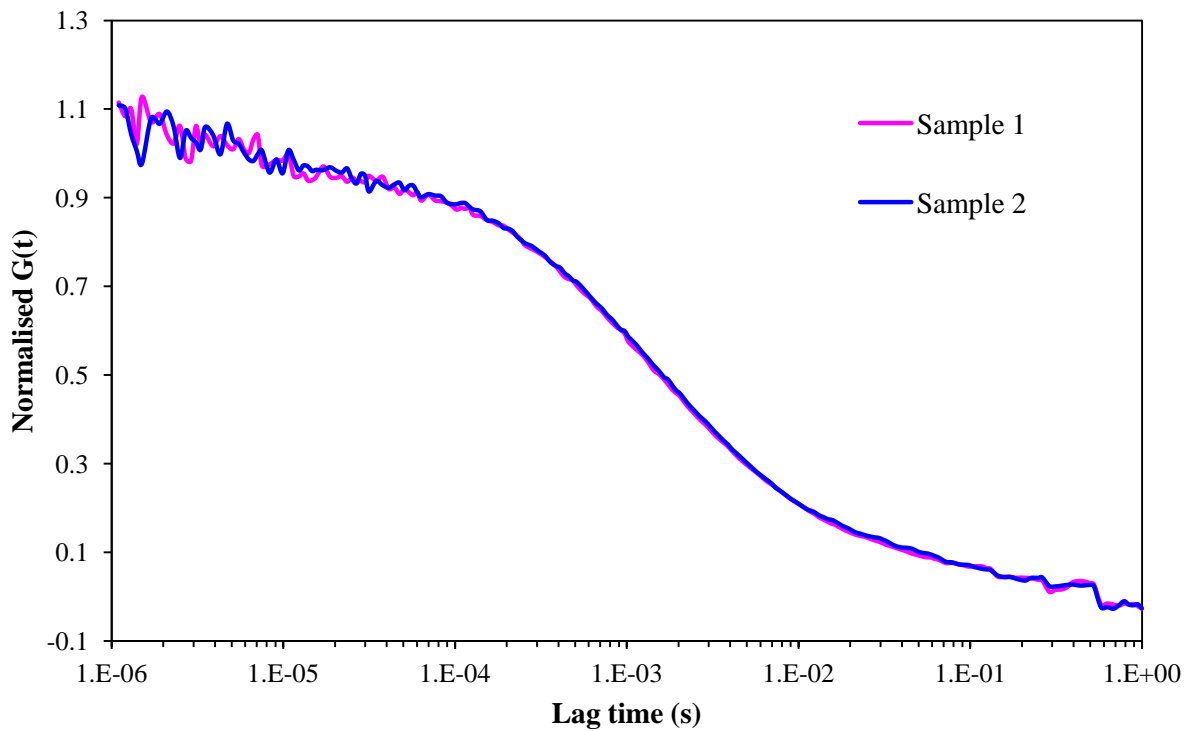
Figure 22: The comparison of ACF curves of first focus for samples of HyaRh at the highest concentration in physiological solution.

4.3   Behaviour of Hya-Rh in presence of alkali metal ions

On the basis of knowledge of behaviour of polyelectrolyte in solutions with presence of ions, the Hya-Rh diffusion characteristics were studied in presence of increasing concentration of alkali metal ions, especially Li^+, Na^+, K^+ and Cs^+. The main assumption was that the polymer chains should compress with increasing ionic strength, and therefore the Hya-Rh molecules movements in solution should be faster because of the smaller hydrodynamic radius. Afterwards, some differences between univalent ions of alkali metal ions as influence of radius of cations can be determined, which are shown in Table 7 together with appropriate ionic strength of various concentrated solutions. As can be seen, the ionic strength was similar for alkali metal ions solutions; however, the radius of cations is increasing with the order of first group in periodic table of elements, whereas Li^+ possesses the smallest radius and Cs^+ possesses the largest radius.

*Table 7: The comparison of size radii of cations and ionic strength of salt solutions used for studying of Hya-Rh*

Concentration $(mol \cdot L^{-1})$		0.000 1	0.001	0.01	0.1	1
Cation	Radius (pm) [71]	Ionic strength $(mol \cdot L^{-1})$				
Li^+	76					
Na^+	102	0.000 1	0.001	0.01	0.1	1
K^+	138					
Cs^+	167					

Table 8: The comparison of values of diffusion coefficient of Hya-Rh in solutions of alkali metal ions

Concentration $(mol \cdot L^{-1})$	Diffusion coefficient $(10^{-7}\, cm^2 \cdot s^{-1})$			
	Li^+	Na^+	K^+	Cs^+
0.000 1	3.49 ± 0.09	3.43 ± 0.09	3.67 ± 0.33	3.81 ± 0.14
0.001	3.35 ± 0.08	3.49 ± 0.04	3.45 ± 0.04	3.75 ± 0.09
0.01	3.48 ± 0.21	3.49 ± 0.16	3.53 ± 0.20	3.63 ± 0.41
0.1	3.38 ± 0.11	3.79 ± 0.02	3.47 ± 0.04	3.44 ± 0.10
1	4.43 ± 0.19	4.39 ± 0.22	4.25 ± 0.33	5.21 ± 0.64

Furthermore, the diffusion coefficient values of Hya-Rh in presence of these ions were determined by 2f-FCS and are shown in Table 8 with appropriate deviations. One can note that the values changed, and significant increasing can be seen between values of salt concentration of 0.1 and 1 $mol \cdot L^{-1}$. In addition, the dependence of diffusion coefficient values on concentration of each salt is shown in Figure 23, where deviation curves were not shown because of better visualisation of averaged values of diffusion coefficients and their differences. As can be seen, the values of diffusion coefficient of Hya-Rh in presence of Li^+ and Na^+ do not differ very much and they can be considered as almost similar in the concentration range of 0.000 1 to 0.01 $mol \cdot L^{-1}$. In presence of K^+ cations, the Hya-Rh molecules possess higher value at the 0.000 1 $mol \cdot L^{-1}$ of concentration than in presence of Li^+

and Na$^+$, but in following concentration range the behaviour of Hya-Rh in K$^+$ presence is almost similar as in Li$^+$ and Na$^+$ environment. On the contrary, the dependence of diffusion coefficient values in presence of Cs$^+$ is slightly decreasing in range of 0.000 1 to 0.1 mol·L^{-1}. However, all of these discussed values of diffusion coefficients are affected by deviations mentioned in Table 8. Therefore, the sole observation can be noted that the significant change of mobility of Hya-Rh occurs between 0.1 and 1 mol·L^{-1} of salt concentrations.
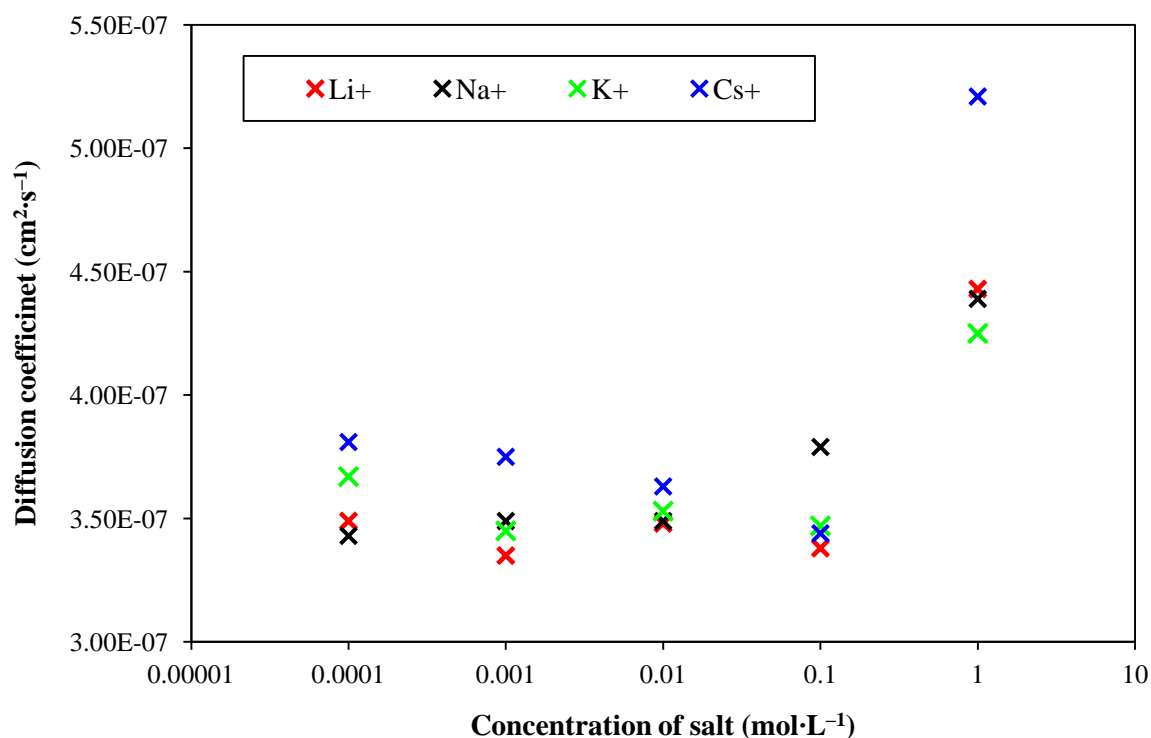
Figure 23: The dependence of diffusion coefficient values of Hya-Rh on concentration of alkali metal ions.

Table 9: The values of diffusion coefficient, hydrodynamic radius and appropriate information of 2f-FCS measurement for samples of Hya-Rh in dependence on Na$^+$ concentration

| c (mol·L^{-1})	D (cm^2·s^{-1})	R$_H$ (nm)	Counting rate (CPS)	G(t$_0$)	Brightness (CPSM)
0.0001	$(3.43 \pm 0.09) \times 10^{-7}$	65 ± 2	19 177	0.20	3 691
0.001	$(3.49 \pm 0.04) \times 10^{-7}$	65 ± 1	17 049	0.22	3 616
0.01	$(3.49 \pm 0.16) \times 10^{-7}$	65 ± 3	8 255	0.45	3 567
0.1	$(3.79 \pm 0.02) \times 10^{-7}$	60 ± 0.3	12 741	0.33	4 344
1	$(4.39 \pm 0.22) \times 10^{-7}$	52 ± 3	11 005	0.37	3 983

Moreover, the dependence of the diffusion coefficient values and calculated hydrodynamic radius of Hya-Rh on concentration and ionic strength of NaCl salt solution is depicted in Figure 24. As can be seen, the values of diffusion coefficient does not change in range of

0.000 1 to 0.01 mol·L^{-1}. However, since the values of 0.1 mol·L^{-1} of concentration, the mobility of Hya-Rh starts to increase as a consequence of shrinking of polymer molecule. All the values of diffusion coefficient are noted in Table 9, whereas calculated approximate values of hydrodynamic radius are also shown with appropriate deviations. Then, the values of G(t$_0$), molecular brightness and counting rate are also shown, and as can be seen it does not change significantly except the counting rate at 0.01 mol·L^{-1} concentration, which is apparently caused by lower concentration of Hya-Rh in measured solution. The molecular brightness at 0.1 mol·L^{-1} concentration of salt is higher than other molecular brightness values; however, these values are not exactly accurately known and the value does not differ significantly than others.

Subsequently, the ACF curves of first focus for samples of Hya-Rh in presence of 0.000 1, 0.1 and 1 mol·L^{-1} were compared, as can be seen in Figure 25, and for better visualisation the lag time axis was reduced to range between 0.000 1 and 0.01 s. Hence, the obvious shift of ACF curves between solutions contained 0.1 and 1 mol·L^{-1} of salt can be determined. These facts proved that by increasing concentration of ions and ionic strength the shape of Hya-Rh molecule compresses and significant change of diffusion mobility of Hya-Rh occurs between concentration of 0.1 and 1 mol·L^{-1} of salt.
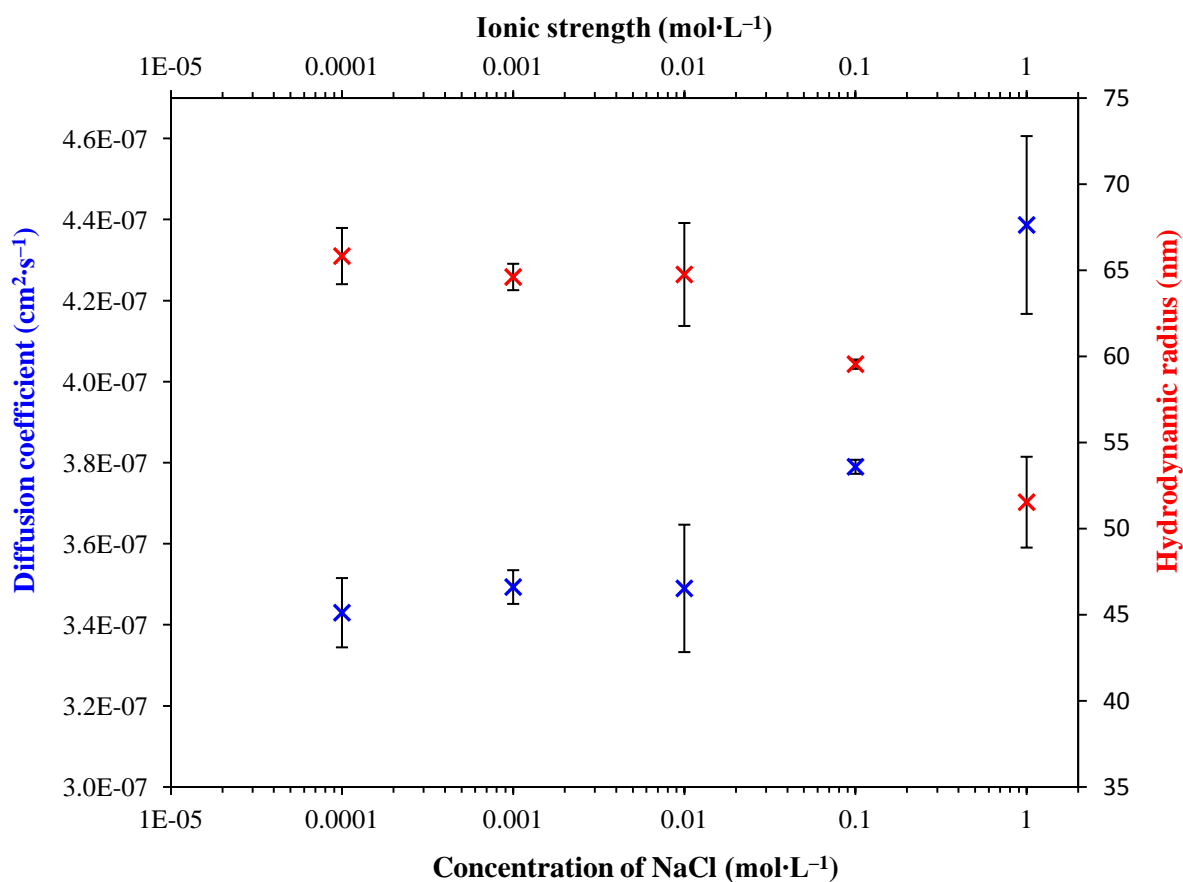
Figure 24: The dependence of Hya-Rh diffusion coefficient and hydrodynamic radius on concentration of NaCl.
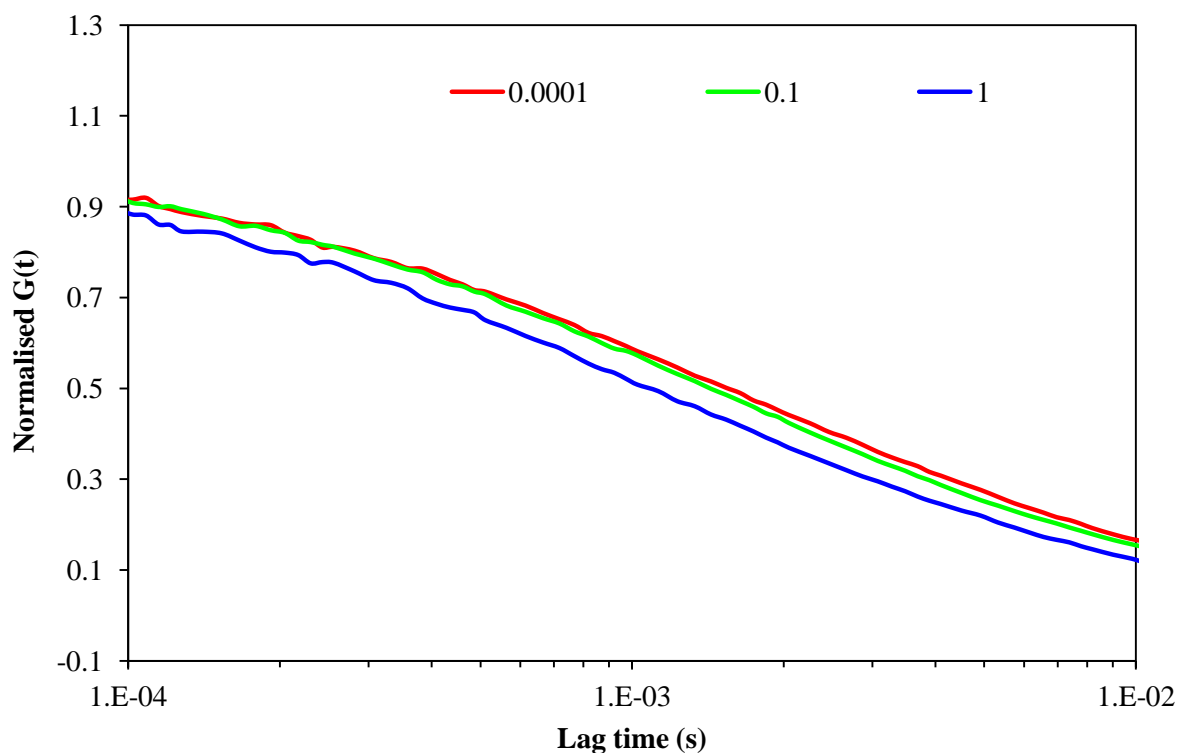
Figure 25: The normalised ACF curves of first focus for sample of Hya-Rh in presence of different concentrations of NaCl.

## 4.4 Study of diffusion of HyaRh in presence of VLMW HA

The diffusion characteristics of Hya-Rh at the presence of varied concentrations of VLMW HA were measured by 2f-FCS technique and performed in aqueous solution and also in physiological solution. Furthermore, the transitions between concentration regimes from diluted to semi-diluted in aqueous and physiological solution of VLMW HA were studied and compared.

4.4.1 Aqueous solution

At the beginning before all following measurements, the diffusion characteristics of free probe Rhodamine 110 in 0.001 g·L^{-1} and 3 g·L^{-1} solution of VLMW HA were measured, and then compared with the measured data of fluorescently labelled hyaluronan at similar conditions to prove any interactions between chains of VLMW HA and fluorescently labelled hyaluronan. These experiments were performed for aqueous solutions.

As can be seen in Figure 26, the difference between normalised ACF curves of first focus of samples contained VLMW HA and Rhodamine 110 is minimal and almost imperceptible. Because the molecules of probe are very small, they can freely diffuse through polymer domains and then the diffusion coefficient of free probe does not change significantly. On the contrary, the significant shift of normalised ACF curves of first focus for samples of Hya-Rh in presence of lowest and highest concentration of VLMW HA can be recognized. This fact signalises the change of mobility of Hya-Rh molecules, which can be caused by transition between diluted to semi-diluted concentration regimes of VLMW HA solutions.

Consequently, the diffusion coefficients of Hya-Rh in solutions of VLMW HA were determined according to the 2f-FCS measurements with appropriate standard deviations obtained by performing of measurements of three similar series of studied concentration range of VLMW HA. The plot of diffusion coefficient values of Hya-Rh against the increasing concentration of VLMW HA is shown in Figure 27. As can be noted, the value of diffusion coefficient at the lowest concentration of VLMW HA is higher than values measured in pure water. It means that observed diffused Hya-Rh molecule moved faster in solution of lowest concentrated VLMW HA than in pure water. One of explanations can be the fact, that polymer chains of Hya-Rh are not monodisperse and since that the measured molecule was smaller than the molecule measured in pure water and this caused the difference.
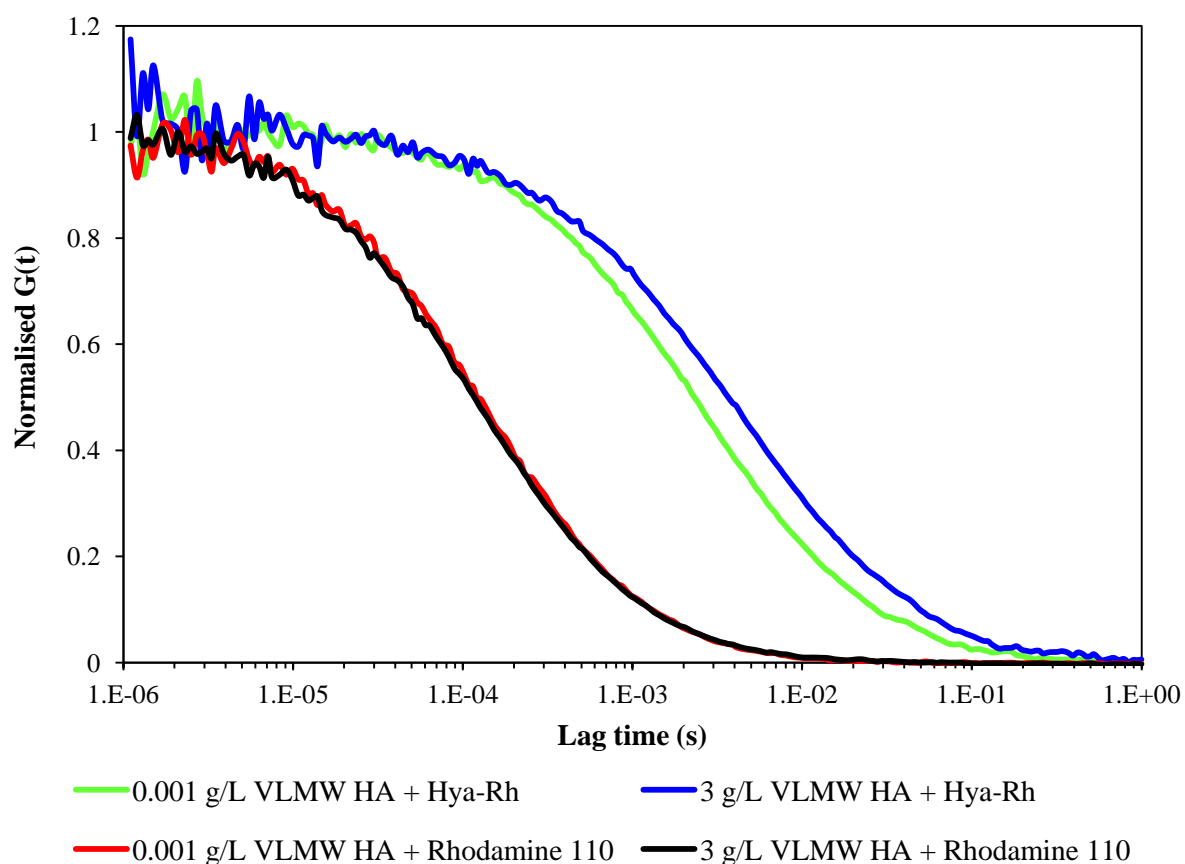

Figure 26: The comparison of normalised ACF curves of first focus of Rhodamine 110 and Hya-Rh at presence of lowest and highest concentration of VLMW HA in aqueous solution.

Furthermore, the change of mobility of Hya-Rh happens with increasing concentration of unlabelled hyaluronan molecules, whereas the first significant change starts at the 0.005 $g \cdot L^{-1}$ concentration of unlabelled hyaluronan. Moreover, the values of diffusion coefficient at the concentration of 0.005 $g \cdot L^{-1}$ and at 0.01 $g \cdot L^{-1}$ contain large standard deviations, which can be a consequence of non-equilibrium states and can signalise that the system is not stable. The diffusion coefficient values are related with the size of molecule and varies from 2.5×10^{-7} to

3.3×10^{-7} cm^2·s^{-1}. It can also signalise the beginning of crossing over from diluted to semi-diluted mode, which usually happens in a broad range of concentration variation, as was mentioned. In addition, it can be seen that the reach of the transition is not sharp and takes almost two orders of magnitude until the system reaches the semi-diluted regime of concentration. After crossing of the concentration of 0.05 g·L^{-1}, the diffusion coefficient values are gaining some plateau and velocity of diffusion does not change significantly until the concentration of 3 g·L^{-1}.
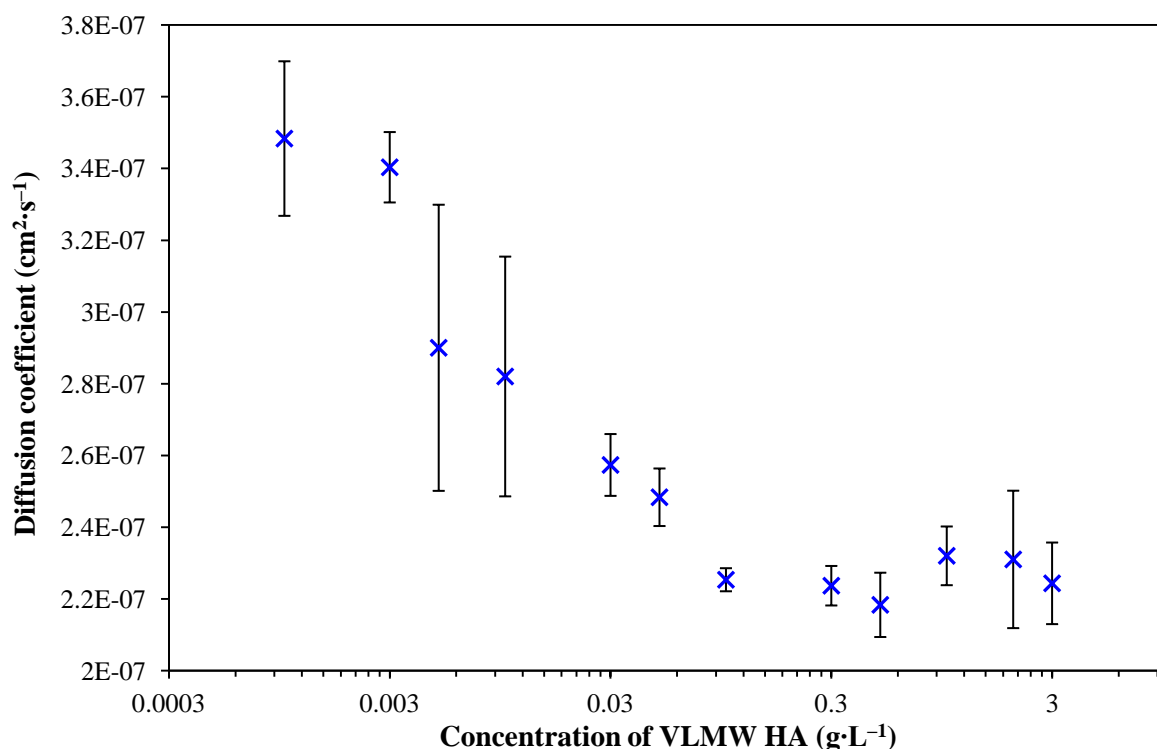
Figure 27: The dependence of diffusion coefficient values of Hya-Rh on the concentration of VLMW HA in aqueous solution.

However, one can note that the values of diffusion coefficient of Hya-Rh could not sufficiently denote the diluted to semi-diluted transitions because of the difference between molecular weight and also between size of VLMW HA molecules and Hya-Rh molecules. The molecular weight of Hya-Rh molecule is roughly ten times smaller than molecular weight of unlabelled hyaluronan molecules. Hence, it is also possible that the molecules of Hya-Rh are able to diffuse through the meshes of unlabelled hyaluronan nets and then the diffusion coefficient values are not related with the concentration regime transition, whereas the cross-over concentration could not be determined. This idea is shown in Figure 28, where four situations are described. The first one denotes the diffusion of labelled polymer alias Hya-Rh in diluted solution of unlabelled hyaluronan. It is apparent that the movement is almost similar as in pure water because the concentration of hyaluronan in solution is very low, and the probability of encountering of unlabelled molecules with labelled molecules is very small. However, it is important to note that for 2f-FCS measurements the concentration of labelled

polymer molecules was almost six orders of magnitude lower than the concentration of unlabelled molecules. The second picture denotes the situation when the concentration of unlabelled molecules has increased. Then, the solution was generally inhomogeneous, and the probability of encountering of labelled molecules with unlabelled polymer chains is much higher. This can cause the change of diffusion movement of Hya-Rh. Moreover, this explanation could be able to establish the question about the deviation curves at the concentration of 0.005 g·L^{-1} and at 0.001 g·L^{-1} of unlabelled polymer. If this assumption is right, the values of diffusion coefficient at these concentrations were composed of signal from Hya-Rh molecules diffused through pure water and through polymer chains and their aggregates.
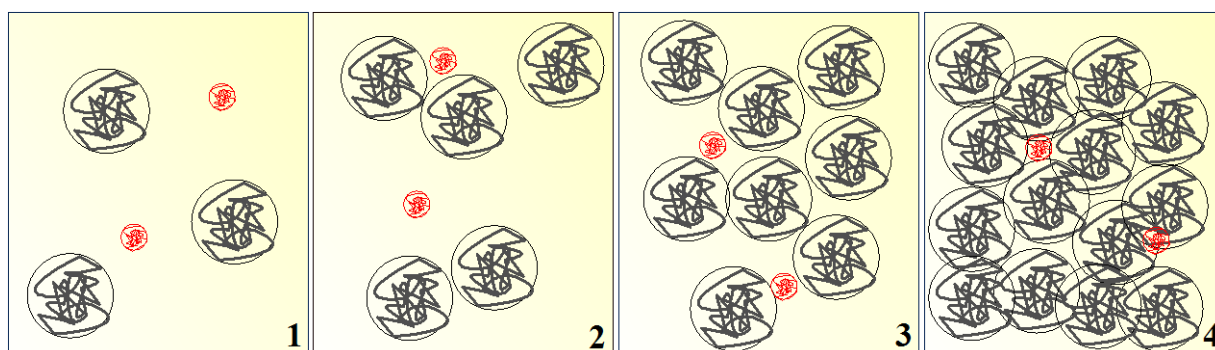
Figure 28: The pictures of behaviour of Hya-Rh in solutions of VLMW HA.

Subsequently, the third picture shows the diffusion of labelled hyaluronan molecules through starting polymer nets, when the chains of unlabelled hyaluronan start to overlap and form physically bonded net. If the concentration of unlabelled hyaluronan increases, as is shown in fourth picture in Figure 28, the molecules of Hya-Rh would be approximately able to diffuse through the polymer net meshes, but the significant decreasing of diffusion coefficient would be noted.

However, all of this explanations are only suggestions, how one can explicate the measured data of diffusion coefficients of Hya-Rh at different concentration of VLMW HA in aqueous solution, and it has to be noted that all of the deviation curves can be also partially caused by the polydispersity of measured Hya-Rh molecules.
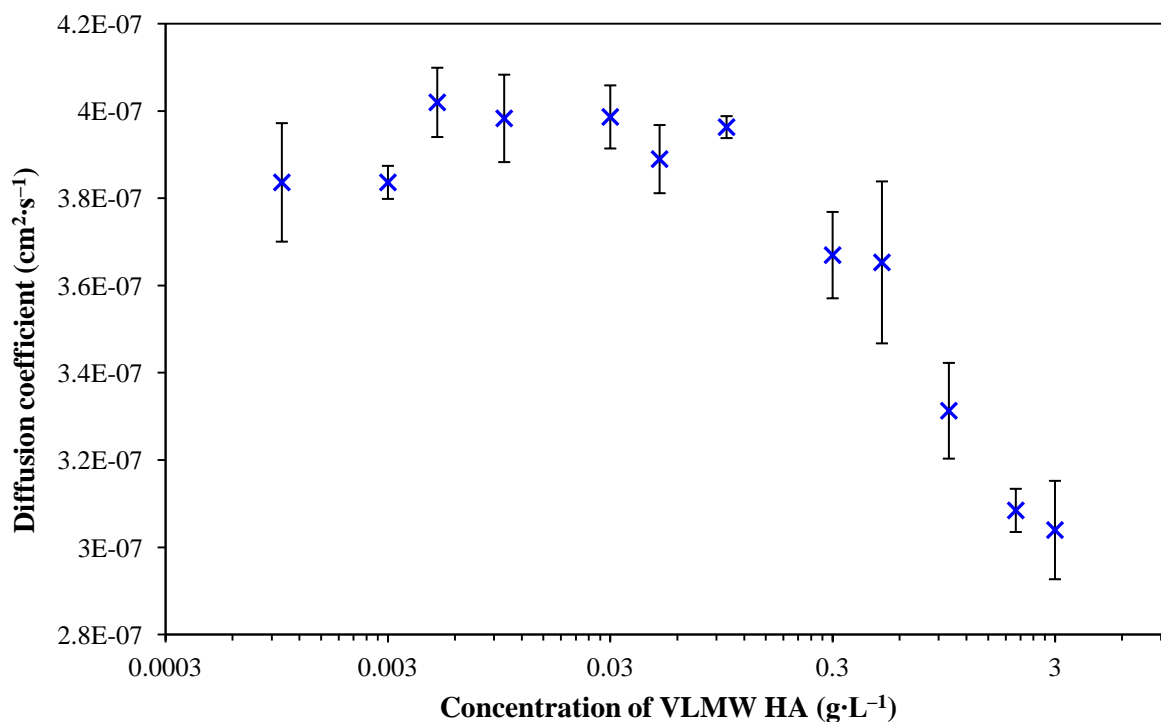
4.4.2 Physiological solution

The dependence of diffusion coefficient values of Hya-Rh on increasing concentration of VLMW HA was also measured by 2f-FCS in physiological solution, and the determined values are shown in Figure 29. As can be seen, at the beginning the diffusion coefficient values slightly increase with increasing concentration of unlabelled polymer molecules between concentration values of 0.001 and 0.1 g·L^{-1}. However, if one take in note that these diffusion coefficient values are affected by errors, the change would not be very significant with increasing concentration of VLMW HA, and it would mean that the diffusion coefficient

values possess some plateau through two orders of magnitude. Moreover, the value of the diffusion coefficient at the lowest concentration of VLMW HA and also the mean value of the plateau are almost similar with the value of diffusion coefficient of Hya-Rh in presence of $0.1 \ \text{mol·L}^{-1}$ NaCl, which was determined to $(3.79 \pm 0.02) \times 10^{-7} \ \text{cm}^2 \cdot \text{s}^{-1}$.

Decreasing of diffusion movement of Hya-Rh molecules is obvious between concentrations of $0.3 \ \text{g·L}^{-1}$ to $3 \ \text{g·L}^{-1}$, whereas all these values are also affected by large standard errors. The deviations can be caused at first by the instability of polymer system, at second by the polydispersity of studied labelled polymer molecules, at third by interactions and different origin of diffusion movement of labelled polymer, and at the end by the presence of salt, which can contribute to the general instability of the whole system.

It is known that the presence of salt in polyelectrolyte solution as hyaluronan solution causes shrinking and compressing of polymer coils. If the dependence of diffusion coefficient of labelled hyaluronan on the concentration of VLMW HA in aqueous and physiological solution are compared (Figure 30), the higher values of diffusion coefficients in physiological solution are significant. This fact signalises that the polymer shapes are more compressed and molecules move faster in physiological solution, while in aqueous solution the chains are a little bit more stretched and possess bigger shapes in solution, so the diffusion movement is slower than in the presence of salt.

Figure 29: The dependence of diffusion coefficient of Hya-Rh on the concentration of VLMW HA in physiological solution.

In addition, the effect of salt also induces the shift of beginning of transition between diluted to semi-diluted concentration regime to higher concentrations of VLMW HA. If one

compare the deviations of diffusion coefficient at the concentration of 1 g·L^{-1} in physiological solution with the deviations of diffusion coefficient at the concentration of 0.005°g·L^{-1} and 0.01 g·L^{-1}, which all are significantly higher than other errors, a possible similarity could be noted. Consequently, the suggestion about the behaviour of Hya-Rh in aqueous solution of VLMW HA described in Figure 28 can be applied also for behaviour of Hya-Rh molecules in physiological solution. However, the beginning of chains overlapping is shifted to higher concentration of unlabelled polymer by the reason of affect of salt on the polyelectrolyte molecules.
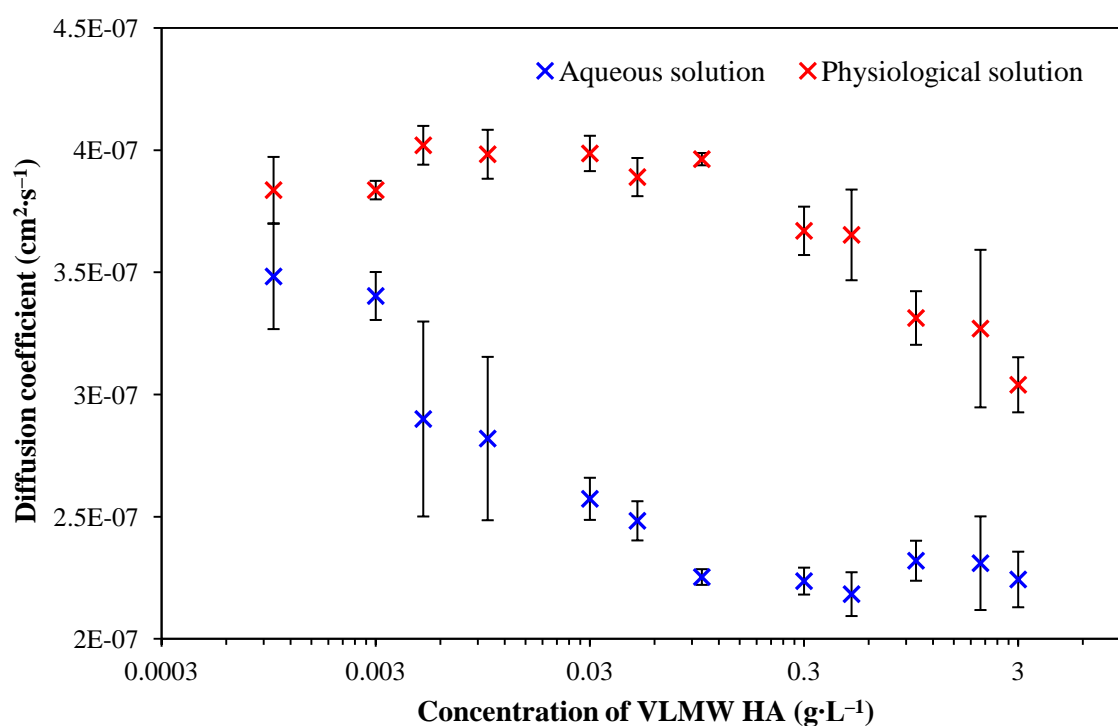
Figure 30: The comparison of dependence of diffusion coefficient values of Hya-Rh on the concentration of VLMW HA in aqueous and physiological solution.

5 CONCLUSION

Based on the first FCS measurements, it was recognized that the sample of Hya-Rh contained an amount of free probe molecules which brought incorrect results. Hence, it was found that every Hya-Rh store solution had to be separated by SEC separation process to get pure labelled polymer molecules and to prepare the storage solution of Hya-Rh used for following 2f-FCS measurements. In addition, the difference behaviour of Hya-Rh before and after SEC separation process and Rhodamine 110 were compare by fluorescence emission and excitation spectra to prove the difference base of each sample. So the calibration process and improvement of preparation of Hya-Rh samples for next measurements was devised, whereas it was also observed that the storage solution can be stored for three days, and then the new one had to be prepared to successfully determine the diffusion coefficient of labelled Hya-Rh.

Subsequently, the influence of concentration of Hya-Rh on value of diffusion coefficient in aqueous and physiological solution was checked because the concentration of Hya-Rh for next 2f-FCS measurements was not accurately known in virtue of the SEC separation process. Since that, it was determined that the concentration of Hya-Rh in aqueous solution did not change significantly with increasing concentration of Hya-Rh; however, in physiological solution the value of diffusion coefficient at the highest concentration of Hya-Rh differed and was affected by high deviation. Hence, this highest concentration of Hya-Rh in physiological solution was not used for next 2f-FCS measurements.

Then, diffusion characteristics of labelled hyaluronan were measured and discussed as a function of influence of ionic strength even presence of different alkali metal ions. Even if the values of diffusion coefficient changed with increasing concentration of salt in solution and for each cation, they were affected by deviations, and only the observation about apparent change of diffusion coefficient values at 0.1 and 1 $mol \cdot L^{-1}$ of salt could be noted.

Moreover, values of diffusion coefficient radius of labelled hyaluronan in solution of VLMW HA were studied in the dependence on concentration of the unlabelled polymer at different conditions such as in pure aqueous solution and physiological solution of 0.15 $mol \cdot L^{-1}$ NaCl. It was determined that significant change of diffusion coefficient of Hya-Rh occurs with increasing concentration of unlabelled hyaluronan, and assumption of explanation of measured data was described, whereas values of diffusion coefficient of Hya-Rh in physiological solution and in aqueous solution were compared.

Finally, as was proved in this thesis, the usage of 2f-FCS method has a great potential for measuring of hydrodynamic behaviour of fluorescently labelled hyaluronan in solutions, and this method enables to study solutions of this unique polymer in dependence on many conditions such as temperature, presence of bivalent ions or amphiphilic molecules in next future. These facts denote the future outlook and directions of following subject of hyaluronan research by using of 2f-FCS method.

6 REFERENCES

[1]   CROUZIER, Thomas, Thomas BOUDOU and Catherine PICART. Polysaccharide-based polyelectrolyte multilayers. *Current Opinion in Colloid & Interface Science*. 2010, vol. 15, issue 6, pp. 417-426. ISSN 0079-6700.

[2]   SCOTT, J. E., C. CUMMINGS; A. BRASS and Y. CHEN. Secondary and tertiary structures of hyaluronan in aqueous solution, investigated by rotary shadowing-electron microscopy and computer simulation. Hyaluronan is a very efficient network-forming polymer. *The Biochemical journal*. 1991, vol. 274 (Pt 3), pp. 699-705. ISSN 0264-6021.

[3]   SHEEHAN, John and Andrew ALMOND. Hyaluronan: Static, Hydrodynamic and Molecular Dynamic Views. *Glycoforum* [online]. 2001, [ref. 19. 3. 2015]. Available from: http://glycoforum.gr.jp/science/hyaluronan/HA21/HA21E.html

[4]   GRIBBON, Philip, Boon C. HENG and Timothy E. HARDINGHAM. The Molecular Basis of the Solution Properties of Hyaluronan Investigated by Confocal Fluorescence Recovery After Photobleaching. *Biophysical Journal*. 1999, vol. 77, issye 4, pp. 2210-2216. ISSN 0006-3495.

[5]   ALMOND, Andrew and Timothy E. HARDINGHAM. Hyaluronan: Current Macromolecular and Micromolecular Views. *Glycoforum* [online]. 2008, [ref. 19. 3. 2015]. Available from: http://www.glycoforum.gr.jp/science/hyaluronan/HA31/HA31E.html

[6]   MAGDE, D., E. L. ELSON and W. W. WEBB. Thermodynamic fluctuations in a reacting system–measurement by fluorescence correlation spectroscopy. *Phys. Rev. Lett*. 1972, vol. 29, pp. 705-708. ISSN 0031-9007.

[7]   SCHWILLE, Petra and Elke HAUSTEIN. Fluorescence Correlation Spectroscopy: An Introduction to its Concepts and Applications. *Biophysics Textbook Online* [online]. 2004. [cit. 2014-11-16] DOI: 10.1.1.405.2487. Article availability: http://www.biophysics.org/Portals/1/PDFs/Education/schwille.pdf

[8]   ATKINS, Peter and Julio DE PAULA. *Atkins' Physical chemistry*. 8th ed. Oxford: Oxford University Press, 2006, 1064 p. ISBN 01-987-0072-5.

[9]   BIRDI K.S. *Handbook of surface and colloid chemistry*. 2nd ed. Boca Raton: CRC Press, 2003, 765 p. ISBN 08-493-1079-2.

[10]   SHAW, Duncan J. *Introduction to Colloid and Surface Chemistry*. 4th Ed. New York: Butterworth Heinemann, 1992, 306 p. ISBN 07-506-1182-0.

[11]   ELIAS, Hans-Georg. *Macromolecules*. Weinheim: WILEY-VCH, c2008, xxxiv, 665 p. ISBN 978-3-527-28790-1.

[12]   PATTERSON, Gary. *Physical chemistry of macromolecules*. 2nd ed. Boca Raton: CRC Press, 2007, 136 p. ISBN 08-247-9467-2.

[13]   MASARO, L. and X.X. ZHU. Physical models of diffusion for polymer solutions, gels and solids. *Progress in Polymer Science*. 1999, vol. 24, issue 5, pp. 731-775. ISSN 0079-6700.

[14]   MARCUS, Yizhak. *Ions in water and biophysical implications from chaos to cosmos*. Dordrecht. Dordrecht: Springer, 2012. ISBN 978-940-0746-473.

[15]   BURKE, Matthew D., Jung O. PARK, Mohan SRINIVASARAO and Saad A. KHAN. Diffusion of Macromolecules in Polymer Solutions and Gels: A Laser Scanning

Confocal Microscopy Study. *Macromolecules*. New York: Elsevier Science, 2000, vol. 33, issue 20, pp. 7500-7507. ISSN 0024-9297.

[16] NYDÉN, Magnus and Olle SÖDERMAN. An NMR Self-Diffusion Investigation of Aggregation Phenomena in Solutions of Ethyl(hydroxyethyl)cellulose. *Macromolecules*. 199807, vol. 31, issue 15, pp. 4990-5002. ISSN 0024-9297.

[17] SEIFFERT, Sebastian and Wilhelm OPPERMANN. Diffusion of linear macromolecules and spherical particles in semidilute polymer solutions and polymer networks. *Polymer*. 2008, vol. 49, issue 19, pp. 4115-4126. ISSN 0032-3861.

[18] PHILLIES, George D. J., Thomas PIRNAT, Miklos KISS, Nancy TEASDALE, David MACLUNG, Heather INGLEFIELD, Craig MALONE, Anand RAU, Li Ping YU and James ROLLINGS. Probe diffusion in solutions of low-molecular-weight polyelectrolytes. *Macromolecules*. 198910, vol. 22, issue 10, pp. 4068-4075. ISSN 0024-9297.

[19] DE SMEDT, S. C., T. K. L. MEYVIS, J. DEMEESTER, P. VAN OOSTVELDT, J. C. G. BLONK and W. E. HENNINK. Diffusion of Macromolecules in Dextran Methacrylate Solutions and Gels As Studied by Confocal Scanning Laser Microscopy. *Macromolecules*. 199708, vol. 30, issue. 17, pp. 4863-4870. ISSN 0024-9297.

[20] SCOTT John E. Secondary and Tertiary Structures of Hyaluronan in Aqueous Solution. Some Biological Consequences. *Glycoforum* [online]. 1998, [ref. 19. 3. 2015]. Available from: http://glycoforum.gr.jp/science/hyaluronan/HA02/HA02E.html

[21] HASCALL Vincent C. and Torvard C. LAURENT. Hyaluronan: Structure and Physical Properties. *Glycoforum* [online]. 1997, [ref. 19. 3. 2015]. Available from: http://glycoforum.gr.jp/science/hyaluronan/HA01/HA01E.html

[22] ALBERTS, Bruce et al. *Molecular biology of the cell*. 4th ed. New York: Garland Science, 2002, 1463 s. ISBN 0-8153-4072-9.

[23] GHOSH Peter, Nongporn HUTADILOK, Naomi ADAM and Aldo LENTINI. Interactions of hyaluronan (hyaluronic acid) with phospholipids as determined by gel permeation chromatography, multi-angle laser-light-scattering photometry and ^{1}H-NMR spectroscopy. International Journal of Biological macromolecules. 1994, vol. 16, issue 5, pp. 237-244. ISSN 0141-8130.

[24] HEJNÁ, J. *Hyaluronan micro- and nanoparticles*. Brno: Brno University of Technology, Faculty of Chemistry, 2013. 68 p. Supervisor prof. Ing. Miloslav Pekař, CSc..

[25] SHENOY, V. and J. ROSENBLATT. Diffusion of Macromolecules in Collagen and Hyaluronic Acid, Rigid-Rod-Flexible Polymer, Composite Matrixes. *Macromolecules*. 199512, vol. 28, issue 26, pp. 8751-8758. ISSN 0024-9297.

[26] NOGOVITSIN, E.A. and Yu.A. BUDKOV. Self-consistent field theory investigation of the behaviour of hyaluronic acid chains in aqueous salt solutions. *Physica A: Statistical Mechanics* and its Applications [online]. 2012, vol. 391, issue 8, pp. 2507-2517. ISSN 0378-4371.

[27] MATTEINI, Paolo, Luigi DEI, Emiliano CARRETTI, Nicola VOLPI, Andrea GOTI a Roberto PINI. Structural Behavior of Highly Concentrated Hyaluronan. *Biomacromolecules*. 2009, vol. 10, issue 6, pp. 1516-1522. ISSN 1525-7797.

[28] FURLAN, Sara, Giovanni LA PENNA, Angelo PERICO a Attilio CESÀRO. Hyaluronan chain conformation and dynamics. *Carbohydrate Research*. 2005, vol. 340, i. 5, pp. 959-970. ISSN 0008-6215.

[29] COWMAN, Mary K. a Shiro MATSUOKA. Experimental approaches to hyaluronan structure. *Carbohydrate Research*. 2005, vol. 340, i. 5, pp. 791-809. ISSN 0008-6215.

[30] BILEROVÁ H. *Rheology of hyaluronan solutions*. Brno: Brno University of Technology, 2012, 109 p. The thesis on faculty ofchemistry, , Institute of Physical and Applied Chemistry. Supervisor Prof. Ing. Miloslav Pekař, CSc.

[31] FUDALA, Rafal, Mark E. MUMMERT, Zygmunt GRYCZYNSKI a Ignacy GRYCZYNSKI. Fluorescence detection of hyaluronidase. *Journal of Photochemistry & Photobiology, B: Biology*. 2011, vol. 104, i. 3, p. 473-477. ISSN 1011-1344.

[32] RICH, Ryan M., Mark MUMMERT, Zeno FOLDES-PAPP, Zygmunt GRYCZYNSKI, Julian BOREJDO, Ignacy GRYCZYNSKI and Rafal FUDALA. Detection of hyaluronidase activity using fluorescein labeled hyaluronic acid and Fluorescence Correlation Spectroscopy. *Journal of Photochemistry & Photobiology, B: Biology*. 2012, vol. 116, p. 7-12. ISSN 1011-1344.

[33] *Detection of hyaluronidase activity using fluorescence lifetime correlation spectroscopy to separate diffusing species and eliminate autofluorescence*. Single Molecule Spectroscopy and Superresolution Imaging VI, 2013, Virich, R. M., Mummert M., Gryczynski Y., Borejdo J., Gryczynski I., Sørensen T.J., Laursen B.W., Fudala R., Enderlein J., Gregor I., Gryczynski Z.K., Erdmann R. and F. Koberling.

[34] HALASOVÁ, T. *Interactions Between Hyaluronan and Amphiphilic Molecules*. Brno: Brno University of Technology, Faculty of Chemistry, 2013. 160 p. Supervisor prof. Ing. Miloslav Pekař, CSc..

[35] MEUNIER, Françoise and Kevin J WILKINSON. Nonperturbing fluorescent labeling of polysaccharides. *Biomacromolecules*. 2002, vol. 3, issue. 4, p. 857. ISSN 1525-7797.

[36] THERMO FISHER SCIENTIFIC INC. *Life Technologies* [online]. 2015 [ref. 2015-03-19]. Available from: https://www.lifetechnologies.com/de/en/home.html

[37] SAUER, Markus, Johan HOFKENS and Jörg ENDERLEIN. *Handbook of fluorescence spectroscopy and imaging: from single molecules to ensembles*. Weinheim: Wiley-VCH, 2011, ix, 281 p. ISBN 978-3-527-31669-4.

[38] ENDERLEIN, Jörg, Ingo GREGOR, Digambara PATRA and Jörg FITTER. Art and Artefacts of Fluorescence Correlation Spectroscopy. *Current Pharmaceutical Biotechnology*. 2004, vol. 5, issue 2, p. 155-161. ISSN 1389-2010.

[39] LAKOWICZ, Joseph R. *Principles of Fluorescence Spectroscopy*. 2nd Ed. New York: Kluwer Academic Publishers, 1999, 698 s. ISBN 0-306-46093-9.

[40] MACHÁŇ, Radek a Thorsten WOHLAND. Recent applications of fluorescence correlation spectroscopy in live systems. *FEBS Letters*. 2014, vol. 588, issue. 19, pp. 3571-3584. ISSN 0014-5793.

[41] KOYNOV, Kaloian a Hans-Jürgen BUTT. Fluorescence correlation spectroscopy in colloid and interface science.*Current Opinion in Colloid & Interface Science*. 2012, vol. 17, issue. 6, pp. 377-387. ISSN 1359-0294.

[42] ZETTL, H, W HAFNER, A BOKER, H SCHMALZ, M LANZENDORFER, Ahe MULLER and G KRAUSCH. Fluorescence correlation spectroscopy of single dye-labeled polymers in organic solvents. *Macromolecules*. AMER CHEMICAL SOC, 2004, vol. 37, i. 5, pp. 1917-1920. ISSN 0024-9297.

[43] LIU, RG, X GAO, J ADAMS a W OPPERMANN. A fluorescence correlation spectroscopy study on the self-diffusion of polystyrene chains in dilute and semidilute solution. *Macromolecules*. AMER CHEMICAL SOC, 2005, vol. 38, i. 21, pp. 8845-8849. ISSN 0024-9297.

[44] GRABOWSKI, Ca and A MUKHOPADHYAY. Diffusion of polystyrene chains and fluorescent dye molecules in semidilute and concentrated polymer solutions. *Macromolecules*. AMER CHEMICAL SOC, 2008, vol. 41, i. 16, pp. 6191-6194. ISSN 0024-9297.

[45] CHERDHIRANKORN, T, A BEST, K KOYNOV, K PENEVA, K MUELLEN and G FYTAS. Diffusion in Polymer Solutions Studied by Fluorescence Correlation Spectroscopy. *Journal Of Physical Chemistry B*. AMER CHEMICAL SOC, 2009, vol. 113, i. 11, pp. 3355-3359. ISSN 1520-6106.

[46] ZETTL, U, M BALLAUFF a L HARNAU. A fluorescence correlation spectroscopy study of macromolecular tracer diffusion in polymer solutions. *Journal Of Physics-Condensed Matter*. IOP PUBLISHING LTD, 2010, vol. 22, i. 49. ISSN 0953-8984.

[47] ZETTL, U, St HOFFMANN, F KOBERLING, G KRAUSCH, J ENDERLEIN, L HARNAU and M BALLAUFF. Self-Diffusion and Cooperative Diffusion in Semidilute Polymer Solutions As Measured by Fluorescence Correlation Spectroscopy. *Macromolecules*. AMER CHEMICAL SOC, 2009, vol. 42, i. 24, pp. 9537-9547. ISSN 0024-9297.

[48] MICHELMAN-RIBEIRO, A, F HORKAY, R NOSSAL and H BOUKARI. Probe diffusion in aqueous poly(vinyl alcohol) solutions studied by fluorescence correlation spectroscopy. *Biomacromolecules*. AMER CHEMICAL SOC, 200705, vol. 8, i. 5, p. 1595-1600. ISSN 1525-7797.

[49] PRISTINSKI, D, V KOZLOVSKAYA a SA SUKHISHVILI. Fluorescence correlation spectroscopy studies of diffusion of a weak polyelectrolyte in aqueous solutions. *Journal Of Chemical Physics*. AMER INST PHYSICS, 2005, vol. 122, i. 1. ISSN 0021-9606.

[50] PAPADAKIS, CM, P KOSOVAN, W RICHTERING and D WOLL. Polymers in focus: fluorescence correlation spectroscopy. *Colloid And Polymer Science*. SPRINGER, 201410, vol. 292, i. 10, p. 2399-2411. ISSN 0303-402X.

[51] ENDERLEIN, Jörg, Ingo GREGOR, Digambara PATRA, Thomas DERTINGER and U. Benjamin KAUBB. Performance of Fluorescence Correlation Spectroscopy for Measuring Diffusion and Concentration. *ChemPhysChem*. 2005-11-11, vol. 6, issue 11, pp. 2324-2336. ISSN 1439-4235.

[52] ENDERLEIN, Jörg. Fluorescence correlation spectroscopy (IUPAC Technical Report): A New Tool for Accurate and Absolute Diffusion Measurements. *Pure and Applied Chemistry*. 2013-01-2, vol. 85, issue 5, p. -. ISSN 0033-4545.

[53] *Recent Advances in Fluorescence Lifetime Correlation Spectroscopy (FLCS) and Two Focus FCS*. 10th Workshop on FCS and Related Methods Sapporo, 2007; Ortmann U., Enderlein J., Krämer B., Koberling F., Kapusta P., Ewers B., Buschmann V., Patting M., Wahl M. and R. Erdmann.

[54] DERTINGER, Thomas, Victor PACHECO, Iris VON DER HOCHT, Rudolf HARTMANN, Ingo GREGOR and Jörg ENDERLEIN. Two-Focus Fluorescence Correlation Spectroscopy: A New Tool for Accurate and Absolute Diffusion

Measurements. *ChemPhysChem*. 2007-02-19, vol. 8, issue 3, pp. 433-443. ISSN 1439-4235.

[55] DERTINGER, Thomas. *Two-Focus Fluorescence Correlation Spectroscopy*. Köln, 2007. Ph.D. Thesis. Universität zu Köln. Supervisor Priv. Doz. Dr. Jörg Enderlein.

[56] MÜLLER, Claus B., Anastasia LOMAN, Walter RICHTERING and Jörg ENDERLEIN. Dual-Focus Fluorescence Correlation Spectroscopy of Colloidal Solutions: Influence of Particle Size. *The Journal of Physical Chemistry B*. 2008, vol. 112, issue 28, pp. 8236-8240. ISSN 1520-6106.

[57] MÜLLER, Claus Bernard. *Applications of Two Focus Fluorescence Correlation Spectroscopy in Colloid and Polymer Science*. Aachen, 2008. Ph.D. Thesis. Aachen University.

[58] MÜLLER, Claus B., Walter RICHTERING, Qui VAN, Stefanie KRAMER, Ingo GREGOR and Jörg ENDERLEIN. Sealed and temperature-controlled sample cell for inverted and confocal microscopes and fluorescence correlation spectroscopy. *Colloid and Polymer Science*. 2008, vol. 286, issue 11, pp. 1215-1222. ISSN 0303-402X.

[59] MÜLLER, Claus B., Kerstin WEIß, Anastasia LOMAN, Jörg ENDERLEIN and Walter RICHTERING. Remote temperature measurements in femto-liter volumes using dual-focus-Fluorescence Correlation Spectroscopy. *Lab on a Chip*. 2009, vol. 9, issue 9, p. 1248-. ISSN 1473-0197.

[60] ARBOUR, Tyler J. and Jörg ENDERLEIN. Application of dual-focus fluorescence correlation spectroscopy to microfluidic flow-velocity measurement. *Lab on a Chip*. 2010, vol. 10, issue 10, p. 1286-. ISSN 1473-0197.

[61] LOMAN, Anastasia, Ingo GREGOR, Christina STUTZ, Markus MUND and Jörg ENDERLEIN. Measuring rotational diffusion of macromolecules by fluorescence correlation spectroscopy. *Photochemical and Photobiological Sciences*. 2010, vol. 9, issue 5, pp. 627-636. ISSN 1474-905X.

[62] WEIß, Kerstin, Jörg ENDERLEIN, Christina STUTZ and Markus MUND. Lipid Diffusion within Black Lipid Membranes Measured with Dual-Focus Fluorescence Correlation Spectroscopy. *ChemPhysChem*. 2012, vol. 13, issue 4, pp. 990-1000. ISSN 1439-4235.

[63] WEIß, Kerstin, Andreas NEEF, Qui VAN, Stefanie KRAMER, Ingo GREGOR and Jörg ENDERLEIN. Quantifying the Diffusion of Membrane Proteins and Peptides in Black Lipid Membranes with 2-Focus Fluorescence Correlation Spectroscopy. *Biophysical Journal*. 2013, vol. 105, issue 2, pp. 455-462. ISSN 0006-3495

[64] MAFFRE, Pauline, Karin NIENHAUS, Faheem AMIN, Wolfgang J PARAK and G Ulrich NIENHAUS. Characterization of protein adsorption onto FePt nanoparticles using dual-focus fluorescence correlation spectroscopy. *Beilstein Journal of Nanotechnology*. 2011, vol. 2, issue 11, pp. 374-383. ISSN 2190-4286.

[65] WONG, John E., Claus B. MÜLLER, Ana M. DÍEZ-PASCUAL, Walter RICHTERING and G. Ulrich NIENHAUS. Study of Layer-by-Layer Films on Thermoresponsive Nanogels Using Temperature-Controlled Dual-Focus Fluorescence Correlation Spectroscopy. *The Journal of Physical Chemistry B*. 2009-12-10, vol. 113, issue 49, pp. 15907-15913. ISSN 1520-6106.

[66] RIES, Jonas, Zdeněk PETRÁŠEK, Anna J GARCÍA-SÁEZ and Petra SCHWILLE. A comprehensive framework for fluorescence cross-correlation spectroscopy. *New Journal of Physics*. 2010-11-01, vol. 12, issue 11, p. 113009-. ISSN 1367-2630.

[67] KORLANN, You, Thomas DERTINGER, Xavier MICHALET, Shimon WEISS and Jörg ENDERLEIN. Measuring diffusion with polarization-modulation dual-focus fluorescence correlation spectroscopy. *Optics Express*. 2008, vol. 16, issue 19, pp. 14609-14616. ISSN 1094-4087.

[68] ŠTEFL, Martin, Aleš BENDA, Ingo GREGOR, Martin HOF, Walter RICHTERING and Jörg ENDERLEIN. The fast polarization modulation based dual-focus fluorescence correlation spectroscopy. *Optics Express*. 2014, vol. 22, issue 1, p. 885-. ISSN 1094-4087.

[69] LAVIS, Luke D., Tzu-Yuan CHAO and Ronald T. RAINES. Fluorogenic label for biomolecular imaging. *ACS chemical biology*. 2006, vol. 1, issue 4, pp. 252-260. ISSN 1554-8929.

[70] KAPUSTA, Peter. PICOQUANT GMBH. *Absolute Diffusion Coefficients: Compilation of Reference Data for FCS Calibration: Application Note*. Berlin, July 2010. Avaible from:
http://www.picoquant.com/images/uploads/page/files/7353/appnote_diffusioncoefficients.pdf

[71] SHANNON, R. D. Revised effective ionic radii and systematic studies of interatomic distances in halides and chalcogenides. *Acta. Crystallographica Section A*. 1976, vol. 32, issue 5, pp. 751-767. ISSN 2053-2733.

7   LIST OF USED ABBREVIATIONS AND SYMBOLS

2f-FCS	Dual-focus fluorescence correlation spectroscopy
A1	Autocorrelation function of first volume
A2	Autocorrelation function of second volume
ACF	Autocorrelation function
CAS	Chemical abstract service registry number
CCF	Crosscorrelation function
CPS	Counts per second
CPSM	Counts per second per molecule
DIC	Differential interference contrast microscopy
DLS	Dynamic light scattering
FCS	Fluorescence correlation spectroscopy
FLCS	Fluorescence life-time correlation spectroscopy
FRAP	Fluorescence recovery after photo-bleaching
FRET	Fluorescence resonance energy transfer
GUV	Giant unilamelar vesicles
HMW HA	High molecular weight hyaluronan
Hya-Rh	Hyaluronan Rhodamine 110
LMW HA	Low molecular weight hyaluronan
MDF	Molecule detection function
NB	Number of batch
NP	Nomarski prism
pfNMR	Pulsed-field nuclear magnetic resonance
PIE	Pulsed interleaved excitation
pmFCS	Polarization modulated fluorescence correlation spectroscopy
SEC	Size exclusion chromatography
SEC-MALLS	Size exclusion chromatography with multi-angle laser light scattering
SPAD	Single photon avalanche diode
VLMW HA	Very low molecular weight hyaluronan
X	Crosscorrelation function between both volumes
A	Absorption
a	Scaling factor
b	Exponential factor
c	Concentration
c^*	Chain overlap concentration
c^{**}	Critical entanglement concentration
c_{App}	Approximated concentration of Hya-Rh
c_P	Mass concentration of polymer in solution
$\langle c \rangle$	Mean value of concentration in time
D_0	Diffusion coefficient in pure solvent
D_i	Diffusion coefficient
f_i	Friction coefficient

F	Motive force of diffusion
$G_{ACF}(\tau)$	Autocorrelation function
$G_{CCF}(\tau)$	Crosscorrelation function
$G(t_0)$	Value of correlation in time zero
h	Radius of pinhole divided by magnification of objective
I	Intensity
I_1, I_2	Fluorescence intensity in first focus and in second focus
j	Refractive index of medium
k_B	Boltzmann constant
K	Constant
l	Optical distance
m	Weight
M	Molar mass
M_w	Mass average molar mass
n	Molar amount
N	Number of dispersed particles
N_A	Avogadro's constant
$P(\delta c)$	Probability density function
$P(x,t)$	Probably distribution function of shift of particle
q	Intensity of diffusion flow
$\mathbf{r}$	Vector of position in one of detection volumes
R	Exponential term
R_H	Hydrodynamic radius
$\langle R^2 \rangle$	Quadratic mean distance of ends of polymer chain
$R(z)$	Model parameter of MDF denoting radius of confocal volume
t	Time
T	Thermodynamic temperature
$U(\mathbf{r})$	Molecule detection function
$w_0, R_0,$	Parameters of detection volume
$w(z), ,$	Model parameter of MDF denoting radius of confocal volume
x	Distance
$\hat{\mathbf{x}}$	Unit vector along x axis
$\langle x^2 \rangle$	Mean square distance of particle in time t
α	Solvent quality factor
δ	Distance of Nomarski prism
δc	Deviation of the mean concentration
δG	Deviation of Gibbs energy
ΔG_{diss}	Gibbs energy of polymer dissolving in solvent
ΔH_{diss}	Enthalpy of dissolving
ΔS_{diss}	Entropy of dissolving
ε	Molar extinction coefficient
$\varepsilon_1, \varepsilon_2$	Factors related with excitation power and detection efficiency

$[\eta]$	Limiting viscosity number
η_0	Viscosity of solvent
θ	Theta solvent
$\kappa(z)$	Model parameter of MDF denoting eccentricity of detection volume
λ	Wavelength
λ_{em}	Emission wavelength
λ_{ex}	Excitation wavelength
μ_i	Chemical potential of dispersed part
$\overline{\mu}$	Mean velocity of translational movement
ρ	Density of polymer solution
ρ_P	Bulk density of polymer solution
υ	Flory exponent
φ_1	Volume fraction of solvent
φ_2	Volume fraction of polymer
χ	Flory-Huggins interaction parameter

8 LIST OF APPENDIX

Appendix 1: Jabłoński diagram
Appendix 2: Manual for 2f-FCS measurement
Appendix 3: SEC-MALLS analysis of Hyaluronan Rhodamine 110
Appendix 4: SEC separation data

APPENDIX

Appendix 1: Jabłoński diagram
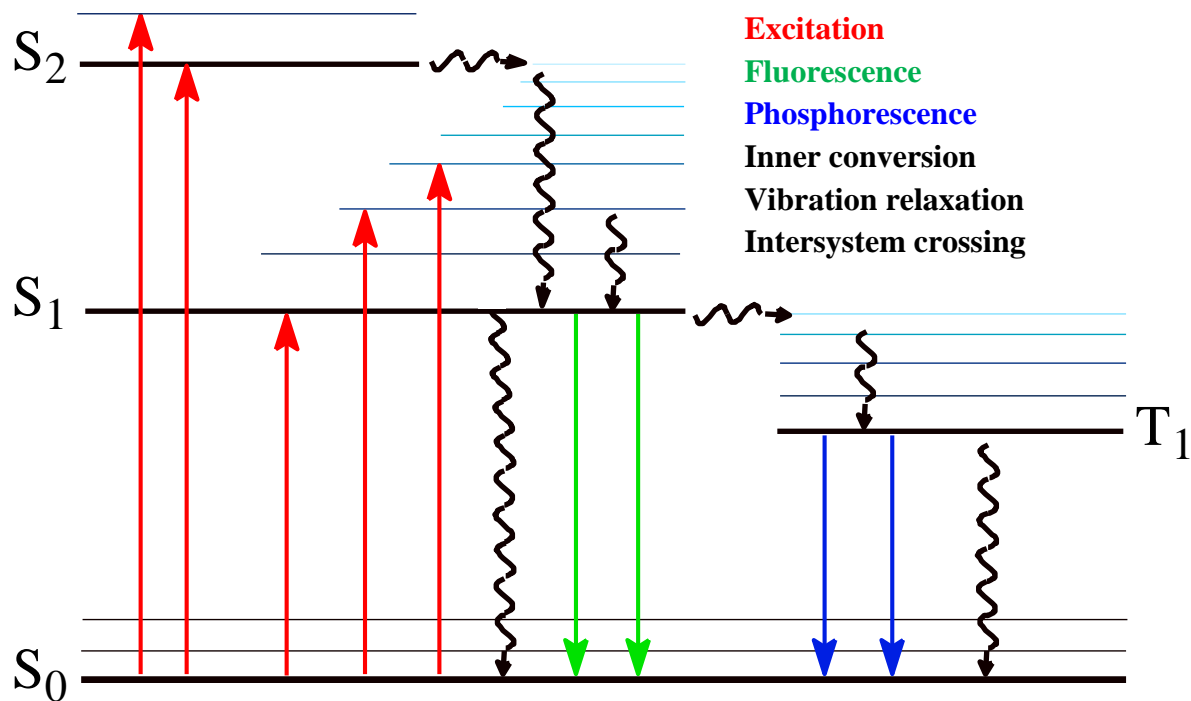
Appendix 2: Manual for 2f-FCS measurement

The aim of this work is describing 2f-FCS measurement set up, which deals with depicting of details how to adjust the instrument to the right state to start measure by 2f-FCS technique. At the beginning, it is necessary to note some information about the instrument. The 2f-FCS measurements are performed at the inverted epifluorescent time-resolved confocal microscope (Microtime 200, PicoQuant GmbH) with water immersion objective (Olympus, UPLSAPO 60XW). Horizontally and vertically polarized pulsed diode lasers of 640 nm, 510 nm or 470 nm wavelength (LDH Series) could be used as an excitation source. The excitation power is set to optional excitation power together with adjustable TCSPC resolution and overall repetition rate (20, 40 or 80 MHz). The size of pinhole is usually 150 μm and 10 min measurement time of each sample is recommended. The signal is collected in four photon counting detectors (two τ-SPAD or two MPD). For analysis, software SymphoTime 64 and then for calculations programme Matlab are used. Finally, the most essential component is Nomarski prism, which generates two shifted and overlapped foci. The determination of the distance of Nomarski prism by probe with known diffusion coefficient is performed after every measurement at the similar conditions as the measurements of your samples are done.
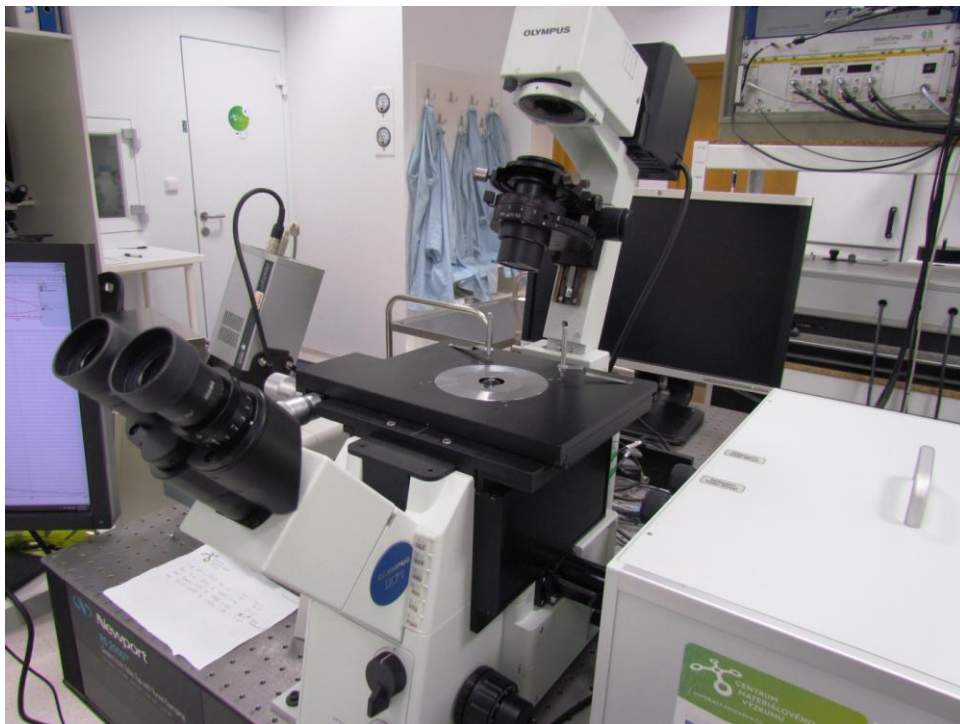
Fig. 1: The photo of confocal fluorescence microscope in lab at FCH BUT.

Procedure

This description is composed of several steps how to adjust the instrument to measure by 2f-FCS technique:

1) Before switching on the instrument and PC, it is necessary to check the dichroic mirror (red arrow in Fig. 2) and emission filters (green arrow in Fig. 2) according to the used

lasers wavelength. Then, the objective has to be adjusted, alternatively changed to the right one with the magnification of 60 (Fig. 3).
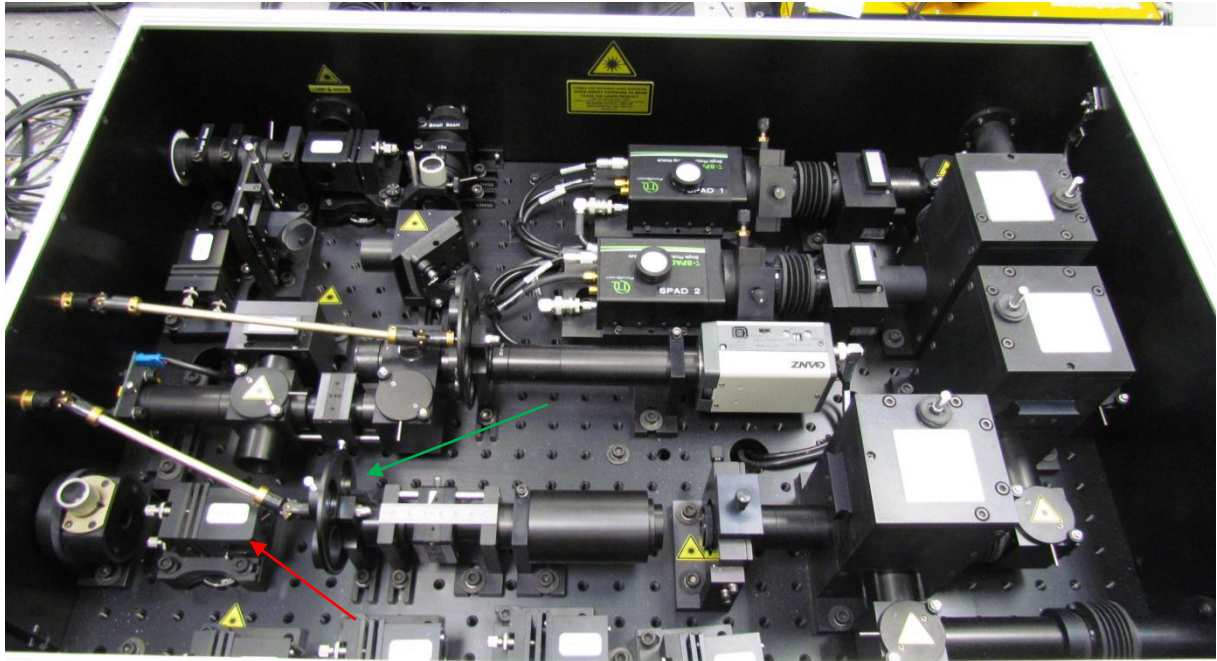
Fig. 2: The optical arrangement of FCS unit.
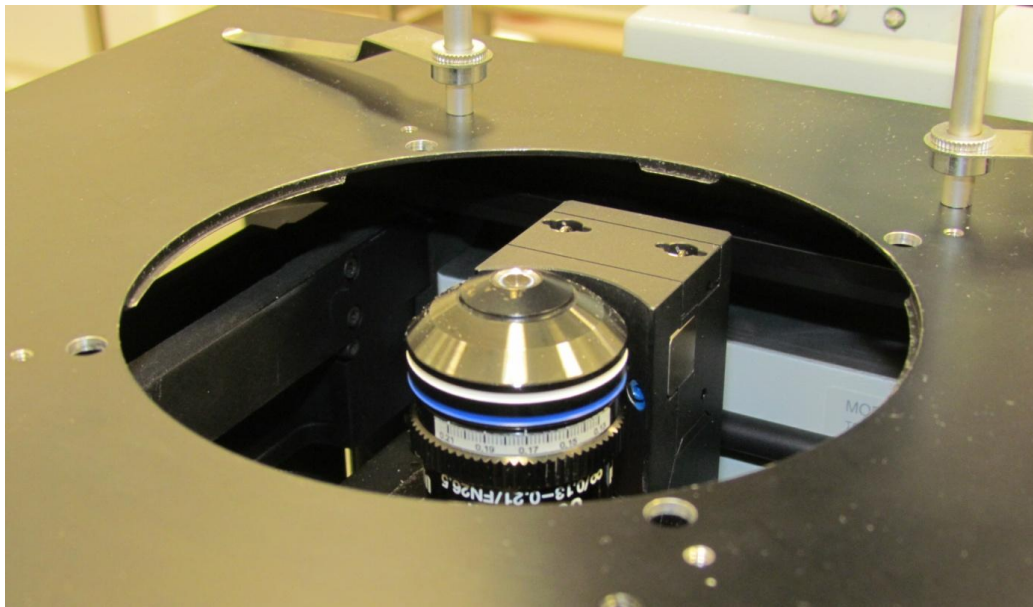
Fig. 3: The objective with magnification of 60 which is used for 2f-FCS measurements.

2) For 2f-FCS technique it is necessary to use two orthogonally polarized lasers, so check the connection of lasers which will be used. Then, turn on the red adaptor to start all units simultaneously.

Fig. 4: The connections of laser heads to multichannel diode laser unit.

3) Adjust the position of button in the laser combining unit to the small beam regime (Fig. 5). It is also necessary to move down with the mirror in the optical unit, how it is shown in Fig. 6 by yellow arrow.

4) Switch on the programme SymphoTime and turn on the manual control.

5) Drop a small amount of water on the objective and put on it the holder with glass slide. Then by using of camera, find the interface of glass and air.

6) Find the cross of laser beam and if it is needed, move with the beam displacer (blue arrow in the Fig. 6) to adjust the cross to the symmetrical position in the middle of the screen.

7) Turn on the detectors; however, be aware of the intensity of signal and decrease at first the intensity of light by dim filters (OD3).

8) Check the size of pinhole in the instrument and change it to the 150 μm sized pinhole (Fig. 7).

Fig. 5: The position of button in the small beam regime.
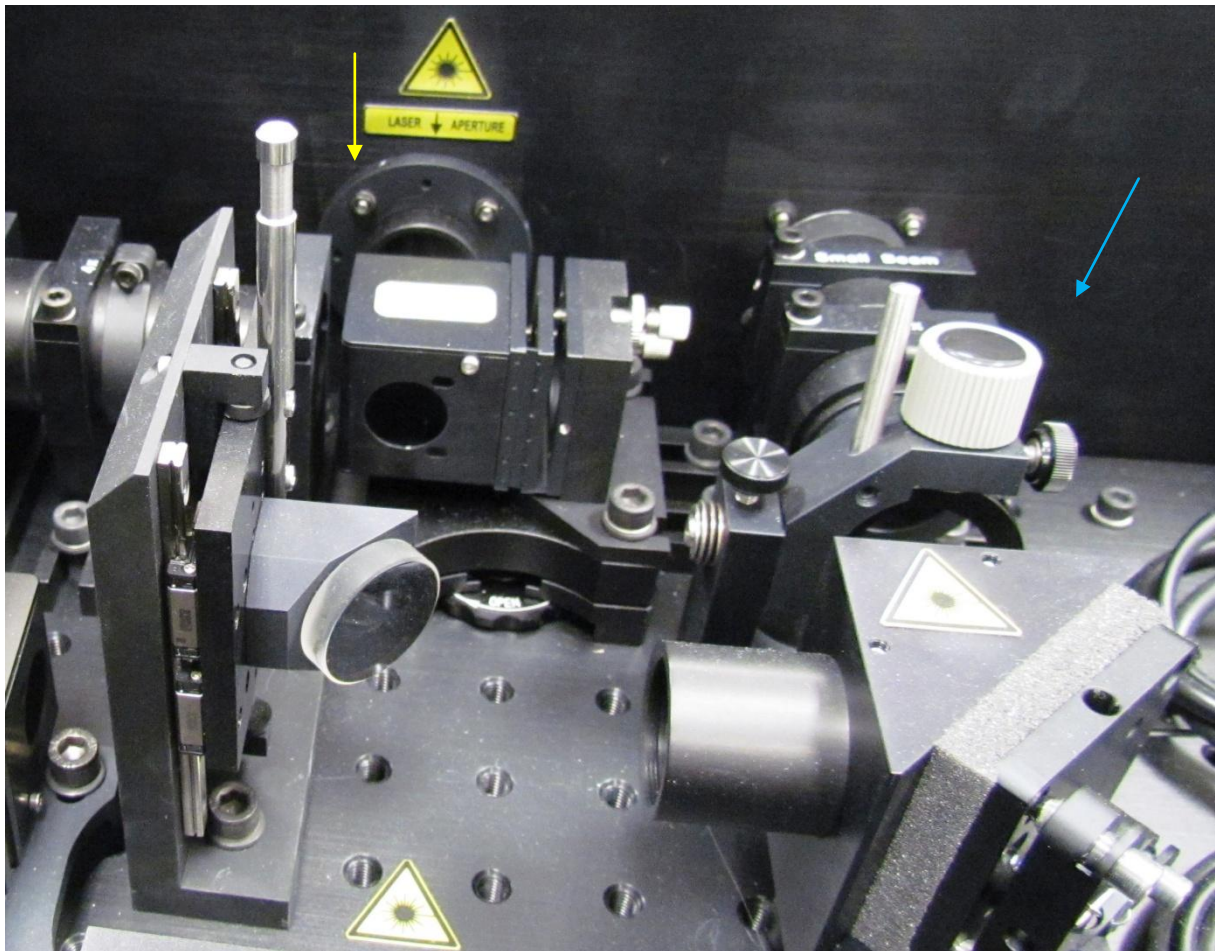
Fig. 6: The picture of mirror for adjusting of small beam regime (yellow arrow) and beam displacer (blue arrow).

9) On the screen of the programme, choose the *test regime* and start the time-trace mode. By using of backscattering signal, optimize and adjust the position of pinhole manually to get the maximum signal by moving of the micro-screw simultaneously with pinhole rotational screws. Then, turn on the TCSPC mode and also adjust the right position of used detectors by moving of rotational screws to get very sharp TSCPC curves.
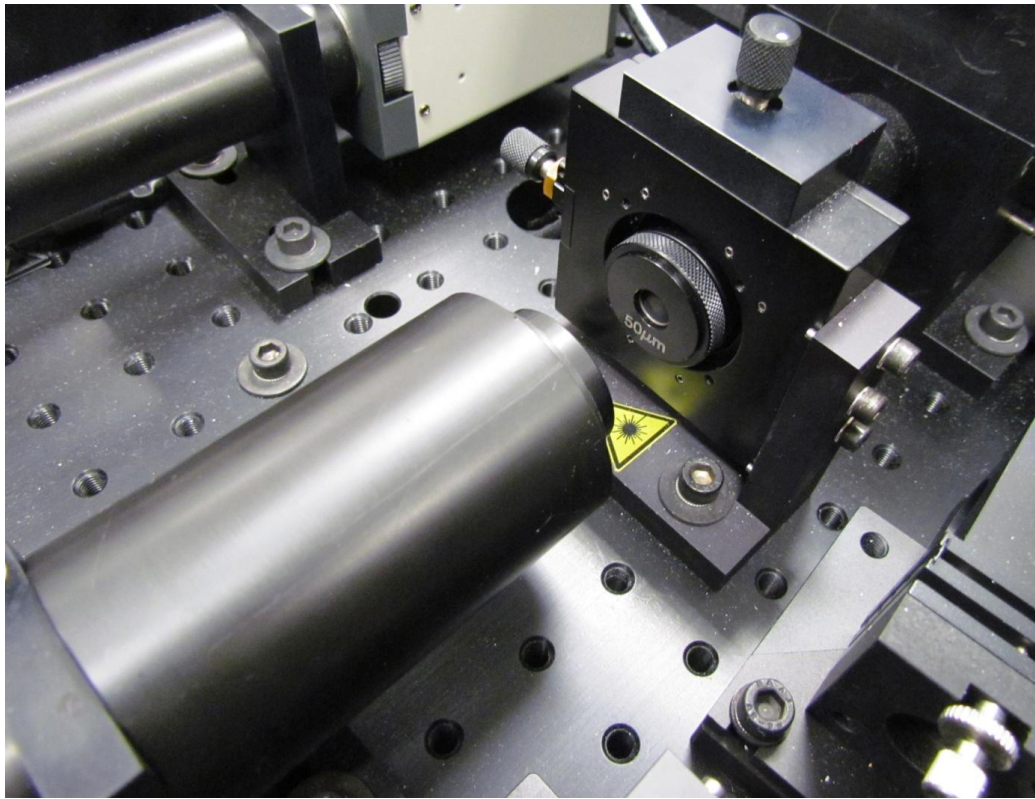
Fig. 7: The picture of pinhole in optical unit.

Fig. 8: The sample holder with glass slide and drop of sample.
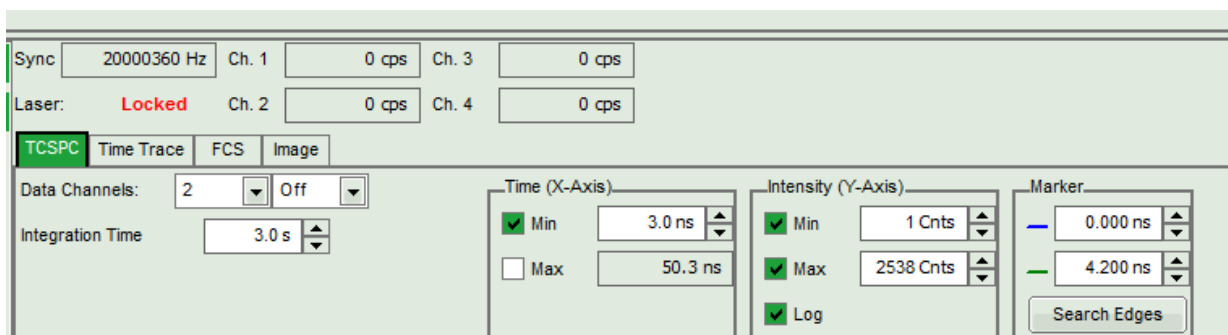
Fig. 9: Image of SymphoTime programme TCSPC mode set-up.

10) Drop your sample on the glass slide and cover it. Then, rotate with micro-screw to get to the sample and adjust the emission filter, which you want to use.

11) Optimize the excitation power and recalculate the laser power in arbitrary units with the table of power diode conversion factors which you can find in lab to get the absolute laser power in µW units. It is necessary to decrease or increase the excitation power of lasers according to changes of the signal which you can see to come to the detector. However, you have to also switch on both lasers, whereas choose the pulsed interleaved excitation (PIE), and look in the TCSPC mode to adjust the intensity of each laser to get the same high of both TCSPC curves. Fig. 10 shows the TCSPC mode, where two lifetime curves can be seen, but according to increasing or decreasing of the excitation power of one of the lasers their heights have to be adjusted to the almost similar value of intensity.

12) As the next step, put the prism to the microscope body (red arrow in the Fig. 12).

13) Now, you can start to measure. Change the regime to Measurement regime and choose FCS mode. Do not forget to measure also 2f-FCS of probe standard, which value of diffusion coefficient has already been accurately specified and which can be excited by used laser wavelength.
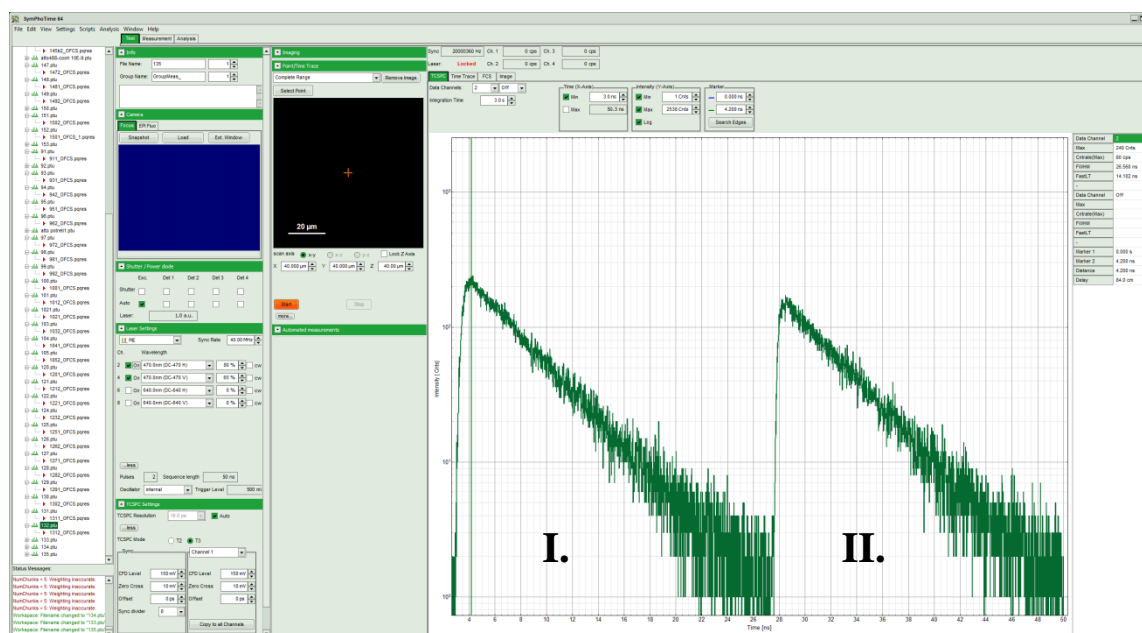
Fig. 10: The TCSPC mode with life-time curves, where the first one relates to the first focus and the second one relates with the second focus.
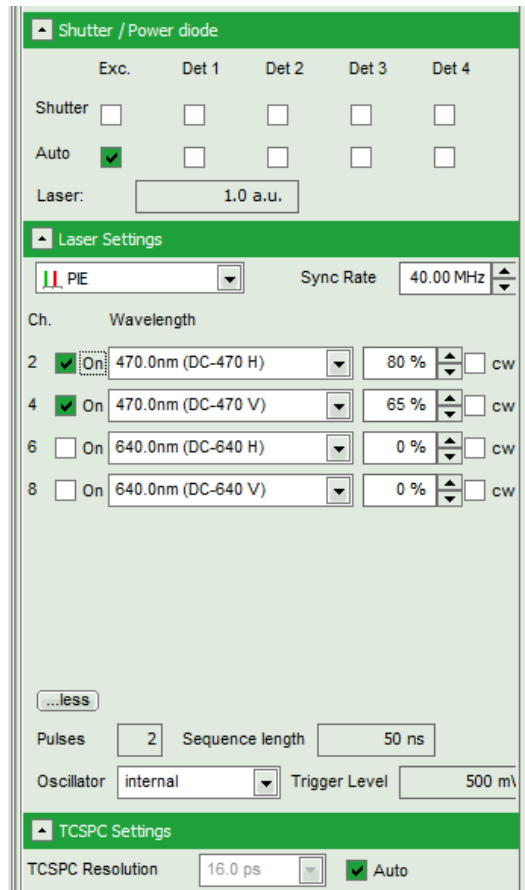
Fig. 11: Image of laser excitation power set up.

*Fig. 12: The microscope body with description where put the Nomarski prism (red arrow).*

14) Note the temperature. It is also recommended to temperate your samples at laboratory temperature, if you store it in a fridge. For any cases, you can use sample chamber.

15) Analysis of measured data is simple. At first, choose the file which contains obtained data, then start FCS analysis as is describe in Fig. 13.

16) After the loading of data, start to generate at first the autocorrelation function of the first focus, the autocorrelation function of the second focus and finally, the crosscorrelation of both foci with each other, whereas choose the data channels which you used as detectors. In case you used just one detector, it is necessary to enable FLCS background correction. For the other case, if you use two detectors in your measurement set-up, then it is not necessary; however, it is better to use it to eliminate the noise. The example of crosscorrelation analysis by using of one detector is shown in Fig. 14.
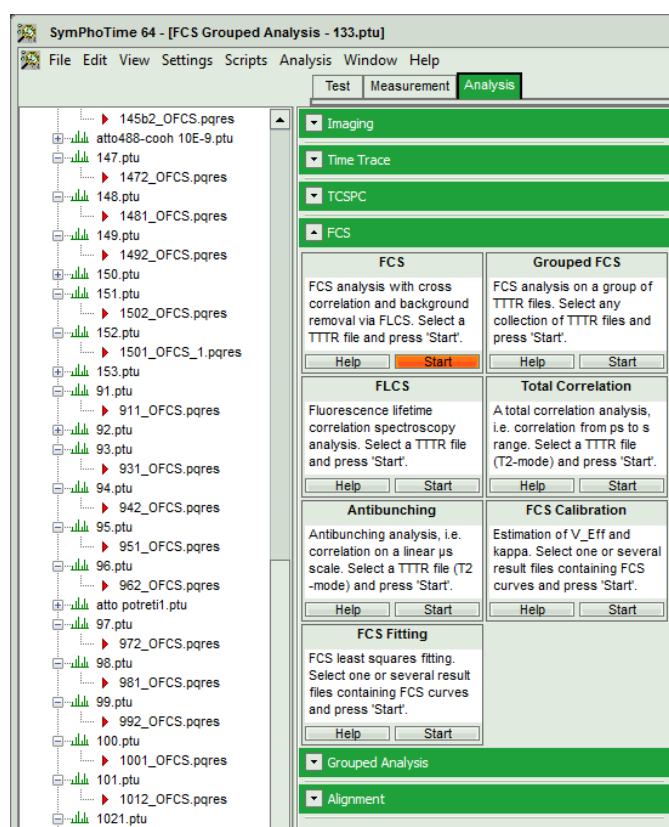

Fig. 13: The description of pathway how to analyse measured data.

17) After calculation, you will obtain the correlation curve. For Matlab analysis, export the data as a data file (.DAT) by clicking on the right button of your mouse. Choose to export all cells, how it is shown in Fig. 16, and save the data file.

18) In the end, please, set the instrument to the original state (change the pinhole to 50 μm size, change the small beam to the large beam regime in optical unit as well as in laser combining unit, and get the prism out of the microscope body).
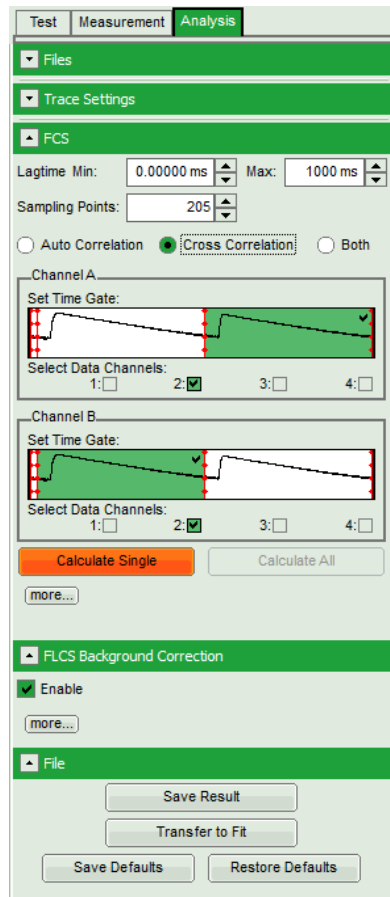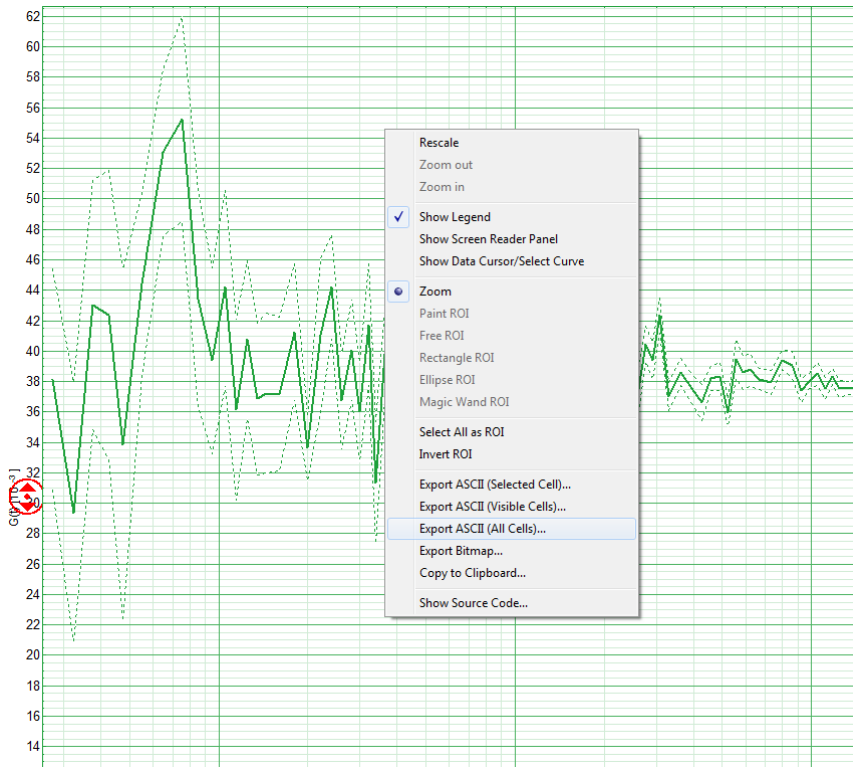
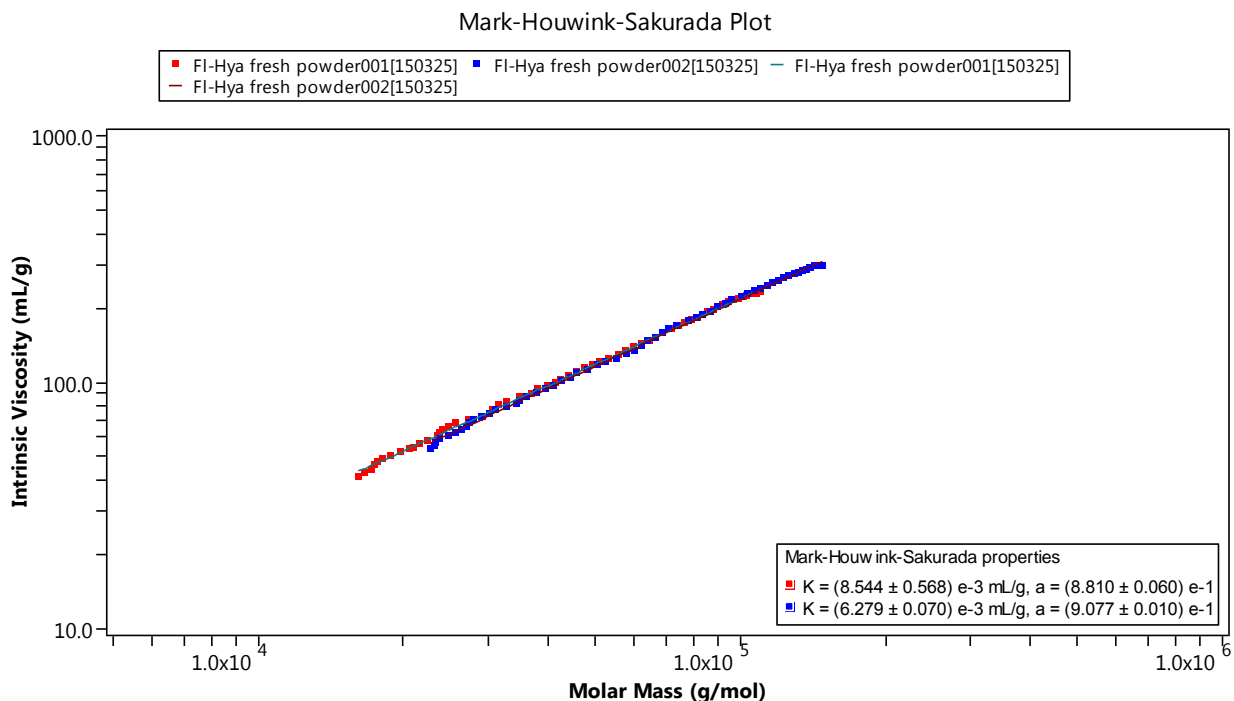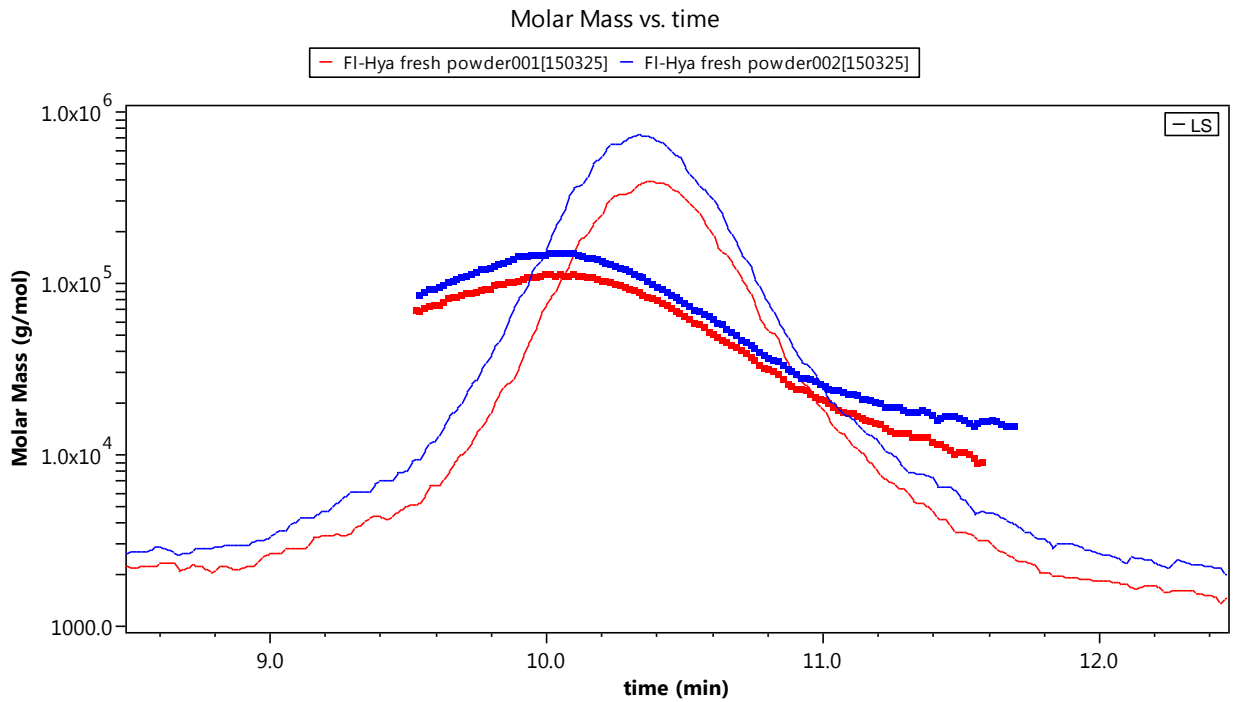*Fig. 14: The example of crosscorrelation analysis by programme SymphoTime.*
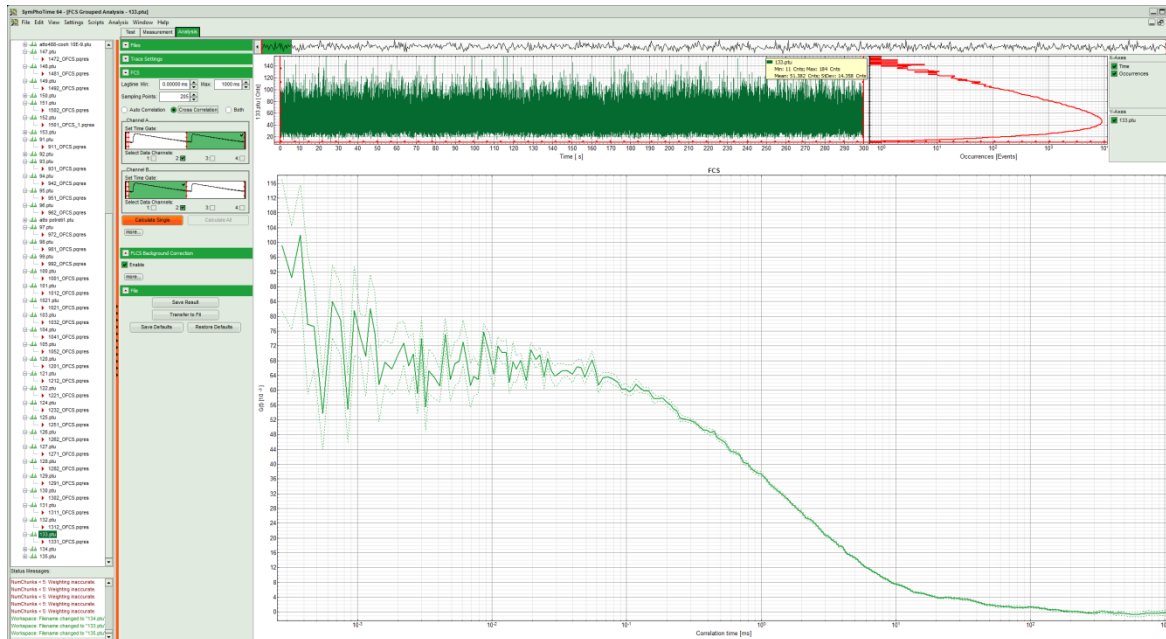
Fig. 15: The obtained correlation curve determined by analysis of measured data.

Fig. 16: The description of steps how to export data.

Appendix 3: SEC-MALLS analysis of Hyaluronan Rhodamine 110

According to SEC-MALLS measurement, molar mass of Hya-Rh sample was determined to 40 kDa. Random coil conformation is denoted by value of *a* between 0.5 and 0.8, and for rigid rod conformation the value of *a* is 1.8. Because of this, the samples are already too short to form a random coil conformation and the coefficients determined by Mark-Houwink-Sakurada plot showed a conformation between random coil and rod.

Appendix 4: SEC separation data